

# **AN INVESTIGATION ON INTERCONNECTION OF MICRO WIND TURBINES USING MULTILEVEL CONVERTERS**

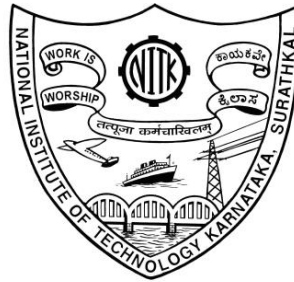
Thesis

Submitted in partial fulfillment of the requirements for the degree of

**DOCTOR OF PHILOSOPHY**

by

**KODEESWARA KUMARAN. G**



**DEPARTMENT OF ELECTRICAL AND ELECTRONICS  
ENGINEERING,  
NATIONAL INSTITUTE OF TECHNOLOGY KARNATAKA,  
SURATHKAL, MANGALURU - 575025.**

**October - 2018**

# DECLARATION

*by the Ph.D. Research Scholar*

I hereby *declare* that the Research Thesis entitled '**An Investigation on Interconnection of Micro Wind Turbines using Multilevel Converters**' which is being submitted to the National Institute of Technology Karnataka, Surathkal in partial fulfillment of the requirements for the award of the Degree of Doctor of Philosophy in Electrical and Electronics Engineering is a *bonafide report of the research work carried out by me*. The material contained in this Research Thesis has not been submitted to any University or Institution for the award of any degree.

Kodeeswara kumaran G

Register Number: EE09P03

Department of Electrical and Electronics Engineering

Place : NITK-Surathkal

Date :

## **CERTIFICATE**

This is to *certify* that the Research Thesis entitled '**An Investigation on Interconnection of Micro Wind Turbines using Multilevel Converters**' submitted by **Kodeeswara kumaran G**, (Register Number: **EE09P03**) as the record of the research work carried out by him, is *accepted as the Research Thesis submission* in partial fulfillment of the requirements for the award of degree of Doctor of Philosophy.

Research Guide  
(Name and  
Signature with Date  
and Seal)

Chairman - DRPC  
(Signature with Date and Seal)

## **ACKNOWLEDGEMENTS**

I would like to express my profound gratitude to my guide Dr. P. Parthiban, Department of Electrical and Electronics Engineering, NITK, for his valuable guidance which enabled me to complete the research work. I will be indebted to him for the constant support and the enormous patience shown in guiding me during the research.

I would like to thank Dr. Venkatesa Perumal, HoD, Department of Electrical and Electronics Engineering, NITK, for the facilities provided and the support given for completion of the work.

Also, I would like to extend my thanks to all the teaching and non-teaching staff of the department of Electrical and Electronics Engineering for their cooperation and support.

I would like to thank all those who are directly and indirectly involved in enabling me to complete the research work.

Finally, I would like to thank and acknowledge the grace of the almighty for everything.

Kodeeswara kumaran. G

## ABSTRACT

The increase in demand for electricity coupled with the obligation to use sustainable technologies has extended research and development to small and micro wind turbine based electricity generation systems. When it comes to micro wind energy systems, one of the important criteria in commissioning/operating is overall simplicity of the system apart from the system's capability to produce power adhering to established standards. To meet these requirements, a novel switching network, referred in this research work as comparator based switching signal selection (CSSS) network, has been proposed for controlling the series connected inverters of the micro wind energy system. The CSSS network eliminates the complexity in switching signal generation process like generation of multiple carrier waveforms or performing complex calculations. The network also enables the use of any two level inverter modulation schemes to control any levels of series connected inverter. To demonstrate the effectiveness of employing this switching network in a micro wind energy system, a comprehensive analysis has been performed using performance parameters like output rms value, harmonic distortion of output voltage and current, and k-factor of the transformer. A comparative analysis of the parameters under wide operating conditions has also been performed to understand how comparable the performance of the CSSS network is, to the existing modulation schemes. The results indicate that by employing the CSSS network, satisfactory performance can be obtained from the system for wide operating conditions. The structure of the network can also simplify the implementation of control algorithm.

**Keywords:** Micro wind turbines, series connected inverters, comparator based switching signal selection (CSSS) network, root mean square value, total harmonic distortion, k-factor.

## TABLE OF CONTENTS

<i>Abstract</i> .....	i
<i>Nomenclature</i> .....	iv
<i>List of symbols</i> .....	v
<b>1 INTRODUCTION</b> .....	1
1.1 Background of the Research Work .....	1
1.2 Literature Survey.....	3
1.3 Scope and Objective of the Research Work.....	13
1.4 Organization of the Thesis .....	13
<b>2 OVERVIEW OF MICRO WIND ENERGY SYSTEMS</b> .....	15
2.1 Wind Turbines.....	15
2.2 Generators .....	18
2.3 Power Converters in Micro Wind Energy Systems .....	19
2.3.1 Power converters for rectification and inversion.....	20
2.3.2 Power converters for turbine safety .....	22
2.4 System Controller .....	22
2.4.1 Control of power generated by the wind turbine.....	23
2.4.2 Control of dc-ac converter .....	24
2.5 Summary .....	26
<b>3 MODELING AND SIMULATION OF MICRO WIND ENERGY SYSTEM</b> .....	28
3.1 Modeling of Turbine-Generator Unit.....	28
3.2 Modeling of ac-dc Converter .....	31
3.3 Modeling of dc-ac Inverter.....	33
3.4 Switching Signal Generation using SHE Technique .....	34
3.4.1 Equal source condition .....	35
3.4.2 Unequal source conditions.....	38
3.4.3 Usage of computation tools for SHE equations.....	40
3.5 Switching Signal Generation using Multicarrier Modulation	

Techniques .....	41
3.6 Switching Signal Generation by using a Novel Switching Network ..	44
3.7 Modeling of Wind Turbine Braking Mechanism.....	49
3.8 Modeling of Reference Signal Generator .....	50
3.9 Summary .....	51
<b>4 PERFORMANCE ANALYSIS OF THE MICRO WIND ENERGY SYSTEM .....</b>	<b>52</b>
4.1 MWES Inverters with Equal Sources .....	54
4.2 MWES Inverters with Delta Modulator and CSSS Network.....	67
4.3 MWES Inverters with Un-equal Sources.....	73
4.4 Generation of Switching Signals using Digital Signal Controllers...	80
4.5 Summary .....	83
<b>5 CONCLUSION.....</b>	<b>84</b>
5.1 Future Scope of the Research Work.....	86
<b>APPENDIX I Specification of SPVAWT1-650W VAWT .....</b>	<b>88</b>
<b>APPENDIX II C Program for generating switching signals using CSSSN .</b>	<b>89</b>
<b>REFERENCES.....</b>	<b>92</b>

## NOMENCLATURE

<b>MWES</b>	Micro Wind Energy System
<b>DDG</b>	Decentralized Distributed Generation
<b>VAWT</b>	Vertical Axis Wind Turbine
<b>HAWT</b>	Horizontal Axis Wind Turbine
<b>PMSM</b>	Permanent Magnet Synchronous Machine
<b>MLI</b>	Multi-Level Inverter
<b>PWM</b>	Pulse Width Modulation
<b>SPWM</b>	Sinusoidal Pulse Width Modulation
<b>SHE</b>	Selective Harmonic Elimination
<b>PD</b>	Phase Disposition
<b>POD</b>	Phase Opposition Disposition
<b>APOD</b>	Alternate Phase Opposition Disposition
<b>CSSSN</b>	Comparator based Switching Signal Selection Network
<b>QI</b>	Quantization Index
<b>THD</b>	Total Harmonic Distortion
<b>DSC</b>	Digital Signal Controller
<b>ePWM</b>	Enhanced Pulse Width Modulation



## LIST OF SYMBOLS

<b>W/MW/GW</b>	Watt/ Mega Watt/ Giga Watt
<b><math>v</math></b>	Wind velocity
<b><math>\rho</math></b>	Density of air
<b><math>A_r</math></b>	Swept area of wind turbine rotor
<b><math>C_p</math></b>	Wind turbine power coefficient
<b><math>r</math></b>	Height and radius of wind turbine rotor
<b><math>\lambda</math></b>	Tip to speed ratio of a wind turbine
<b><math>\omega</math></b>	Angular speed of wind turbine shaft
<b><math>V_{dc}</math></b>	Rectifier output voltage/ DC source voltage
<b><math>V_L</math></b>	Three phase line to line voltage
<b>S</b>	Number of dc sources in a series connected inverter
<b><math>\theta_1, \theta_2, \dots, \theta_s</math></b>	Inverter switching angles
<b><math>V_f</math></b>	Magnitude of fundamental voltage
<b><math>V_{ref}(i)</math></b>	Instantaneous voltage of reference(modulating) waveform
<b><math>V_{ref}(p)</math></b>	Peak voltage of reference(modulating) waveform
<b><math>N_T</math></b>	Number of threshold levels used in the CSSS network
<b><math>m_a</math></b>	Amplitude modulation ratio
<b><math>f_c</math></b>	Carrier frequency
<b><math>f_m</math></b>	Modulator frequency
<b><math>m_f</math></b>	Frequency modulation ratio
<b><math>V_1</math></b>	Input dc voltage of the lower most inverter in a series connected inverter
<b><math>V_2, V_3, \dots</math></b>	Input dc voltages of the next higher inverters in a series connected inverter



# Chapter-1

## Introduction

# **1. INTRODUCTION**

## **1.1 Background of the Research Work**

Electricity has almost become one of the basic needs for human beings apart from food, fodder and shelter. As humans depend more and more on electrical equipment in their everyday life, the demand for electricity is steadily rising. The advancement of technology and improvement of lifestyle is further going to increase humans' dependence on electrical energy. Even though increased efficiency of the electric systems may result in less electricity consumption, the demand is only set to increase on account of growing economy in developing countries and electrification of transport and heating. In 2012, world electrical energy consumption stood at 18,608 TWh/year. The world energy council sees world electricity consumption increasing to more than 40,000 TWh/Year in 2040. This means the energy demand in future will be almost double than that of 2012 levels. Increased demand will be most dramatic in Asia. Energy demand of this magnitude can only be met by aggressively adding up to the existing generating capacity.

Majority of the existing electrical energy generating capacity is based on conventional methods using coal fired thermal power stations and oil/gas powered stations. Any attempt to increase the generating capacity through these types of conventional power stations will only aggravate the existing environmental problems. A conservative estimate reveals that in order to generate 1kWh of electrical energy from the conventional thermal power plants, 0.8 kg of CO<sub>2</sub> is being released in to the atmosphere (Mittal M L, Sharma C et al. 2012). The profound impact of these conventional power stations on the environment is a matter of grave concern. The solution to the energy demand issue should therefore be viable, both environmentally and economically.

The electricity generating systems are shifting towards cleaner technologies, driven by environmental needs and technological advances. Among the various technologies existing in theory and practice, for generating electricity, technologies involving renewable sources look quite promising. Meeting the future energy

demand from renewable energy sources, would therefore be the viable solution. The governments around the globe are making renewable energy resources competitive, and targeting their use in remote areas and for installation of decentralized power generation stations.

As a developing country, India too has the obligation to select a sustainable path in development. Not only it will contribute to reduction in carbon foot print, but also it will help in achieving the energy security in the future. At present, the energy policy of India is dictated by the growing energy deficit and the need to develop alternate energy sources. Approximately 70% of India's electricity generation capacity comes from fossil fuels, majority of which is being imported from other countries. This is a point of concern, both in terms of energy security and growing trade deficit. So, the policies and acts drafted by various government agencies focus on development and deployment of technologies involving renewable energy sources.

Energy from wind is one of the cleanest forms of energy. It can be used to meet part of the total electrical energy demand. Right now India stands 5<sup>th</sup> in terms of installed capacity of wind power in the world. Roughly 9% of the total electrical energy generated comes from wind power projects. Almost all of these projects incorporate a set of large megawatt capacity wind turbines. While the large wind turbines may be suitable for areas with high wind speeds like parts of Tamilnadu, Gujarat and Karnataka, the smaller counterparts may be suitable for much of the less windy areas. The prospect of installing small wind turbines provides additional scope of using wind power to augment the existing generation capacity.

The technology of extracting energy through micro and small wind turbine systems is less mature when compared to the technology involved in large wind turbine systems. This fact makes research and development in micro and small wind turbine based electricity generation systems more attractive. Plethora of possibilities is there to incorporate developmental aspects in the area of wind energy conversion systems, power electronic converters and system controllers.

Though the amount of energy generated by the small and micro wind turbine systems seems to be comparatively less to satisfy the enormous needs, they do provide a part of the solution to the power demand issues. The technology of generating electrical energy from micro and small wind turbines can be an extremely advantages feature when it comes to rural electrification, developing greener buildings or even deploying distributed generation plant with option to export power to the main grid. Most energy demands which are considered local may be addressed by using this technology of extracting power from wind using micro and small wind turbines.

## **1.2 Literature Survey**

Often energy is attributed to people's standard of living and there is always a direct correlation between the consumption of energy and the development of a country. Keeping this in mind, government energy policies have focused on raising per capita energy consumption and production. The energy policy of India has four key objectives: Access at affordable prices, improved security and independence, greater sustainability and economic growth. It is estimated that 304 million people in India live without access to electricity, and about 500 million people, are still dependent on solid bio-mass for cooking. The government is drafting and enacting policies to provide electricity for all and has set an ambitious target of providing electricity to all by 2022. The government policies coupled with fast improving economy has helped to improve the quality of life. As the standard of living improves, so does the growing need for electrical energy. India's annual energy consumption was around 4,926 TWh in 2012 and is projected to be around 15,820 TWh in 2040 (NITI Aayog June, 2017).

As the demand for electrical energy grows, scientists and engineers are prompted to look for solutions to increase the generation capacity through all possible means. India's share of conventional energy resources like oil, gas and coal out of global capacity is just 0.4%, 0.6% and 7%, respectively (NITI Aayog June, 2017). This implies that the demand should be met by importing these resources from other countries, if the dependency on conventional power generation technologies

continues. This may not be feasible for reasons like increased fiscal deficits arising due to imports, concerns about deteriorating environment etc. Hence, new and alternate power generation technologies are required. The need to produce electricity with least impact to environment has given a new dimension for research and development in renewable energy source based electricity generation technologies.

Approximately 1% of the total solar energy absorbed by the Earth is converted in to kinetic energy in the atmosphere, dissipated ultimately by friction at the Earth's surface. Based upon this fact, an analysis indicates that “a network of land based 2.5 megawatt turbines restricted to non-forested, ice-free, non-urban areas operating at as little as 20% of their rated capacity, could supply more than 40 times present worldwide consumption of electricity” (Lu, McElroy et al. 2009). This is more than 5 times total global use of energy in all form. The above estimation is based upon the annual average wind speeds in excess of 6.9 m/s at an elevation of 80 meters.

As a tropical country India is blessed with abundant wind and solar energy. Of all the renewable sources like wind, solar, geothermal and other similar other sources, wind energy seem attractive for various reasons. The National Institute for Wind Energy's (NIWE) latest estimate for India's wind power potential is 302 GW at 100 meters height (Rishi Dwivedi 2016). India's Integrated Energy Policy projects 800 GW installed capacity in 2031-32. Around 40 per cent of this, or 320 GW, will come from renewable energy as per currently announced plans of the government (Rishi Dwivedi 2016). Considering the renewable energy potential in India, a rapid push is needed to meet this goal. Most of the estimated energy potential and government drafted policies are based upon the potential in high wind speeds and large scale wind turbines.

The fact that there is considerable amount of potential to be exploited in low speed winds and the fact that not always it will be feasible to install large wind turbines in high wind speed regions due to geographical and environmental reasons, highlights the option to use micro and small wind turbines to augment the electrical

energy need. Conservative estimates say that huge untapped potential exists for small wind and hybrid systems. The potential to generate power using small wind turbines in Indian subcontinent alone is approximately 80,000 MW (Kshirsagar July, 2016). This energy can be used for off-grid applications like street lighting, rural electrification, public building electrification, signaling, remote houses, mini wind farms, desalination plants, communication towers and grid integrated applications.

There are numerous advantages of opting for micro and small wind turbines for electricity generation like absence of transmission loss, suitability for low wind speed areas, better suited for hybrid plants in combination with other sources, enhancement of energy independence and much less impact on environment. Also, there are other attractive feature for a small wind energy systems like increased recognition by government, opportunity for obtaining subsidy, feed-in tariffs, concept of net metering, which indirectly cuts down the cost of battery banks, increased retailability (Kharu, 2018). The Decentralized Distribute Generation (DDG) under Rajiv Gandhi Grameen Vidyutikaran Yojana also encourages use of small wind turbine based systems for rural electrification. But, in spite of the encouragement given by the government, micro and small wind turbine market has not yet reached its full potential. Among the challenges for small and micro wind energy systems, lack of mature technology, high initial system cost and comparatively complex system configuration are the important ones. In order to make effective use of micro and small wind energy systems in meeting the electrical energy demand, simple and better technology is required.

Every wind energy system consists of aerodynamic system, a generator, power electronic converter and system controller. The aerodynamic system comprises of a wind turbine, mechanical gear arrangements, tower structure, and the yaw mechanism such as the tail vane (in case of a horizontal axis wind turbine). Depending upon the axis of arrangement of turbine blades, the wind turbine may be classified as Horizontal Axis Wind Turbine (HAWT) type or Vertical Axis Wind Turbine (VAWT) type. Each of these turbine types has its own advantages and disadvantages. In VAWTs, the main rotor shaft is set perpendicular to the wind

while the main components are placed at the bottom of the turbine. This arrangement allows the generator and gearbox to be located close to the ground, facilitating easy service and repair. VAWTs do not need to be pointed into the wind, which removes the need for wind-sensing and orientation mechanisms.

VAWTs offer a number of advantages over traditional horizontal-axis wind turbines (HAWTs) such as (Wikipedia contributors 2018):

- they are omni-directional and do not need to track the wind. This means they don't require a complex mechanism and motors to yaw the rotor and pitch the blades
- ability to take advantage of turbulent and gusty winds. Such winds are not harvested by HAWTs, and in fact cause accelerated fatigue for HAWTs
- the gearbox of a VAWT takes much less fatigue than that of a HAWT. Motor and gearbox failures generally increase the operational and maintenance costs of HAWT wind farms both on and offshore
- some VAWTs can use a screw pile foundation, allowing a huge reduction in the carbon cost of an installation as well as a reduction in road transport of concrete during installation. They can be fully recycled at the end of their life
- wings of the Darrieus type have a constant chord and so are easier to manufacture than the blades of a HAWT, which have a much more complex shape and structure
- can be grouped more closely in wind farms, increasing the generated power per unit of land area
- can be installed on a wind farm below the existing HAWTs; this will improve the efficiency (power output) of the existing farm

Research at Caltech has shown that a carefully designed wind farm using VAWTs can have an output power ten times that of a HAWT wind farm of the same size (Svitil July, 2011). In 2011, Sandia National Laboratories wind-energy researchers began a five-year study of applying VAWT design technology to offshore wind farms (Wikipedia contributors 2018). The researchers stated: "The economics of



offshore wind power are different from land-based turbines, due to installation and operational challenges. VAWTs offer three big advantages that could reduce the cost of wind energy: a lower turbine center of gravity; reduced machine complexity; and better scalability to very large sizes. A lower center of gravity means improved stability afloat and lower gravitational fatigue loads. Additionally, the drivetrain on a VAWT is at or near the surface, potentially making maintenance easier and less time-consuming, fewer parts, lower fatigue loads and simpler maintenance all lead to reduced maintenance costs."

The VAWT may be suitable for installation in building mounted applications and sparsely populated areas where the wind is turbulent and weak. Traditional guideline is to install a wind turbine at a place which is at a horizontal distance of 10-20 times the vertical height of an obstruction or twice the height above any obstruction (Burton, Sharpe et al. 2002). Few studies have concluded that the wind flow over the roof is enhanced, providing possibility of application of the wind turbines in low speed areas. And also the studies have suggested that VAWT are much more suitable for built in environments due to their better performance in turbulent and skewed wind flow (Liang and Liu 2010). Increasing the solidity of the blades leads to increased power co-efficient at low tip speed ratios, which eliminates the problem of starting the turbine in low wind speeds.

From the view point of generators employed in micro and small wind energy systems, permanent magnet synchronous machine (PMSM) and brushless DC (BLDC) machines are mostly used because of their high power density and reliability (Liang and Liu 2010). The criterion commonly used to compare different generators is power density and torque density. PMSM and permanent magnet BLDC machines are mostly used in small scale wind energy systems. The concept of direct drive generators is being explored due to its advantages such as omission of gearbox between the turbine and the shaft of the generator. Contra rotating generators are also being explored for usage in small scale non grid connected wind turbines. Wind turbines with contra-rotating generators achieve higher energy conversion efficiency than traditional wind turbines (Li, Wang et al. 2010). Also contra-rotating generators have the advantage of high torque at slow

speed, so the gearbox can also be omitted, the power density goes up and starting torque becomes low which makes it fit for operating in the breeze.

For a wind turbine, the maximum power that can be possibly extracted, at a wind velocity ' $v$ ', is given by Betz's law as (Burton, Sharpe et al. 2002),

$$P_{max} = \frac{16}{27} \left( \frac{1}{2} \rho r h v^3 \right) \quad (1.1)$$

where  $h$  and  $r$  are the height and radius of the rotor. However, under practical conditions, the extractable power is just half of the value. Thus,

$$P_{max} = 0.36 \text{ kg m}^{-3} h r v^3 \quad (1.2)$$

The angular frequency of a rotor is given by  $\omega = \lambda \cdot v \cdot r$ , where  $\lambda$  is a dimensionless factor called the tip-speed ratio.  $\lambda$  is a characteristic of each specific windmill.

From the energy conversion equation (1.1), it can be seen that the output power of the wind turbine is sensitive to wind speed. This implies that the terminal voltage of the generators will not be constant due to the varying nature of wind. This stipulates that the output of these generators cannot be connected directly to a battery bank or a load. Apart from this fact, the blades of the micro wind turbines have a lower mass when compared to its bigger counterparts, which further aggravates the problem of maintaining the output voltage constant. The blades of the wind turbines act as a fly wheel and prevents sudden variation in turbine speed, in case of sudden variation in the wind speed. Lesser blade mass means lesser speed stability and in turn large variation in generators output during varying wind speeds. This fact is kept in consideration while designing micro wind energy systems.

The generators used in micro wind turbines are usually designed to give output in sub-hundred voltage range. So, to meet the power requirement of standard electrical loads designed to operate at single phase supply of 230V, or three phase supply of 440V, a group of such turbines would be required to be connected in series/parallel configuration. In this context, processing the output voltage and

current of the micro wind turbine generators to satisfy the load requirements will need appropriate power converter topology.

Several topologies of rectifiers have been suggested that can be used along with an inverter to connect the load to the generator such as uncontrolled diode rectifier, single-switch switched mode rectifier and full-bridge controlled rectifiers. It has been reported that a single-switch switched mode rectifier offers lesser cost of components, complexity of control and better power at low generator speeds than ordinary rectifiers (Pathmanathan, Tang et al. 2008). In order to control the single-switch switched mode rectifier, phase advance technique has been used and it has been reported that this technique is capable of producing greater power than conventional semi-bridge rectifier modulation. This kind of rectifier circuits doesn't provide solution for interfacing with micro wind energy systems to ac load or a grid.

Small wind turbine generating system configuration with a diode rectifier, dc-to-dc boost converter and a grid connected inverter has also been reported (Liang and Liu 2010). The diode rectifier converts the generated ac supply to uncontrolled dc supply. The dc supply is then boosted to appropriate levels and fed to a grid connected inverter. A grid connected inverter inverts the boosted dc-to-ac and sends it to the grid. It has been reported that the circuit is of low cost, has wide range of power for different rated inverters and dump load power control (Wang, Nayar et al. 2011). This converter doesn't address about the conditions of low power output, efficiency of the inverter, harmonic distortion during low wind speed regimes.

Certain other configurations use a diode rectifier-inverter combination along with a step-up transformer to connect the converters output to the grid (Kortabarria, Ibarra et al. 2010). The maximum power point tracking is controlled by the inverter. This kind of configuration, in spite of its simplicity, requires bulky transformer which increases the system cost, size and weight.

A back to back ac/ac converter uses a controlled rectifier instead of the diode rectifier with a voltage source inverter (Kortabarria, Ibarra et al. 2010). Absence of

diode rectifier eliminates the generator side stator currents with harmonic contents. The converter used is a bidirectional converter and makes it possible to obtain the required current at the generators output with required power factor. But the control of the converter becomes complex and additional sensors are required to sense the current and speed. Also, the use of a two level inverter introduces additional problems as mentioned earlier.

In order to mitigate the power quality issues in a micro wind turbine based energy system, a multilevel inverter (MLIs) along with suitable rectifier configuration may be more suitable. A comparative study has been conducted to determine the suitability of a two level converter and a multilevel converter for wind energy systems. Pulse Width Modulation (PWM) associated with sliding mode is used for controlling the converter. Power factor control is introduced at the output of the converters. It has been observed that the multilevel converter has an enhanced behavior when compared to that of a two level converter and it has been suggested that multilevel converters are much suitable for wind energy system than a two level converters (Melicio, Mendes et al. 2008).

A multilevel inverter has various advantages such as lower common mode voltage, lower voltage stress on power switches, lower  $dv/dt$  ratio to supply lower harmonic contents in output voltage and current. Compared to a two level inverter of the same power rating, MLIs also have the advantages that the harmonic components of line-to-line voltages fed to load are reduced owing to its switching frequencies. Various existing topologies of multilevel inverters such as diode clamped MLI, flying capacitor MLI, cascaded H-bridge MLI have been reviewed in (Colak, Kabalci et al. 2011). Among the three types of multilevel inverters the cascade inverter has the least components for a given number of levels. Cascade MLI consists of a series of H-bridge cells to synthesize a desired voltage from several separate dc sources which may be obtained from solar cells, batteries, fuel cells etc., This makes the cascaded MLI much suitable for a micro wind turbine generator which generates voltage of lower magnitude. With appropriate control strategy, it is possible to bypass any faulty module without having to stop the entire converter operation (Lezana and Ortiz 2009). The power which is obtained from

the micro wind energy systems is directly proportional to the wind speed. It can't be assumed that variation of wind speed will affect the output of all the micro wind turbines in the system, in the same way. Each micro wind energy system may act as a different source of different magnitude. This leads to a situation where the dc link voltages of each cascade MLI stages being different. The cascaded MLI with different dc link voltages (i.e. unequal dc sources) is often referred to as asymmetrical cascaded inverter. It has been suggested in (Malinowski, Gopakumar et al. 2010) that the cascade MLI requires research on fault management, intelligent modularization, and the possibility to change modules and reconfigure on the fly.

Every converter topology needs to be matched with a proper control scheme. Several modulation and control strategies have been developed for multilevel inverters including multicarrier modulation techniques, Selective Harmonic Elimination PWM, space vector PWM (Holmes and Lipo 2003). The efficiency parameters of a MLI such as switching losses and harmonic reduction are principally dependent on the modulation strategies used to control the inverter.

For an m-level converter with equal independent source voltages, (m-1) harmonics can be eliminated (Jih-Sheng and Fang Zheng 1996). The angles for the turn-on and turn-off of the switches can be determined by constraining the Fourier series expansion of the periodic waveform, yielding a set of transcendental equations. Since the resulting waveforms only contain the odd harmonics, the angles are chosen to eliminate them. The dc voltage obtained from each of the micro wind turbines may not be equal at all times, which makes the methods suggested by Lai et al (Jih-Sheng and Fang Zheng 1996) less feasible. A three phase cascaded H-bridge converters supplied by unequal, possibly varying, measurable voltage sources have been proposed in (Chiasson, Tolbert et al. 2005) which makes use of general resultant based algorithm. This kind of technique may be extended to converters of micro wind energy systems, so that the output voltage of the converter will have harmonics within permissible limits.

Apart from resultant algorithms, several other algorithms have also been proposed for eliminating/reducing harmonics and for keeping the total harmonic distortion within acceptable limits. Algorithms such as Genetic algorithms have been used to obtain optimal solutions for inverter circuits but in spite of their advantages, these algorithms are less attractive because of the complex calculations involved. Heuristic algorithms such as Particle Swarm Optimization have been suggested (Al-Othman and Abdelhamid 2008) to deal with harmonics elimination in cascaded multilevel inverters with non-equal dc sources. There is no reference in any of the literatures that these algorithms have been tested on a cascaded MLI in a micro wind energy system with non-equal dc source link voltage. Even if heuristic algorithms are selected, the added complexity of the control algorithms will be a deterrent factor in using them in micro wind energy systems.

Apart from eliminating harmonics and reducing distortion in the output waveform, the control scheme should also take care of extracting maximum power from the wind turbine generator during variable speed operation. In this regard, the operating regions of a micro wind turbine can be divided into two parts according to its rotational speed: below the rated speed and beyond the rated speed. In variable speed operation, a control method designed to extract maximum power from the turbine and provide constant grid voltage and frequency is required. Below the rated speed, laws based on MPPT are commonly used to extract more energy from the wind. All laws based on MPPT track the best operating point according to the energy conversion equation (1.1). Above the rated speed, the over speed protection methods are required. The methods include mechanical protection methods and/or electrical protection methods. The electrical protection method can improve the response of the system compared to the mechanical methods (Liang and Liu 2010). In order to implement this method, information on turbine speed and generator current is required which may be obtained by installing appropriate sensor. Methods similar to the one used by Ashan (Ahshan, Iqbal et al. 2008) uses voltage, frequency, power flow between generator and grid may also be used to indirectly compute the speed and control the system accordingly.

If all of the issues or even a few of them are rectified, micro wind energy systems may become effective and simple, and provide a viable solution for the power demand problem. This requirement led to setting up of the primary focus of this research work which is to find out a simple and effective micro wind energy system configuration.

### **1.3 Scope and Objective of the Research Work**

Based upon the requirements of micro wind energy system discussed in section 1.2, the objective of the research work was framed as follows:

- To model a micro wind-turbine based energy systems with vertical axis wind turbine and necessary power converters
- To analyze the performance of the wind energy system under different test cases (with different inverter configurations, different modulation schemes and different operating conditions)
- To formulate a simple, effective wind energy system controller that may encourage the widespread practical implementation of micro wind turbine based energy systems

### **1.4 Organization of the Thesis**

The research thesis is organized in to five chapters. A brief overview of the contents of individual chapters is presented here:

**Chapter 1** gives an introduction to the background of the research work, motivation for the research work and defines the scope and objectives of the research work. The chapter also gives a detailed overview of the literature related to the research work including the different topologies of power converters in wind energy systems and variety of modulation techniques available to control the power converters.

In **Chapter 2**, the overview of vertical-axis micro wind-turbine based energy systems which is taken up for investigation is discussed elaborately. The discussion includes the explanation of the structure of MWES and the way each functional element operates in the system.

**Chapter 3** discusses about the modeling of the micro wind energy based systems with vertical axis wind turbines and series connected inverters. The chapter also narrates the different MWES system configurations used for performance investigation which includes various levels of series connected inverters and modulation techniques like selective harmonic elimination and multicarrier PWM techniques.

**Chapter 4** elaborately explains about the principles of operation of the proposed comparator based switching signal generation (CSSS) network. A generalized algorithm for realizing the CSSS network using devices like microcontroller, DSP, FPGA is presented in this chapter. This chapter also discusses about the performance analysis of MWES employing the proposed CSSS network and compares the performance with conventional configurations.

**Chapter 5** provides the conclusion of the overall research work and explains about the possible future work that can be carried out based on the proposed CSSS network.



Chapter 2  
Overview of  
Micro Wind Energy  
Systems

## **2. OVERVIEW OF MICRO WIND ENERGY SYSTEMS**

As generation of electricity moves towards using green technologies, research and development in the area of producing electricity using renewable and non-conventional sources has increased. The trend of using wind energy and solar energy has gained momentum due to various reasons. Wind turbine based energy systems owing to its negligible carbon footprint have been deployed in places wherever possible. While large wind turbines have been used to export power to grid, the small and micro wind turbines are employed to satisfy the local energy needs or to form a part of an islanded network in distributed generation network.

The structure of a micro wind turbine based energy systems is similar to the structure of a large wind turbine based energy system in many aspects. The components employed for converting wind energy to electric energy in a typical wind energy system include: the wind turbine, generator, power converters (ac-dc, dc-ac), DC link capacitors, system controller, safety mechanisms, protective elements, power transmission elements, reactive power controllers. This chapter provides an overview of the typical structure of micro wind turbine based energy systems and the functioning of its components.

### **2.1. Wind Turbines**

In any wind energy system, the aerodynamic system plays a crucial role. The aerodynamic system comprises of the parts like turbine blades, hub, guidance mechanism (in case of a horizontal axis wind turbine) and gear arrangements coupled to the generator. The lift/drag force exerted by the wind on the turbine blades does the job of moving the turbine rotor and thereby converting the wind energy to kinetic energy. The wind turbines may be a Horizontal Axis Wind Turbine (HAWT) type or Vertical Axis Wind Turbine (VAWT) type. As depicted in Figure 2.1, the rotor shaft of a HAWT is placed horizontally whereas in a VAWT the rotor shaft is placed vertically.

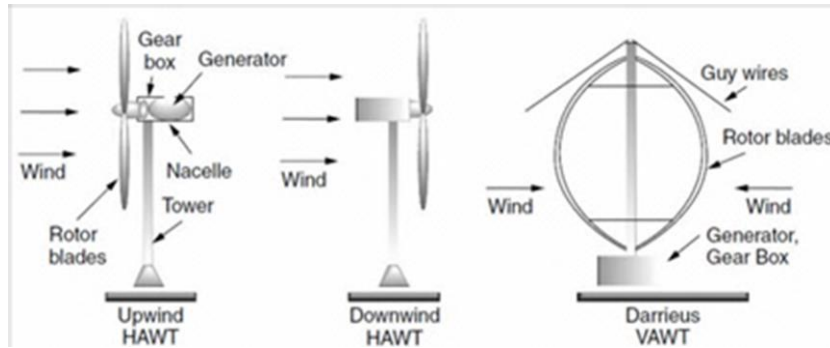


**Figure 2.1** HAWT and VAWT structure

For a micro wind energy system which is supposed to tap the energy from low speed, turbulent winds, VAWT are usually preferred. A VAWT runs slower with high torque when compared to a HAWT, but when mounted on a building, the structure of the roof can double the wind speed and thereby the rotor speed. As far as electricity generation applications are concerned, the generator coupled to the turbine is required to run with high speed rather than with high torque. Optional gear mechanism is employed if the turbine speed has to be appropriately matched with the generator speed. Since the VAWT can operate satisfactorily regardless of the direction of wind and doesn't need a yaw mechanism, the control of VAWT is comparatively much simpler to a HAWT. The control of VAWT is limited to control of rotor speed of the turbine and thereby the power that can be extracted from the turbine.

Theoretically, the amount of power that can be extracted by the wind turbine, from the airflow, is given by the following expression,

$$P_{air} = \frac{1}{2} \rho A_r v^3 \quad (2.1)$$

where,  $\rho$  is the density of air (approximately  $1.225 \text{ kg m}^{-3}$ )

$A_r$  is the swept area of the rotor,  $\text{m}^2$

$v$  is the upwind free wind speed,  $\text{ms}^{-1}$

Although equation 2.1 gives the power available in the wind, the power transferred to the wind turbine rotor is reduced by the power coefficient,  $C_p$  which is expressed as,

$$C_p = \frac{P_{wind\ turbine}}{P_{air}} \quad (2.2)$$

Therefore, the power that can be practically obtained from the wind turbine when expressed in terms of power coefficient of the turbine is written as,

$$P_{wind\ turbine} = C_p P_{air} = C_p \times \frac{1}{2} \rho A_r v^3 \quad (2.3)$$

The maximum value that the power coefficient ( $C_p$ ) can have is defined by the Betz limit, which states that a turbine can never extract more than 59.3% of the power from an air stream. But practically, the value is less than that in the range of 25% to 45% (Burton, Sharpe et al. 2002). At low rotor speed, less amount of wind hits the blades and the efficiency decreases. At high rotor speed, too much wind hitting the blades creates a turbulent effect and thereby reduces efficiency. The maximum efficiency, therefore, occurs at a point in between the minimum rotor speed and maximum rotor speed for a given wind speed. It is possible to obtain maximum turbine efficiency for almost any wind speeds by controlling the rotor speed. A typical wind turbine's power coefficient characteristic is shown in Figure 2.2. It can be observed from the figure that the speed of the rotor indirectly controls the turbine efficiency.

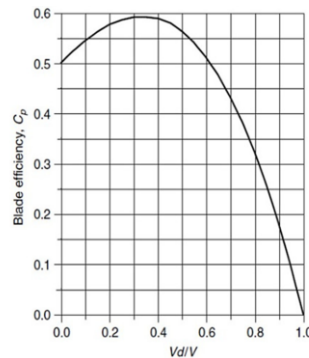


**Figure 2.2** Typical  $C_p$  characteristic of a wind turbine

The power output of a wind turbine at various wind speeds is conventionally described by its power curve. The power curve gives the steady-state electrical power output as a function of the wind speed. Figure 2.3 shows one such power curve of a wind turbine.

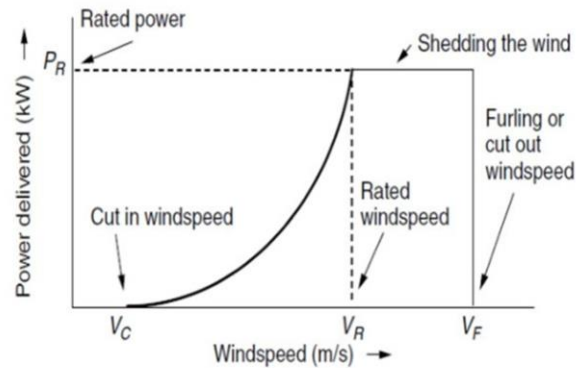


**Figure 2.3** Typical power curve of a wind turbine

Three operating points can be observed in the power curve (Burton, Sharpe et al. 2002):

- Cut-in wind speed – the minimum wind speed at which the wind turbine produces significant power
- Rated wind speed – the wind speed at which rated power is produced (rated power is usually the maximum power produced by the generator)
- Cut-out wind speed – the maximum wind speed until which the wind turbine produces power (usually decided based on the safety aspects)

Below the cut-in speed, the turbine doesn't produce any useful energy. Above the cut-in speed the turbine shaft starts rotating and the generated power increases approximately as a cube of the wind speed (equation 2.3). Beyond the rated wind speed, safety features get activated to limit the rotor speed. Above the cut-out speed or furling speed the rotor is altogether stopped to safeguard the turbine and its associated mechanical structures from damage. So when a wind turbine controller is designed to control the operation of the turbine, the information about cut-in speed, rated speed and cut-out speed is used during the design process.

## 2.2. Generator

The generator coupled to the turbine rotor, with or without gear mechanism, converts the mechanical energy into electrical energy. Different types of generators are used in wind turbine applications. In megawatt range turbines, induction generator and synchronous generators are commonly found. But when it comes to micro wind

turbines, generators with permanent magnet are preferred as obtaining higher efficiency is possible. The presence of permanent magnets in the stator increases power density. It also eliminates the need to supply magnetizing current to the stator windings thereby reducing the control complexity. Among the permanent magnet machine category, Permanent Magnet Synchronous Machines (PMSM) are usually employed for micro and small wind energy systems.

The generators in micro wind turbine systems produce power in the order of few hundred watt and the magnitude of voltage generated is lesser than standard voltage rating of any conventional consumer loads. Commercially available micro wind turbine generators typically generate output voltage in the range of few tens of voltage to around 100V. This fact mandates the usage of a group of such turbines or other appropriate techniques to produce a voltage of standard magnitude to power up the 230V(or 440V) loads. Depending upon the voltage and current requirement of the load, a series-parallel combination of interconnected micro wind turbines may be used. A power converter of appropriate structure is therefore required to connect all the turbines and to process the power obtained from the turbines.

### **2.3. Power Converters in Micro Wind Energy Systems**

The power converters of a wind turbine perform the minimal job of connecting the wind turbine generator to the load/grid. Connecting the generator to the load is always a tricky task as various input and output parameters have to be monitored and controlled. The power obtained from the wind turbine generator is to be conditioned before feeding it to any load. The features required from a power converter used in a wind energy system are therefore derived from the load requirements, which start with selection of appropriate topology of power converter. The overall system requirements may also determine other features related to power quality, overall cost (installation, operation, maintenance) and simplicity of control.

Generally, the features that are required from power converters of a micro wind energy system include:

- Production of appropriate magnitude of output voltage to meet the load requirement
- Conversion of voltage (ac to dc, dc to ac, step-down, step-up)
- Maintain quality of the output to reasonable levels
- Provide electrical braking and a path for excess energy dissipation
- Fault handling

Based upon the functions listed above, the power converters that can be employed in micro wind energy systems can be grouped in to two functional categories: power converters to perform necessary rectification and inversion, and power converters to implement safety aspects.

### **2.3.1. Power converters for rectification and inversion**

Recalling the fact that the PMSM generators used in the micro wind turbines produce ac voltages lower than the standard voltage magnitudes, the generator output has to be boosted to 230VAC or 440VAC. Different configurations of power converters, like the ones listed below, may be used to process the power from the PMSM generators to meet the load requirement.

- a) Controlled rectifier + inverter + step up transformer
- b) Uncontrolled rectifier + PWM inverter + step-up transformer
- c) Uncontrolled rectifier + boost converter + inverter
- d) Uncontrolled rectifier + series connected inverters

Figure 2.4 shows the structure of the different micro wind energy system configurations.

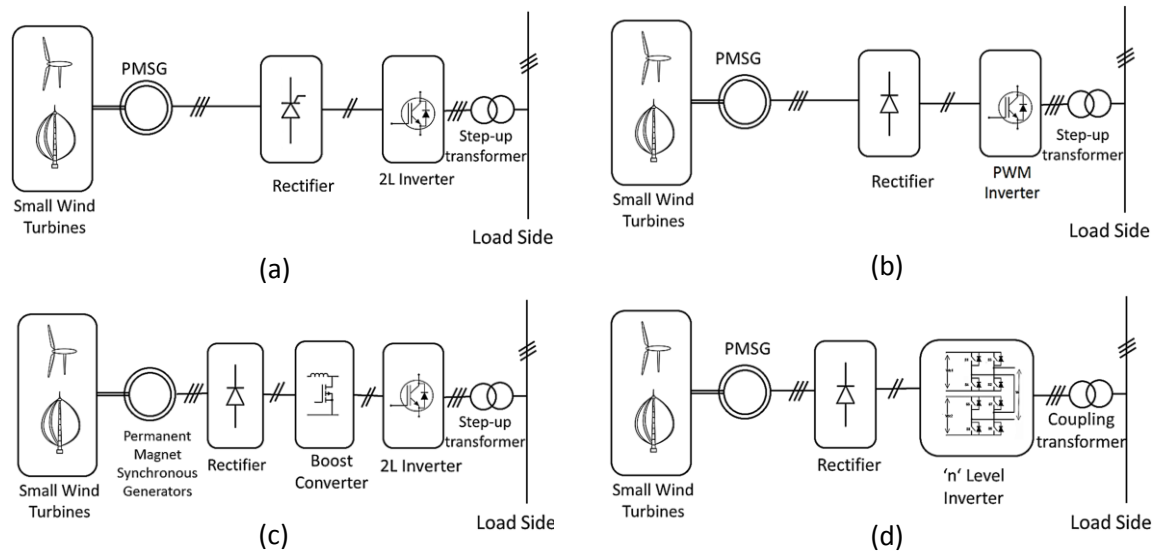


**Figure 2.4** Various power converter configurations for MWES

The converter used in the MWES is required to have features like ability to supply power with least amount of distortion in supply waveform, have least amount of harmonics, higher efficiency, simple operation and lowest possible cost. In the first three configurations listed above, the presence of large reactive element, the inductor, is an element of concern, both in terms of the cost and non-linearity introduced in the circuit operations. The size and cost of the step up transformer which operates at fundamental frequency will significantly outweigh the overall cost of the other power converting elements. As far as the third configuration is concerned, the size of the boost inductor may be reduced by increasing the frequency of operation of the boost converter and thereby reducing the inductor cost, but the effect of the non-linear element on the circuit performance is still a matter of concern.

The fourth configuration on the other hand has no requirement to use a step-up transformer or a boost inductor and uses many dc sources connected in series to raise the magnitude of voltage. This configuration will be the ideal choice for a micro wind energy system where each wind turbine output is processed to form a separate dc source. The number of level of the inverter is decided by the magnitude of the output voltage generated by the turbine generators.



### **2.3.2. Power converters for turbine safety**

Apart from converting power from wind turbine to suitable magnitude and suitable form, the converters also take care of safety aspects like safe guarding the turbine and load during high wind speeds. Referring to the power curve in Figure 2.3, it can be safely stated that the aspects of the power converters handling safety are determined by the information from the power curve.

Due to variation of wind speed during different time of the day and different time of the season, the wind speed may sometimes be very high. The high speed winds may damage the mechanical assembly due to increased centrifugal forces. Also, due to high wind speeds, the turbine may produce more power than the system loads can handle. This may in turn damage the loads. As a safety measure, a dummy load (in the form of a small braking resistance) is used to brake the wind turbine during high winds. As stated in section 2.1, above rated wind speed the turbine speed is required to be controlled and above the cut-off speed the turbine movement should be stopped. A braking resistor in series with a power switch is connected across the output terminals of the turbine. The control of the power switch facilitates the control of the turbine speed. The effective braking resistance is varied by the controlling the duty ratio of the switch based upon the wind speed information. The higher the wind speed, the higher is the braking resistance.

### **2.4. System Controller**

The objective of having a system controller is to enable the wind energy system to operate stably/reliably and deliver power with reasonable standards. This includes producing a sinusoidal output with less distortion, cope up with disturbances on the load side, ensure safety of the wind turbine by controlling the speed of the turbine at high winds and control the active and reactive power. The system controller may also perform other functions like over voltage and under voltage detection, abnormal frequency detection, monitoring and measurement of generator and grid voltages, frequencies and power, disconnection of the system from the load/grid in short

duration of time, measurement of wind speed without wind speed sensor etc.. Various control algorithms are often employed to perform the functions of the system controller.

#### 2.4.1. Control of power generated by the wind turbine

As mentioned in section 2.1, the maximum efficiency from a wind turbine can be obtained by controlling the rotor speed. The Maximum Power Point Tracking (MPPT) algorithms are meant to control the wind turbine rotor speed by controlling torque of the generator. When an uncontrolled rectifier is used to convert the PMSM generated ac voltage to dc voltage, it may not be possible to use MPPT algorithms directly. If a controlled converter is used, the converter may be controlled to extract maximum power from the wind turbine using MPPT algorithms. The energy conversion formula in equation 2.3, for any wind turbine, provides a means to calculate the power that can be obtained from a wind turbine. Only the power coefficient ( $C_p$ ) in equation 2.3 can be controlled according to the power curve in Figure 2.5. The MPPT algorithms are based on finding out the best operating point to extract maximum power from the wind turbine.

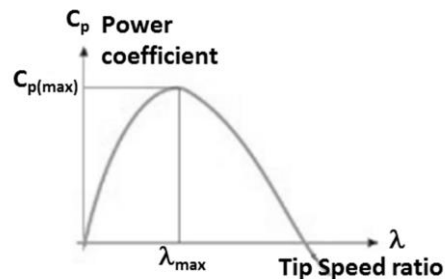


**Figure 2.5** Power co-efficient vs Tip-speed ratio characteristics

This curve shows that the best operating points are obtained around the optimum tip-speed ratio. The tip-speed ratio is expressed using the following equation:

$$\lambda = \frac{r \omega}{v} \quad (2.4)$$

where,  $\lambda$  is the tip to speed ratio,  
 $r$  is the radius of the wind turbine rotor in meters,

$\omega$  is the angular speed of the turbine shaft in rad/sec,  
 $v$  is the velocity of the wind in m/s.

The tip speed ratio can be controlled by controlling the angular speed of the wind turbine rotor and MPPT can be achieved. In general, three main control algorithm are used to track the maximum power points of a wind energy conversion system regardless of the whether the turbine consists of permanent magnet based generator or non-permanent magnet based generator. They are Tip-Speed Ratio (TSR) control algorithm, Hill-Climb Search (HCS) algorithm and Power Signal Feedback (PSF) algorithm.

#### 2.4.2. Control of dc-ac converter

The basic operation of a dc-ac converter is to convert the dc bus voltage to ac voltage with desired magnitude and frequency. Since a series connected inverter has been identified as the appropriate inverter topology for a micro wind energy system, relevant modulation strategies may be employed including the use of SPWM with

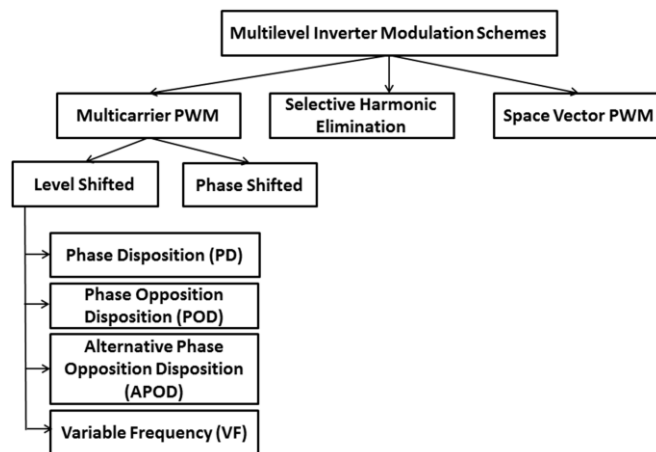


**Figure 2.6** Various modulation schemes for a multilevel inverter

multiple carriers, space vector modulation or selective harmonics elimination technique. The main aim of the modulation strategy of multilevel inverters is to synthesize the output voltage as close as possible to the sinusoidal waveform and to minimize switching losses. Many modulation techniques have been developed for

harmonic reduction and switching loss minimization. The classification of modulation methods used in multilevel inverters is presented in the Figure 2.6.

For instance multicarrier SPWM methods like PD, POD, APOD, VF are employed by exploiting the principles of sinusoidal pulse width modulation technique. The carrier signals are arranged vertically or horizontally to give rise to multicarrier techniques. In phase opposition disposition (POD), the carriers above the zero reference are in phase but shifted by  $180^\circ$  from those carriers below the zero reference. POD method yields an output waveform which has quarter wave symmetry when the frequency modulation ratio ( $m_f$ ) is even and odd symmetry when  $m_f$  is odd. In alternative phase opposition disposition (APOD), each carrier band is shifted by  $180^\circ$  from the adjacent

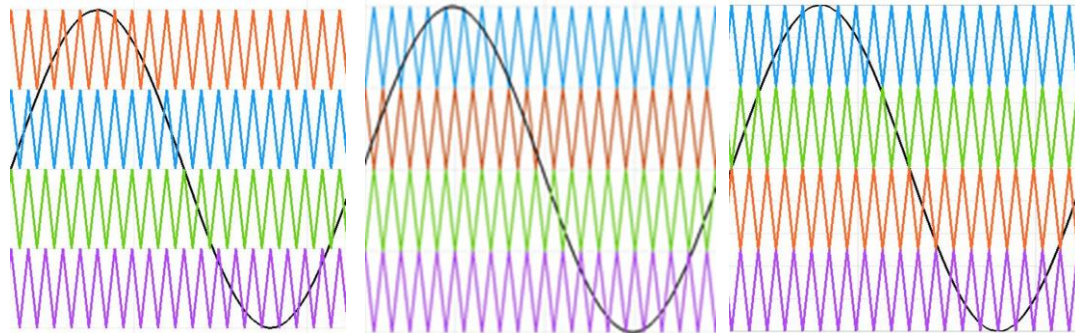


**Figure 2.7** Multicarrier modulation carrier wave and reference wave (a) PD, (b) POD, (c) APOD.

bands. In phase disposition (PD) all the carriers are in phase across all bands which make their band harmonics contiguous. In Variable Frequency (VF) method, the number of switching's for upper and lower devices of chosen MLI is much more than that of intermediate switches in PWM using constant frequency carriers. In order to equalize the number of switching's for all the switches, variable frequency PWM strategy is used in which the carrier frequency of the intermediate switches is increased to balance the number of switching's for all the switches. The number of carrier waves required depends upon on the number of levels present in the inverter output waveform i.e for  $m$ -level inverter;  $(m-1)$  carrier waveforms are required. The carrier waveforms may be level shifted or phase shifted. Comparison of the reference

waveform with the carrier waveforms continuously helps in generating the required switching signals to control the inverter switches.

On the other hand, Selective Harmonic Elimination (SHE) techniques directly estimate the switching angles of different inverter switches from a set of transcendental equations which describe the inverter output voltage. The number of such equations formulated depends upon which order harmonics are targeted for elimination/reduction. Solutions of the transcendental equations (in the form of firing angles) are used to generate appropriate switching signals to control the inverters.

## 2.5 Summary

In this chapter, the overview of the micro wind energy system and the typical

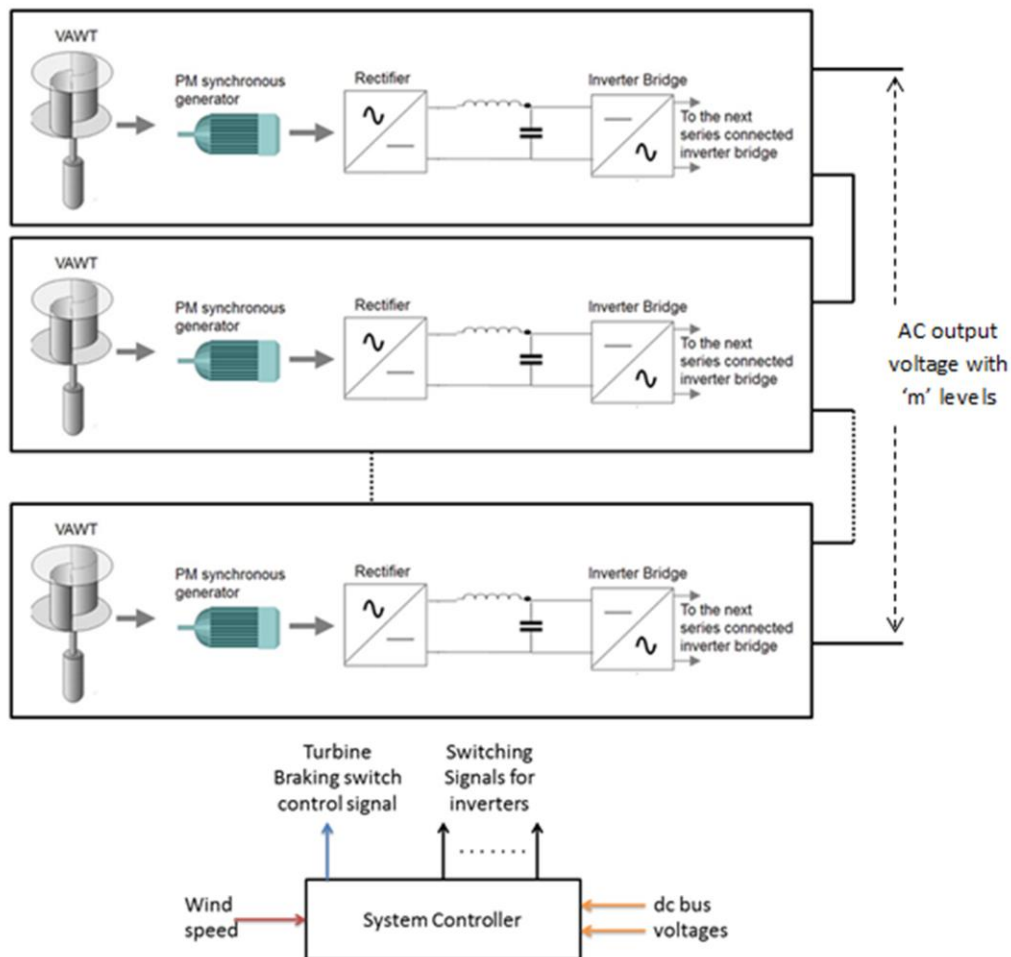


**Figure 2.8** Overall structure of the micro wind energy system

components/blocks which are part of the system have been discussed. Based on the theoretical discussion presented in this chapter, the structure of the micro wind energy system has been formulated as shown in Figure 2.7. The simulation models developed to represent each sub-system of the micro wind energy system are presented in the next chapter.

Chapter 3  
Modeling and  
Simulation of  
Micro Wind Energy  
System

### **3. MODELING AND SIMULATION OF MICRO WIND ENERGY SYSTEM**

In order to study the performance of the micro wind energy system, the entire MWES system with the structure presented in the previous chapter, has been modeled and simulated using MATLAB Simulink. The modeling process involves modeling of all the components of the MWES which include modeling of VAWT with PMSM, modeling of all the converters, modeling of wind turbine braking mechanism, modeling of reference signal generator and system controller.

#### **3.1 Modeling of Turbine-Generator Unit**

As a first step, modeling of the vertical axis wind turbine with permanent magnet synchronous machine (PMSM) has been performed. Just like any other electric machine, a permanent magnet synchronous generator consists of two elements: the field and the armature. The rotor consists of the field circuit in the form of permanent magnets and the stator consists of the armature windings. The rotor of micro wind energy turbines are usually of salient pole type with poles shaped to obtain sinusoidal air-gap flux, which is more suited for low rotor speeds. This structure is especially suitable for micro wind turbine generators, considering the fact that the wind speed is in the order of few tens of meters per second.

The turbine-generator unit is a complex mechanism to model which is made up of several mechanical and electrical components. Since the focus of the research work is limited to suggesting a suitable and simple power converter configuration which may encourage wide spread adoption of the micro wind energy systems, without compromising on the performance, the modeling of turbine unit has been limited to modeling a PMSM generator with a set of speed inputs to mimic the mechanical output of the rotor blades.

The machine parameters of a commercially available 650W vertical axis wind turbine (Model number: SPVAWT1-650W, SunAir Power Pvt.Ltd.,) has been used during simulation. The turbine considered for simulation has direct coupled permanent magnet synchronous generator. The power output curve and the energy



output curve of the chosen VAWT is shown in Figure 3.1. Detailed specifications of the vertical axis turbine are given in APPENDIX I.

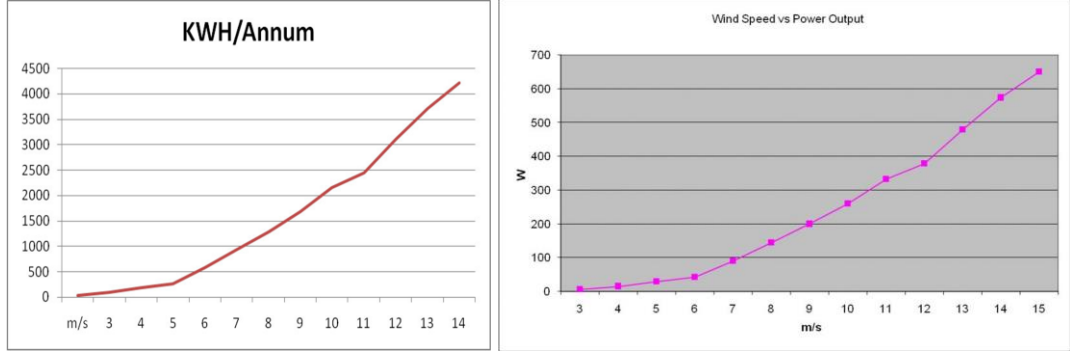


**Figure 3.1** Power and Energy characteristics of SPVAWT1-650W

The permanent magnet synchronous machine block available in Simulink library was used for simulation, after making necessary modifications to the model parameters based upon the specifications of SPVAWT1-650W (Sunair Power 2015). The generator is a three phase permanent magnet synchronous machine with sinusoidal back emf. The equations which are used to model the PMSM are expressed in the rotor reference frame (qd frame) as given in equation (3.1) to (3.3) (Simulink documentation 2017).

$$\frac{d}{dt}i_d = \frac{1}{L_d}V_d - \frac{R}{L_d}i_d + \frac{L_q}{L_d}p\omega i_q \quad (3.1)$$

$$\frac{d}{dt}i_q = \frac{1}{L_q}V_q - \frac{R}{L_q}i_q + \frac{L_d}{L_q}p\omega i_d - \frac{\lambda p\omega}{L_q} \quad (3.2)$$

$$T_e = 1.5p[\Phi i_q + (L_d - L_q)i_d i_q] \quad (3.3)$$

where

$L_d, L_q$  are 'd' and 'q' axis inductances,

(for a salient round rotor,  $L_d=L_q=\max(L_{ab}/2)$ )

$R$  is the resistance of the stator windings,

$i_d, i_q$  are 'd' and 'q' axis currents,

$V_d, V_q$  are 'd' and 'q' axis voltages,

$\omega$  is the angular velocity of the rotor,

$\Phi$  is the amplitude of the flux induced by permanent magnets of the rotor,

$p$  is the number of pole pairs, and

$T_e$  is the electromagnetic torque.

The mechanical system of the PMSM has been modeled using the equations 3.4 and 3.5 (Simulink user manual).

$$\frac{d}{dt} \omega_r = \frac{1}{J} (T_e - T_f - F\omega - T_m) \quad (3.4)$$

$$\frac{d\theta}{dt} = \omega \quad (3.5)$$

where

- $J$  is the combined inertia of rotor and load,
- $F$  is the combined viscous friction of rotor and load,
- $\theta$  is the rotor angular position,
- $T_m$  is the shaft mechanical torque,
- $T_f$  is the shaft static friction torque, and
- $\omega$  is the angular velocity of the rotor (mechanical speed).

Since the PMSM is coupled to the rotor of the wind turbine, the input to the generator block is specified as rotor speed in rad/sec. Using speed as the mechanical input, allows modeling a mechanical coupling of the turbine shaft with the generator. To mimic the variation of wind speed, a look-up table corresponding to the actual wind speed and generated voltage of the turbine has been used. The look up table values serve as a speed input to the PMSM during simulation. Wind speed varying over a wide range (typically from 1m/s to 30m/s i.e. from low wind to high winds) is selected to test the response of the system controller under cut-in speeds, rated speeds and cut-out wind speeds. While performing simulations in Simulink, as per recommended practice, a small parasitic resistive load (around 2% of the total load capacity of the PMSM) was connected across the synchronous machine block to avoid numerical oscillations. The complete Simulink model of the vertical axis wind turbine of the MWES along with the Tip-Speed Ratio control block is shown in Figure 3.2.

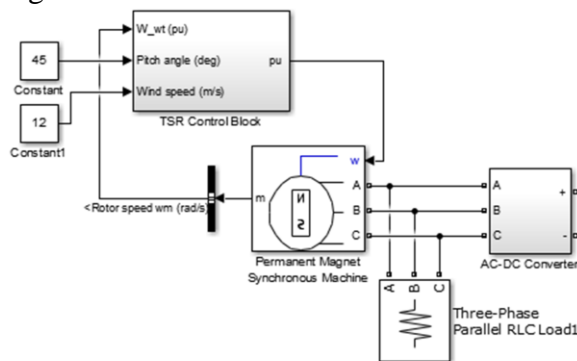


**Figure 3.2** Simulink model of turbine-generator unit with tip-speed ratio control block

The excitation of the synchronous generator remains constant due to the permanent magnet in the field circuit. This makes the control of generator comparatively simpler but does not allow the control of reactive power. With rotor flux remaining fixed due to the permanent magnet arrangement, the PMSM's maximum efficiency is limited to pre-defined rotor speed for a particular wind speed.

Tip-Speed Ratio (TSR) control method is used to track the maximum power point of the permanent magnet synchronous generator which makes use of Equation 2.4. For any wind turbine, the power generated is at its maximum during a particular value of rotor speed called optimum rotor speed ( $\omega_{opt}$ ). The TSR corresponding to the optimum rotor speed is referred as optimum TSR ( $\lambda_{opt}$ ) and it is recommended to operate the wind turbine at this optimum tip speed ratio. By controlling the rotor speed and thereby the tip speed ratio of the wind turbine, maximum power can be extracted from the wind turbine.

For a given wind speed, the synchronous generator generates an induced emf with the synchronous frequency corresponding to the defined number of poles and rotor speed. In other words, the frequency of the emf generated is synchronized with the mechanical rotation of the rotor. A varying wind speed causes the generator speed to vary and in turn the induced emf's frequency varies. Absence of mechanical gears in micro wind turbines requires the usage of static converters which converts the variable frequency ac to dc, and the dc back to ac of fixed 50Hz frequency. These facts are used to frame the requirement of the power converters of MWES and the system controller's functions.

### **3.2 Modeling of ac-dc Converter**

By rectifying the ac voltage of the synchronous generator, the alternating voltage of a particular frequency is converted to a direct voltage which will be later converted to ac voltage. An uncontrolled bridge rectifier, as shown in Figure 3.3, is used to convert the ac voltage to dc voltage. The output dc voltage of the rectifier is expressed as

$$V_{dc} = \frac{3\sqrt{3}}{\pi} V_L \quad (3.6)$$

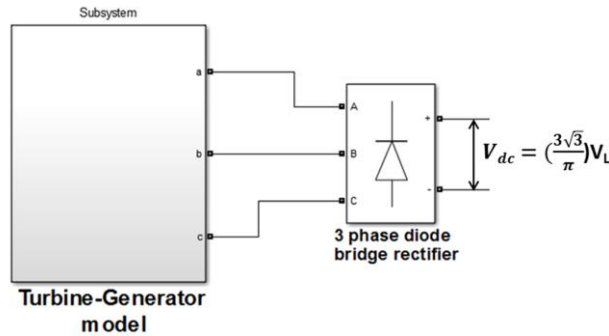


**Figure 3.3** Three phase ac-dc converter

The ripple contents in the output of the ac-dc converter is removed by using a low pass filter. A simple capacitor connected to the output of the rectifier performs the job of the low pass filter and also acts as a dc link capacitor providing the necessary link voltage to the next converter stage. For a ripple content of 5%, load current of approximately 10A, ripple frequency of 1000Hz, the filter capacitor is approximately chosen as 0.2F. The value of the filter capacitor has been calculated using equation 3.7,

$$C = \frac{I_{load}}{f_{ripple} V_{ripple}} \quad (3.7)$$

where  $I_{load}$  is the load current,  $f_{ripple}$  is the ripple frequency and  $V_{ripple}$  is the ripple voltage.

In practical applications, a small filter inductor may also be added to the output of the rectifier to reduce the current ripples and guarantee the safe operation of the capacitor from current surges. In the configuration shown in Figure 3.4 with ac-dc and dc-ac converters, the wind turbine can drive the permanent magnet generator at a frequency independent of the synchronous frequency even though changing the generator speed varies the generator frequency.

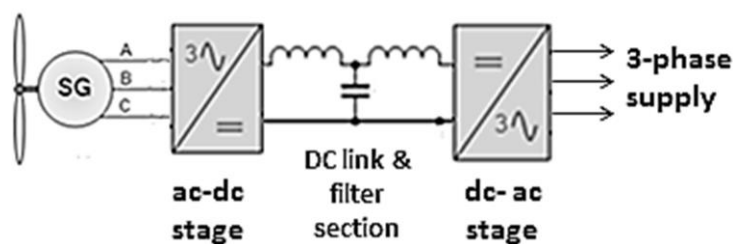


**Figure 3.4** Wind turbine with ac-dc and dc-ac converters

### 3.3 Modeling of dc-ac Inverter

The dc output of the rectifier serves as an input to the inverter stage which follows it. The functions of the dc-ac converter together with the system controller are to convert the dc link voltage to ac voltage of required magnitude and frequency, maintain required phase displacement between each phase and satisfactorily maintain the quality of output power produced. The functions of the system controller like maintaining standard frequency, phase angle and voltage magnitude are implemented using the modulating signal generator block whose operation is discussed elaborately in section 3.8.

Owing to the requirement that MWES has to generate voltage of standard magnitude, it becomes necessary to increase the generators output voltage (which typically is in the sub-hundred voltage range) using appropriate power converter. As mentioned in section 2.3.1, series connected inverter is the best choice to meet this kind of requirement in the micro wind energy system environment. The series connected h-bridges increases the voltage magnitude and reduces the output harmonics. Another important reason to select the series connected topology is that the harmonics cancellation of sideband harmonics is not affected during the over modulation region. Irrelevant of the modulation index similar kind of harmonic benefits can be realized from cascaded bridge configuration. Apart from the other

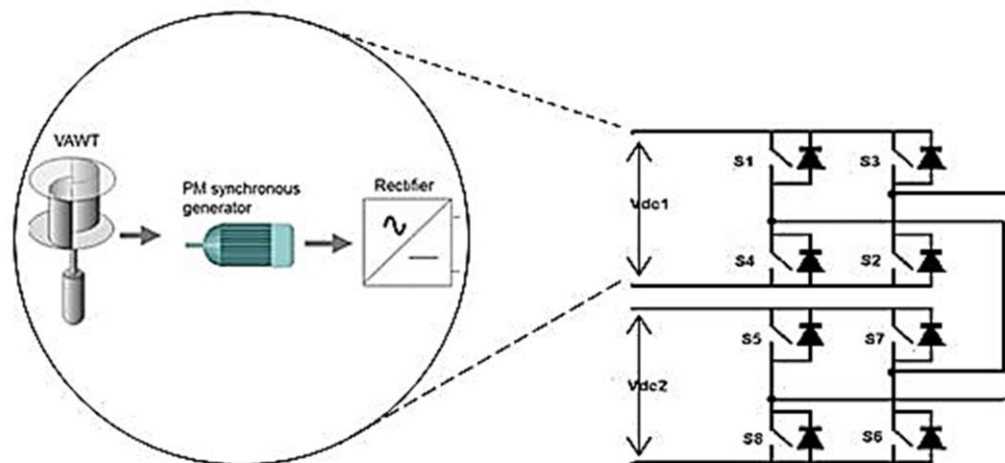


**Figure 3.5** Series connected inverters in MWES

advantages, the modular structure of the series connected inverter also provides a flexible and easy solution for operation and maintenance of the inverter. Also, the

series connected configuration can be scaled to accommodate any number of micro wind turbines in the system. The structure of a series connected inverter used for simulation of MWES is shown in Figure 3.5. The Simulink model of one of the series connected inverters used in the micro wind energy system is shown in Figure 3.6.

The gate signals for the self-commutating semiconductor switches of the inverter

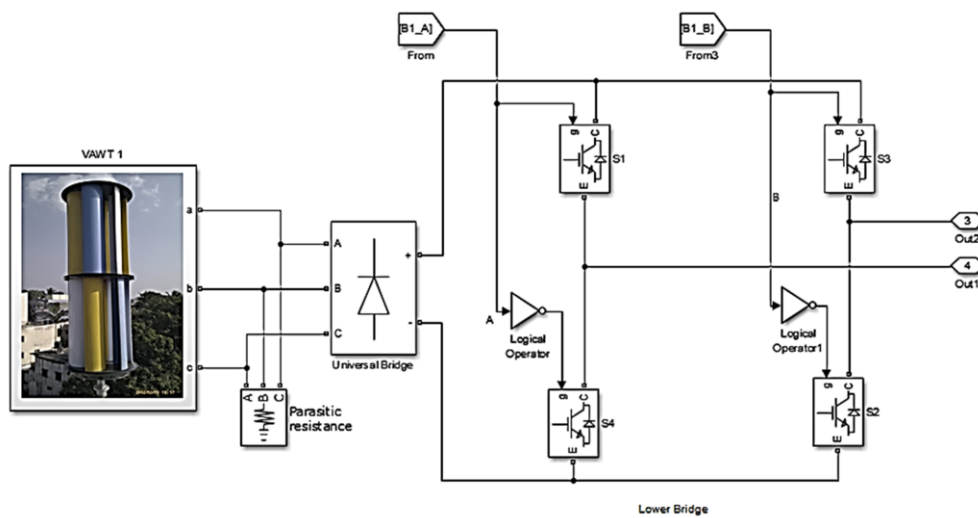


**Figure 3.6** Simulink model of one of the series connected inverters in MWES

can be generated using any of the multilevel inverter modulating techniques discussed in section 2.4.2. Selective harmonic elimination and multicarrier PWM techniques, being the commonly used modulation techniques to control series connected inverters, were considered to begin the simulation study in the micro wind energy system's performance analysis process.

### 3.4 Switching Signal Generation using SHE Technique

This section summarizes the simulation study carried out on the series connected inverters using selective harmonic elimination technique for generation of inverter switching signals. Inverter input conditions related to both, equal and unequal sources was considered during the simulation process.

### 3.4.1 Equal source condition

The series connected inverter shown in Figure 3.8 with equal input source was used for simulation which produces a stepped waveform as shown in Figure 3.7. Any such staircase waveform can be expressed using Fourier series as (Holmes and Lipo 2003),

$$V(\omega t) = \sum_{n=1,3,5,\dots}^{\infty} \frac{4V_{dc}}{\pi} (\cos(n\theta_1) + \cos(n\theta_2) + \dots + \cos(n\theta_S)) \sin(n\omega t) \quad (3.8)$$

where

$V_{dc}$  is the voltage of the dc source,  
 $\theta_1, \theta_2, \theta_3, \dots, \theta_S$  represents the switching angles, and  
 $S$  is the number of dc sources in cascaded h-bridges.

The condition to be satisfied when selecting the optimum switching angles is given by the condition,

$$0 \leq \theta_1 < \theta_2 < \dots < \theta_S \leq \pi/2 \quad (3.9)$$

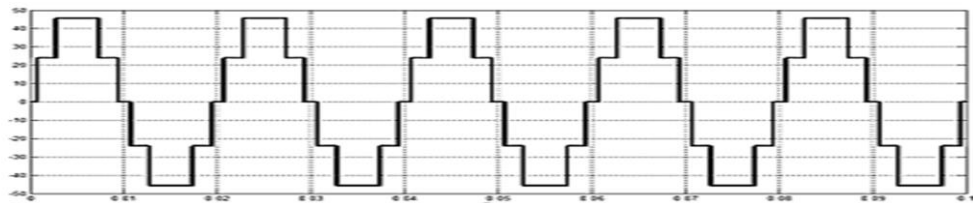


Figure 3.7 A stepped waveform

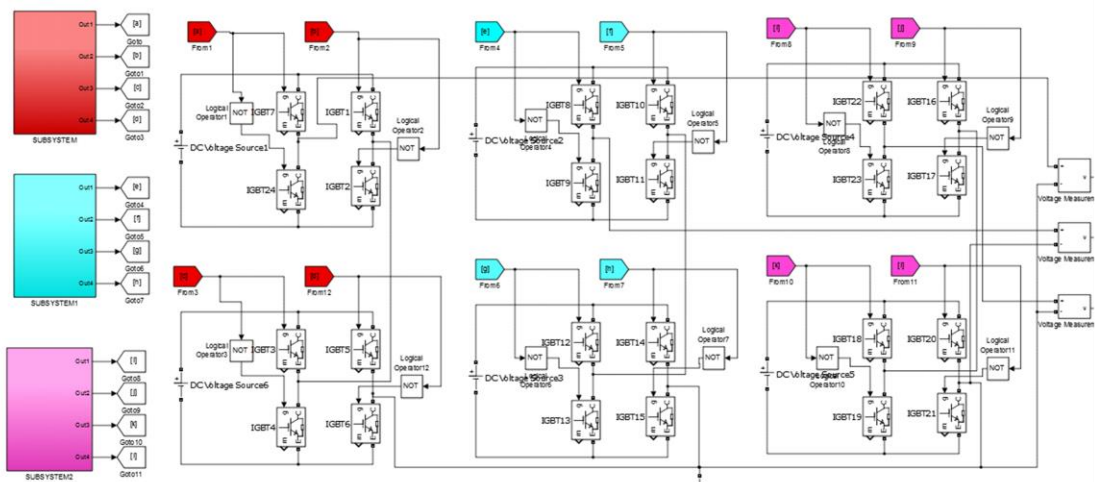


Figure 3.8 Simulink model of a 3-phase, 5-level series connected inverter

The selection of switching angles to control an inverter is based upon the requirement to produce the required magnitude of fundamental voltage ( $V_f$ ) and reduce the distortion in the waveform by eliminating the targeted harmonic components.

The fundamental and  $n^{\text{th}}$  order harmonic components of a stepped waveform generated by a series connected inverter with ‘S’ number of sources can be expressed using transcendental equations 3.10 to 3.13.

$$\left. \begin{aligned} \frac{4V_{dc}}{\pi} [\cos(\theta_1) + \cos(\theta_2) + \dots + \cos(\theta_S)] &= V_f & (3.10) \\ \cos(5\theta_1) + \cos(5\theta_2) + \dots + \cos(5\theta_S) &= 0 & (3.11) \\ \cos(7\theta_1) + \cos(7\theta_2) + \dots + \cos(7\theta_S) &= 0 & (3.12) \\ &\cdot & \\ \cos(n\theta_1) + \cos(n\theta_2) + \dots + \cos(n\theta_S) &= 0 & (3.13) \end{aligned} \right\}$$

The switching angles are selected such that the magnitude of the first order harmonic equals the required fundamental voltage and the higher order harmonic voltages become zero. In order to find the optimum switching angles, the transcendental equations (3.9 to 3.12) need to be solved. Methods like Newton-Raphson method, graphical analysis method, theory of resultants and optimization algorithms can be employed to solve the transcendental equations as described in section 1.2. As the objective of this research work is to identify simple techniques and configurations for a MWES, graphical analysis method has been chosen for solving the transcendental equations as it is comparatively simpler and straight forward. In order to understand the kind of effort one needs to put up for finding the solution of the transcendental equations, the 5<sup>th</sup> harmonic component in the output produced by a 5-level inverter was selected for elimination. The equations considered for finding the solutions are,

$$\cos(\theta_1) + \cos(\theta_2) = \frac{V_f}{4.V_{dc}/\pi} \quad (3.14)$$

$$\cos(5\theta_1) + \cos(5\theta_2) = 0 \quad (3.15)$$



As the first step in finding the optimum value of  $\theta_1$  and  $\theta_2$ , equation 3.14 has been used for plotting the relationship between  $\theta_1$  and  $\theta_2$ . The right-hand side of equation 3.14 refers to the amplitude modulation index ( $m_a$ ) and is expressed as,

$$m_a = \frac{V_f}{4.V_{dc}/\pi} \quad (3.16)$$

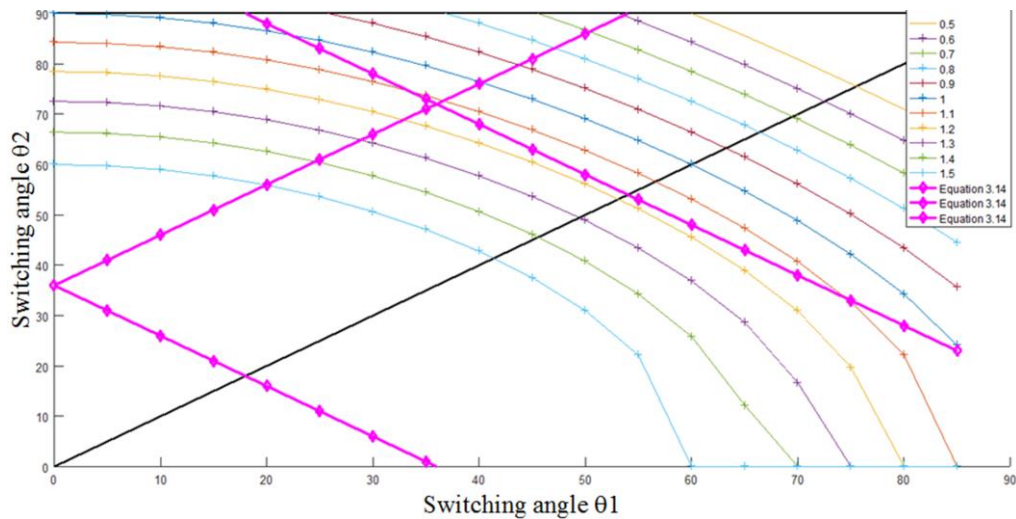


**Figure 3.9** Plot of  $\theta_1$  and  $\theta_2$  under equal voltage conditions using graphical analysis method

For a particular value of modulation index, by varying the value of  $\theta_1$ , the value of  $\theta_2$  is found using equation 3.14. Only those values of  $\theta_1$  and  $\theta_2$  which satisfy the condition mentioned in equation 3.9 has been retained. As the second step, equation 3.15 has been used for plotting the relationship between  $\theta_1$  and  $\theta_2$  using the same procedure. After obtaining all the plots using the above mentioned procedure, the points where the plot of equation 3.14 intersects the plot of equations 3.15 represents the switching angles that can be used to control the multilevel inverter. The resulting plot is shown in Figure 3.9.

Table 3.1 represents the optimum values of  $\theta_1$  and  $\theta_2$  obtained by employing the graphical analysis method. The magnitude of the 5<sup>th</sup> harmonic component which was targeted for elimination is also listed in the tabular column for different modulation indexes.

**Table 3.1** Results obtained through graphical analysis method

Modulation index	$\theta_1$ (degrees)	$\theta_2$ (degrees)	Magnitude of $h_5$ (%)
0.6	54	89	0.3
0.7	50	86	0.0
0.8	47	83	0.1
0.9	45	79	0.0
1.0	40	76	0.0
1.1	33	74	0.3
1.2	33	69	0.0
1.3	29	65	0.0
1.4	24	60	0.9
1.5	19	55	0.0

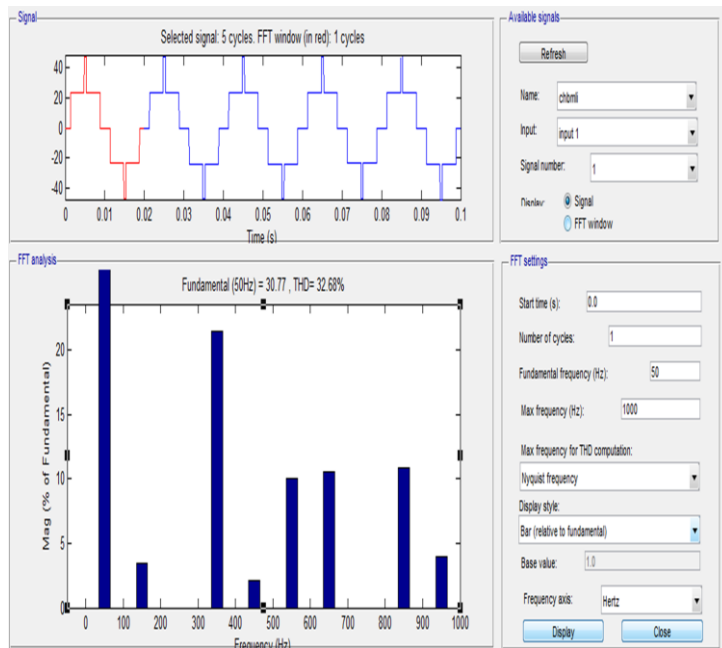


**Figure 3.10** Single phase output voltage of the inverter with FFT analysis when  $m_a = 1.1$

Figure 3.10 shows the inverter output waveform and corresponding FFT analysis for one of the operating conditions.

### 3.4.2 Unequal source condition

In practical cases, the various independent sources of a series connected inverter may not have equal magnitude. Selective harmonic elimination technique can be used to control inverters with unequal sources as well. The procedure described in section 3.4.1 can be repeated after modifying the equation 3.8 as,

$$V(\omega t) = \sum_{n=1,3,5,\dots}^{\infty} \frac{4V_{dc}}{n\pi} (V_1 \cos(n\theta_1) + V_2 \cos(n\theta_2) + \dots + V_S \cos(n\theta_S)) \sin(n\omega t) \quad (3.17)$$

where  $S$  is the number of dc sources and  $V_1, V_2, \dots, V_S$  are the voltage magnitude of the individual sources in per unit.

Equations 3.14 and 3.15 are used to eliminate 5<sup>th</sup> harmonic component at the output of a 5-level inverter, under unequal source conditions.

$$V_1 \cos(\theta_1) + V_2 \cos(\theta_2) = \frac{V_f}{4.V_{dc}/\pi} \quad (3.18)$$

$$V_1 \cos(5\theta_1) + V_2 \cos(5\theta_2) = 0 \quad (3.19)$$

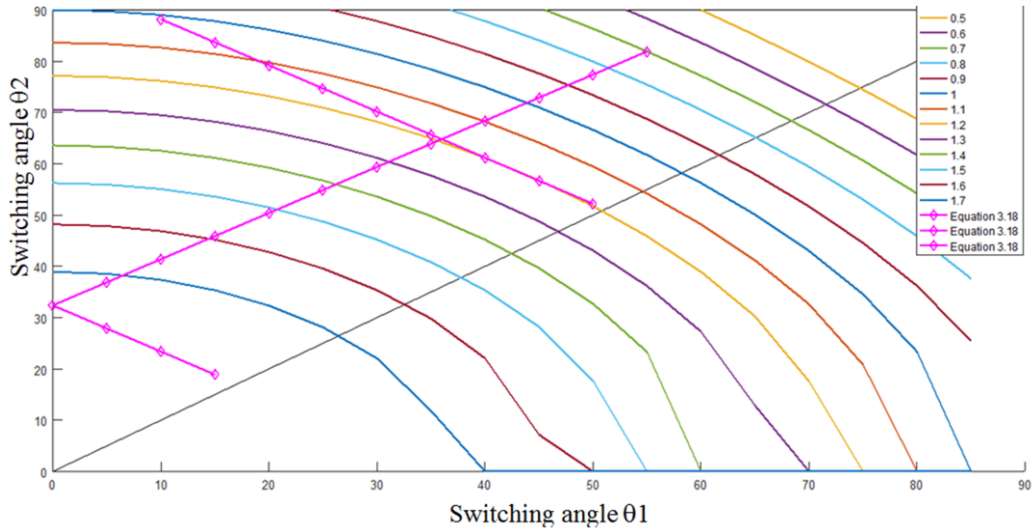


**Figure 3.11** Plot of  $\theta_1$  and  $\theta_2$  under unequal voltage conditions using graphical analysis method

The plot obtained by following the procedure described in section 3.4.1, using equations 3.14 and 3.15 for different modulation indexes, is shown in Figure 3.11. Table 3.2 represents the optimum values of  $\theta_1$  and  $\theta_2$  obtained by employing the graphical analysis method under unequal source conditions. The magnitude of the 5<sup>th</sup> harmonic component is also listed in the tabular column for different modulation indexes.

**Table 3.2** Results for inverter with non-equal dc sources ( $V_1=1$ ,  $V_2=0.9$ )

<b>Modulation index</b>	<b><math>\theta_1</math> (degrees)</b>	<b><math>\theta_2</math> (degrees)</b>	<b>Magnitude of h5 (%)</b>
0.7	50	85	1.1
0.8	47	80	3.6
1.0	44	78	0.7
1.1	22	85	0.6
1.2	30	75	0.1
1.3	30	68	0.1
1.4	22	58	0.4
1.5	17	53	0.1

### 3.4.3 Usage of computation tools for solving SHE equations

Computing tools like Mathematica can be used to calculate the solutions of the transcendental equations formed as a part of selective harmonic elimination process. But finding apt solution will require extra effort as the switching angles obtained should satisfy the condition specified in equation 3.8. Also, whenever new set of transcendental equations are required due to change in the inverter input conditions, new set of optimum switching angles need to be determined. These issues restrict the use of computing tools.

With relation to the discussion in section 3.4, it can be summarized that controlling a series connected inverter using the switching angles computed by selective harmonic elimination technique involves considerable amount of effort. Even though the targeted harmonic components are eliminated, the total harmonic distortion remains considerably high as it is dependent on other dominant harmonics too. Formulating more transcendental equations to describe other harmonic components and finding the optimal solution will require much more effort. Also, new set of switching angles need to be computed when the input conditions (magnitude of the input dc sources) change. These facts compromise on one of the main research objectives which require the control algorithm to be simple.

### 3.5 Switching Signal Generation using Multicarrier Modulation Techniques

As an alternative of using selective harmonic elimination technique for analyzing the complexity and effectiveness of control strategies in controlling the MWES, various multicarrier PWM techniques were also used during simulation. Phase Disposition, Phase Opposition Disposition, Alternative Phase Opposition Disposition were among those used for the simulation experiments. The switching signals generated using these multicarrier modulation techniques are presented in Figures 3.12 to 3.14.

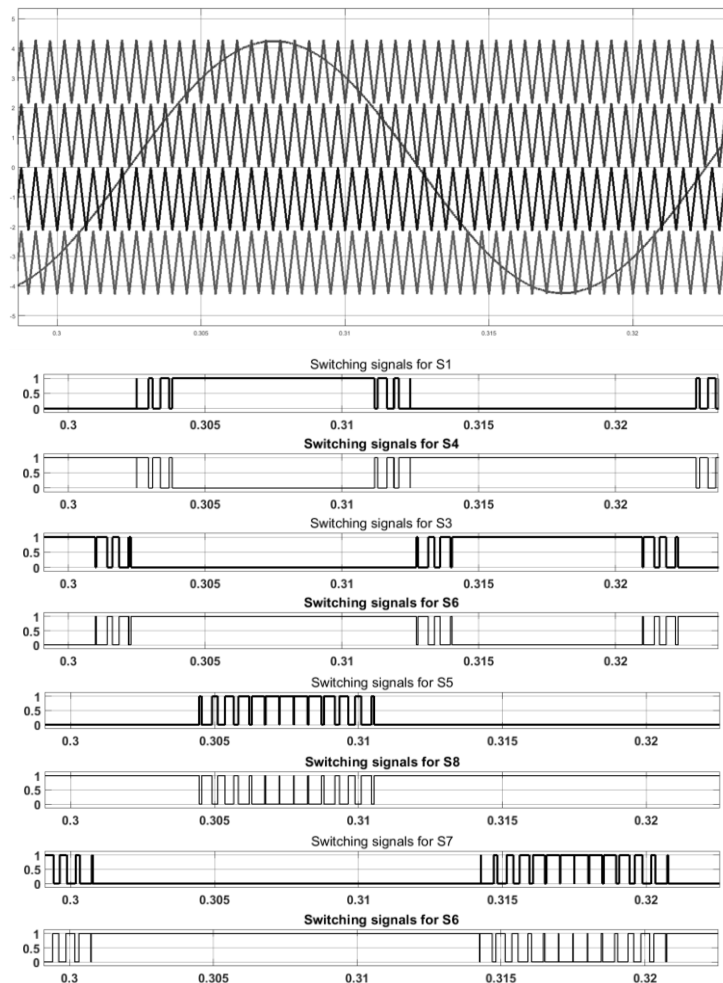


**Figure 3.12** Simulation waveforms - Phase Disposition (PD) (a) Carrier and references waves (b) Generated switching signals for switches S5, S8, S7, S6, S1, S4, S3 and S2

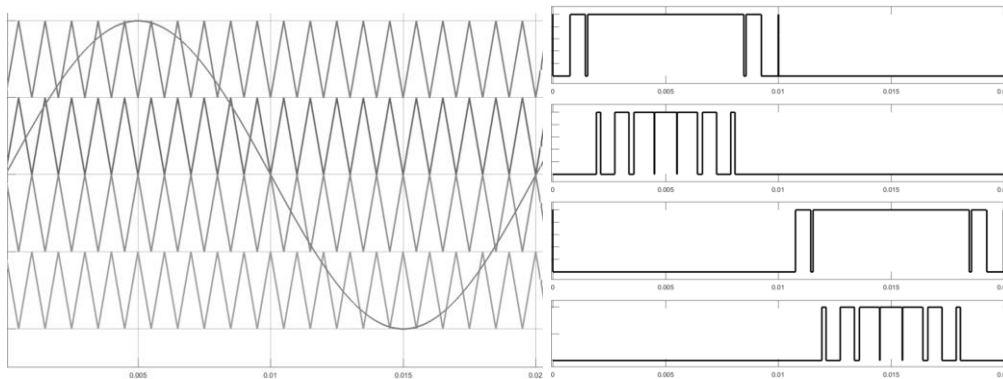


**Figure 3.13** Simulation waveforms - Phase Opposition Disposition (POD)  
 (a) Carrier and references waves (b) Generated switching signals  
 (uncomplemented) for switch S5, S1, S7 and S3

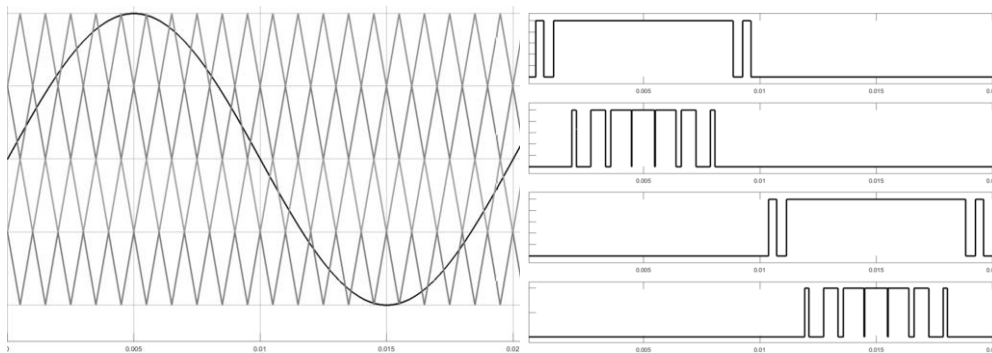


**Figure 3.14** Simulation waveforms - Alternative Phase Opposition  
 Disposition (APOD) (a) Carrier and references waves (b) Generated switching  
 signals (uncomplemented) for switch S5, S1, S7 and S3

Elaborate discussion about the performance analysis of the micro wind energy system using the multicarrier PWM waveform is presented in the chapter 4. One significant inference can be derived from the study of various multicarrier modulation techniques i.e. in the process of generating required switching signals, the number of carrier waveforms increase as the number of inverter levels increase (an  $m$ -level inverter requires  $(m-1)$  carrier waveforms). These carrier waves are to be level shifted (or phase shifted) which means, during implementation, generation of each carrier wave should be done separately. When a stored program computer is used in the control process, this will considerably increase the complexity of the control program and require more processor memory.

On studying the multilevel inverter switching signals, it was observed that the pulse width modulated signals are supplied to various inverters of the series connected inverter only during certain time duration in a cycle and rest of the time either a high or low signal is supplied. For example, observing the switching signals depicted in Figure 3.15, it can be noted that signal in Figure 3.15(a) is used to control lower h-bridge switch S5 and the signal in Figure 3.15(b) is used to control upper h-bridge switch S1, during the positive cycle of the modulating signal.

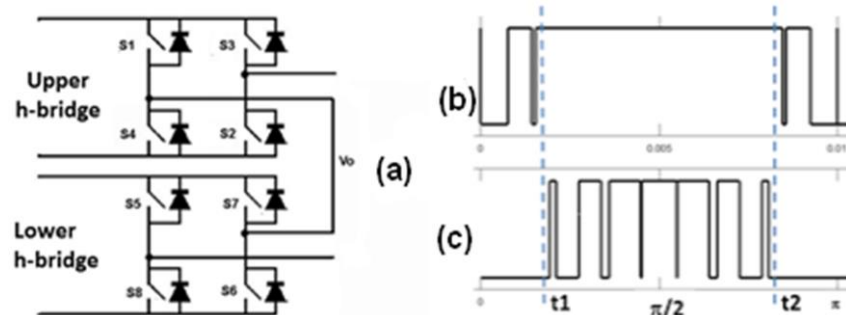


**Figure 3.15** (a) A 5-level inverter. Sample switching signals for (b) lower h-bridge switch S5, (c) Switching signals for upper h-bridge switch S1, during positive half cycle of modulating sine wave.

In Figure 3.15(a), from time instant  $t_1$  to  $t_2$ , logic high signal is continuously applied to the switches S5. Similarly, Figure 3.15(b), from instant  $0$  to  $t_1$  and from  $t_2$  to  $\pi$ , logic low signal is applied continuously to S1. Rest of the time, pulsed width modulated switching signals is applied to the respective switches.

An inference was derived by studying the switching signals of series connected inverters i.e. if a single switching signal generated using a single carrier wave can be time multiplexed to produce several sets of switching signals, then several inverters can be controlled. This idea simplifies the switching signal generation process for controlling any level of multilevel inverters. The idea has been elaborately discussed in the next section along with a simple way to implementing the switching signal generation network.

### 3.6 Switching Signal Generation by using a Novel Switching Network

In this section, a novel switching signal generation process to control multilevel inverters has been discussed. The idea presented at the end of section 3.5 has been used to frame the structure of the novel switching signal generation network, which in turn can be used to control any multilevel inverter. Based upon the operation performed, the network is termed in this thesis as comparator based switching signal selection network (CSSSN). In its simplest form, the network consists of a set of comparators which compares the instantaneous magnitude of the modulating (reference) signal  $V_{ref}(i)$  with *predefined threshold values*. The result of comparison is used to decide whether to send a PWM signal or Logic HIGH/LOW signal to the gate terminal of the power switch in each inverter.

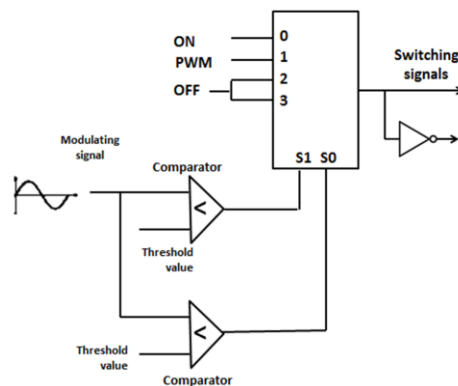


**Figure 3.16** (a) Proposed Comparator based Switching Signal Selection Network (CSSSN) logic (b) Switching signals produced by CSSSN and the reference signal

In order to decide the criteria for selecting the threshold value(s), a simple analysis has been performed. Let's consider one half of the modulating (reference) sinusoidal waveform described by the function  $V_{ref}(i) = V_{ref}(p) \sin(\omega t)$ , as shown in Figure 3.17.

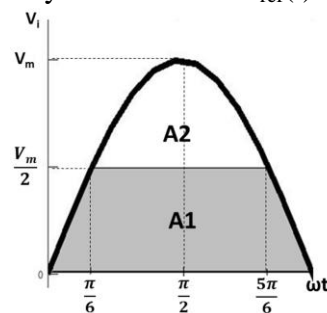


**Figure 3.17** Positive half of a typical sinusoidal waveform



The sinusoidal waveform will reach half of its peak magnitude at  $\pi/6$  rad ( $30^\circ$ ) which means much of the total area of the waveform (and thereby much of the total power) will be covered by the waveform within  $(1/6)^{\text{th}}$  of the total time. This can also be confirmed analytically. Let the area covered by the shaded portion of the waveform in Figure 3.17 (below the half-peak point) be A1 and un-shaded portion (above half-peak point) be A2. The total area covered by the sinusoidal waveform in Figure 3.17 (with peak magnitude  $V_{\text{ref}(p)}=1$ ) is,

$$\begin{aligned} A &= A1+A2 = \int_0^\pi \sin(\omega t) d(\omega t) & (3.20) \\ &= 2 \text{ units} \end{aligned}$$

When the instantaneous value of the waveform is 0.5 (when  $V_{\text{ref}(p)}=1$ ),

$$\text{i.e. } V_{\text{ref}(i)} = \sin(\omega t) = 0.5 \text{ unit}$$

the value of ' $\omega t$ ' is either  $\pi/6$  or  $5\pi/6$ .

Using equal area criterion (Grainger and Stevenson 1994), the area covered by the un-shaded portion is found using the following expression,

$$\begin{aligned} A2 &= \int_{\pi/6}^{5\pi/6} [\sin(\omega t) - 0.5] d(\omega t) & (3.21) \\ &= 0.67 \text{ unit} \end{aligned}$$

which indicates that the area of the un-shaded portion covers about 33.5% of the total area (A). The area covered by shaded portion is found out as,

$$\begin{aligned} A1 &= A - A2 \\ &= 1.33 \text{ unit} \end{aligned}$$

which is 66.5% of the total area (A).

The above computations indicate that major area of the waveform is covered by the time the instantaneous value of waveform reaches half the maximum value (i.e.  $V_{\text{ref}(p)}/2$ ). So, for a CSSS network controlling a five level series connected inverter, the ideal threshold level to maximize the output rms value will be

$(V_{\text{ref}}(p)/2)$  during the positive cycle of the modulating signal and  $(V_{\text{ref}}(p)/2)$  during the negative cycle. In a similar manner, the threshold values can be determined for different levels of inverters.

A five level inverter like the one shown in Figure 3.15(c) will require one threshold value of  $V_{\text{ref}}(p)/2$  during the positive half cycle of the reference wave and another threshold of  $-V_{\text{ref}}(p)/2$  during the negative half cycle. This five-level series connected inverter requires two sets of switching signals for driving the two h-bridge inverters (upper and lower h-bridges). Any of the available two level inverter modulating techniques can be chosen to generate a PWM signal. The CSSS network constantly monitors the magnitude of the modulating signal. Based on the comparison of the modulator's magnitude with the threshold values (i.e.  $V_{\text{ref}}(p)/2$ ), appropriate switching signals are sent to various h-bridge inverters.

During the positive cycle ( $0 < \omega t < \pi$ ) of the modulating signal shown in Figure 3.16(b), the switching signal generation network shown in Figure 3.16(a) functions in the following manner:

(i) Driving lower bridge inverter switches (S5,S6): The PWM switching signal is channeled to drive the inverter switch S5 for the entire time duration when the instantaneous value of the modulating signal is less than the threshold limit( $V_{\text{ref}}(p)/2$ ), which is half the peak value of the reference wave. As long as the condition in (3.22) is satisfied, the inverter switch S5 receives the PWM switching signals.

$$0 < V_{\text{ref}}(i) < V_{\text{ref}}(p)/2 \quad (3.22)$$

where  $V_{\text{ref}}(i)$  is the instantaneous value of the modulating signal and  $V_{\text{ref}}(p)$  is the peak value of the modulating signal. Beyond this time duration, logic high signal is applied to switch S5 until the condition becomes TRUE again, during the rest of the positive cycle. Switch S6 is kept continuously on during the entire positive cycle.

(ii) Driving upper bridge inverter switches (S1, S2): In this case, the PWM switching signals are channeled to drive the switch S1 for a time duration when the condition in (3.23) is satisfied.

$$V_{\text{ref}(p)}/2 < V_{\text{ref}(i)} < V_{\text{ref}(p)} \quad (3.23)$$

Switch S1 is turned off for the rest of the time duration during the positive and negative half cycle of the reference signal. Switch S2 is kept on continuously during the entire positive cycle.

In general, the number of threshold values ( $N_T$ ) required to generate switching signals for an m-level inverter can be determined using the relation,

$$N_T = m - 3 \quad (3.24)$$

where ‘m’ is the number of levels in inverter output.

In the case of a five level inverter, two threshold values are required for comparison during the positive cycle and negative cycle (i.e.  $N_T = 5 - 3 = 2$ ). The peak magnitude of the modulating is divided by  $N_T$  to determine the threshold values in the positive cycle and negative cycle of the modulating signal. For a five level inverter, the threshold value is  $(+V_{\text{ref}(p)}/2)$  and  $(-V_{\text{ref}(p)}/2)$ . Every additional inverter unit in the series connected inverter will require an additional comparator along with the two additional threshold values. The complete switching network along with switch table is shown in Figure 3.18.

The discussed method can be extended to produce switching signals for any levels of inverters. By setting up appropriate number of comparator threshold limits, the PWM signal (in this case, SPWM signals) can be channeled to different inverter bridges at appropriate instances.

Based upon the procedure discussed in this section, a generalized algorithm has been described below, for implementing the CSSS network concept using stored program computers.

For the time duration of  $(0 < \omega t < \pi/2)$ :

**Step-1:** Read ‘m’ (number of output levels of the inverter)

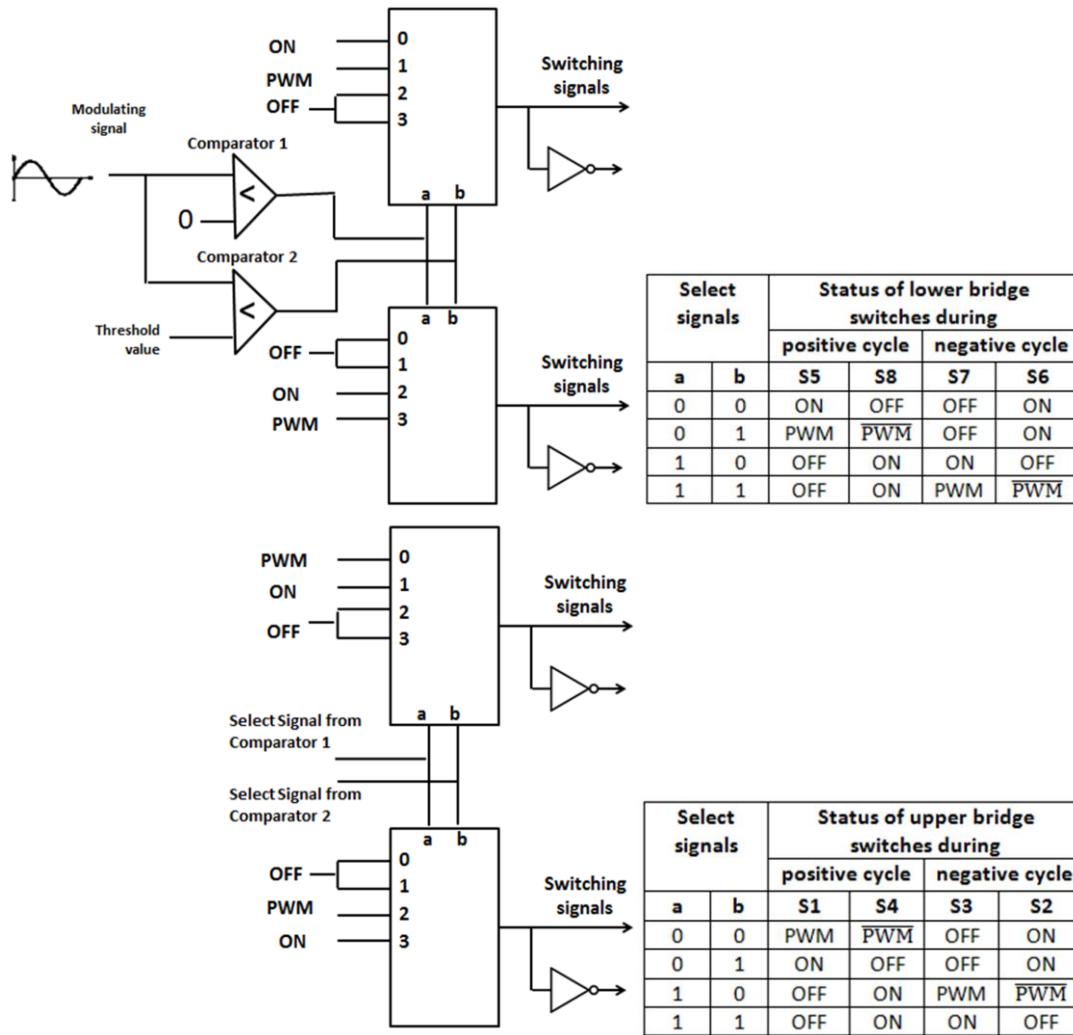


**Figure 3.18** : CSSSN logic to generate switching signals for a 5-level series connected inverter with eight switches

**Step-2:** Compute  $d = (m - 1)/2$

**Step-3:** Compute  $x = d - 1$

**Step-4:** For  $j = 0 : 1 : x$

- i. Read instantaneous value of the reference signal  $V_{ref}(i)$
- ii. If  $[(V_{ref}(p)/d)*j] < V_{ref}(i) < (V_{ref}(p)/d)*(j+1)$ 
  - a. then apply the modulated gate switching signals to inverter bridge 'j'(lower most bridge is bridge '0')
  - b. wait until  $[V_{ref}(i) < ((V_{ref}(p)/d)*(j+1))]$

**Step-5:** When an upper bridge is fed with switching signals, appropriate switches of all lower bridges are kept continuously ON.

In a MWES under practical conditions, the magnitude of voltage produced by the wind turbine generator and thereby the dc voltage produced by the rectifier circuit seldom remains equal. When the dc sources differ in magnitude, the rms value and THD of the output waveform is affected. Changing the position of the inverter bridges will considerably offset this issue. Since physically changing the position of the inverter bridge during the inverter operation is not a feasible solution, the switching signals can be manipulated accordingly to virtually realize the change in position of the inverter bridges. The logic network which does this function is referred as extended CSSS network in this thesis and has been elaborately discussed in the next chapter.

### 3.7 Modeling of Wind Turbine Braking Mechanism

As a safety mechanism every wind turbine has a dump load connected to it which is made use of when the power generated by the turbine is more than what the load can absorb. The dumb load also serves for other purposes like a) to shut down the turbine by stalling the rotor during very high wind speeds b) to limit the turbine speed when required c) to control the output impedance of the turbine and thereby control the maximum power extracted by the turbine.

The converter which helps in realizing this safety mechanism in its simplest form looks like the one shown in Figure 3.19. The duty ratio of the safety switch ( $S_S$ ) is

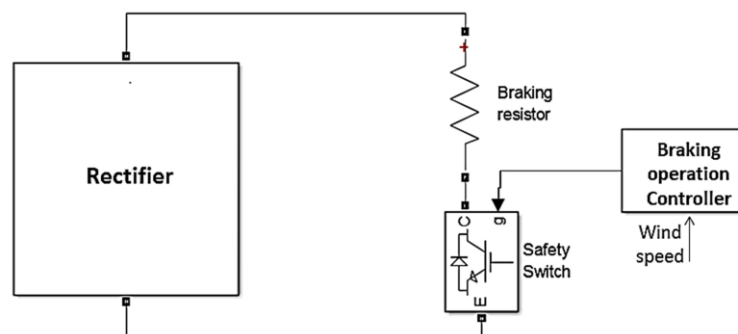


**Figure 3.19** Wind turbine braking mechanism

controlled based upon the wind speed. The wind speed is usually measured using anemometer in case where direct measurement is used. Few methods suggest the use of indirect measurement methods like sensing the output voltage of the rectifier. The later methods remove the cost involved in installation of anemometer but require a proper control algorithm to process the dc link voltage and thereby correlate it with the speed.

### 3.8 Modeling of Reference Signal Generator

The main task for the reference signal generator block is to generate a reference (modulating) signal for proper operation of the inverter. A phase locked loop (PLL) has been used to correct the phase displacement and frequency of the

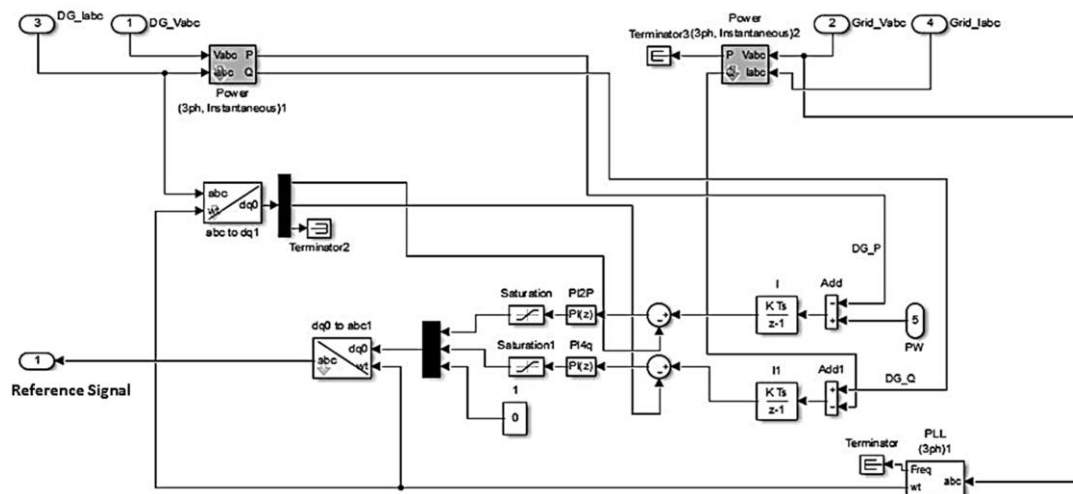


Figure 3.20 Reference signal generator model

generated reference signal. The input for the PLL block may be derived from the grid voltage if the generated input voltage needs to be synchronized with the grid voltage. Alternatively, to operate the MWES in stand-alone mode, the PLL input may be a derived from programmed three phase sinusoidal waveform source with required frequency and phase displacement. The operation of the reference signal generator is also based on the reference frame theory which converts the variables involved back and forth between rotating reference frame variables and stationary reference frame variable. The reference signal generator model used in the simulation of MWES is shown Figure 3.20.

### **3.9 Summary**

This chapter dealt with the modeling of various components/blocks of the micro wind energy system. The discussions related to some of the preliminary simulation studies carried out during the research work have also been presented. From these studies, a new switching network has been formulated to generate series connected inverter switching signals which is simple, flexible and scalable. The performance of MWES controlled by using CSSS network and various multicarrier modulation techniques has been compared and analyzed in the next chapter.

Chapter 4  
Performance  
Analysis of  
Micro Wind Energy  
Systems



#### **4. PERFORMANCE ANALYSIS OF THE MICRO WIND ENERGY SYSTEM**

In order to understand the effect of employing the CSSS network in a micro wind energy system, a simulation study has been performed which is presented in this chapter. The MWES model used for simulation is shown in Figure 4.1. The configuration was tested with different kinds of modulation schemes, with and without the proposed comparators based switching signal selection network (CSSSN). The MWES configuration used for analysis has a set of permanent magnet synchronous machine (PMSM) based micro wind turbines, diode rectifiers and series connected inverter among other protective and control components. The modulation techniques used to control the series connected inverter includes various multicarrier PWM techniques and the proposed CSSS network with single carrier SPWM and delta modulation technique. Series connected inverter conditions related to both, equal sources and un-equal sources, have been covered in the analysis. The performance of the system has been analyzed by observing performance parameters like the output voltage, output current, the total harmonic distortion of current and voltage waveforms, individual harmonic components of the output voltage and current waveforms. The outcome of the analysis and the inferences derived from the analysis has been discussed in this chapter.

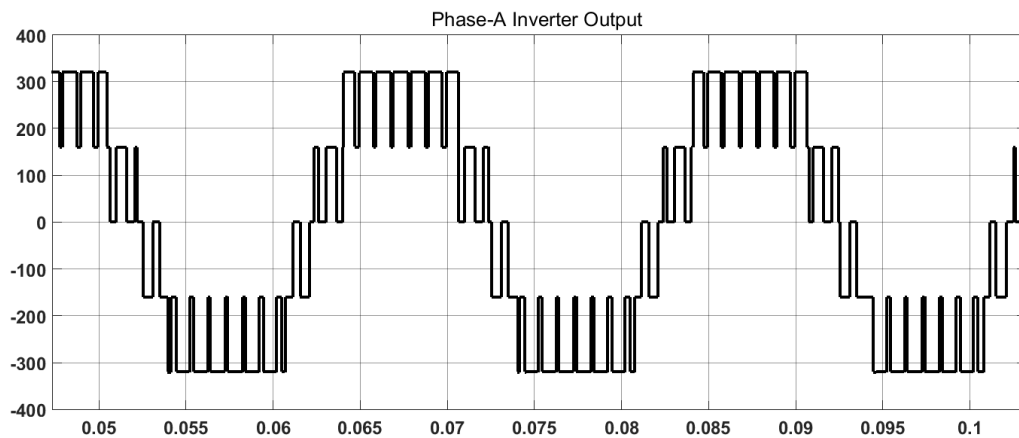
The system which has been simulated consists of a vertical axis wind turbine of 1kW for every inverter level on the source side. The wind speed was assumed constant (12m/s) for all the simulation run . A reactive element with  $X_L=0.5R$  was used as a load to the MWES. Various test cases were considered and the MWES model was simulated to cover a wide range of operating conditions. The amplitude modulation index ( $m_a$ ) was varied from 0.7 to 1.3 to cover both the under-modulated and over-modulated conditions. The frequency modulation index ( $f_c/f_m$ ) was varied from 10 to 360 to analyze the performance of the inverters during low and high switching frequency. As the number of test cases used for simulation study and analysis is more, test scripts were used to automate the test process and to record the results. The results were later plotted using OriginPro and analyzed. Three phase series connected inverter configurations used in the analysis of



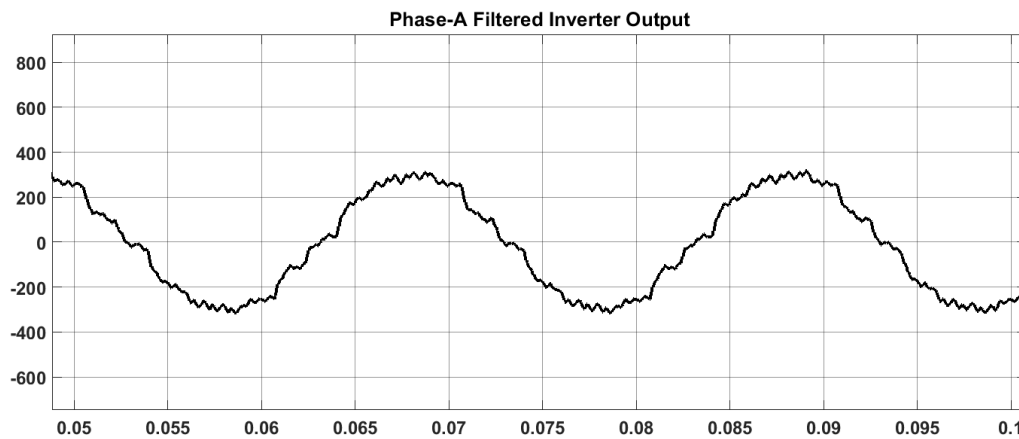
MWES include 5-level and 7-level inverters. The analysis and inferences derived from the results are presented in the following sections.

#### 4.1 MWES Inverters with Equal Sources

The five level inverters and seven level inverters in the micro wind energy system were initially simulated with input sources of equal magnitudes. The modulation schemes used for generation of switching signals during simulation includes phase disposition, phase opposition disposition, alternate phase opposition disposition



(a)



(b)

**Figure 4.2** (a) Output voltage (phase-line) waveform of a 5-level inverter in MWES, (b) Filtered inverter output

and conventional SPWM with the proposed CSSS network. The output voltage waveforms of the MWES (with five level inverter) during one of the test conditions are shown in Figure 4.2. The obtained output waveforms were analyzed

for its rms value, distortion and k-factor. The values of all the parameters' under different test conditions were plotted. The operating points so plotted were fitted using linear fit only to approximately determine the range within which the performance parameters vary under different test conditions.

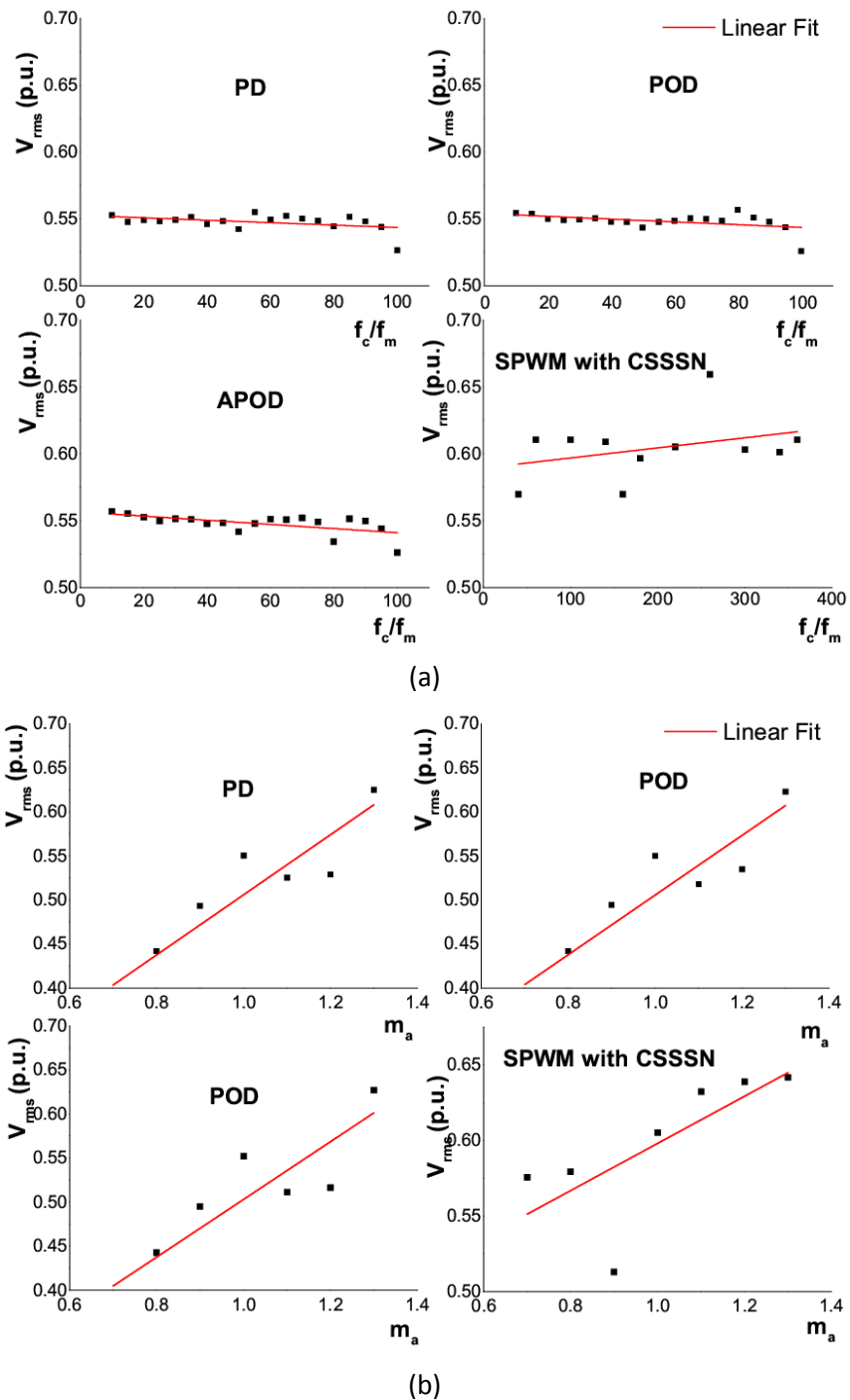
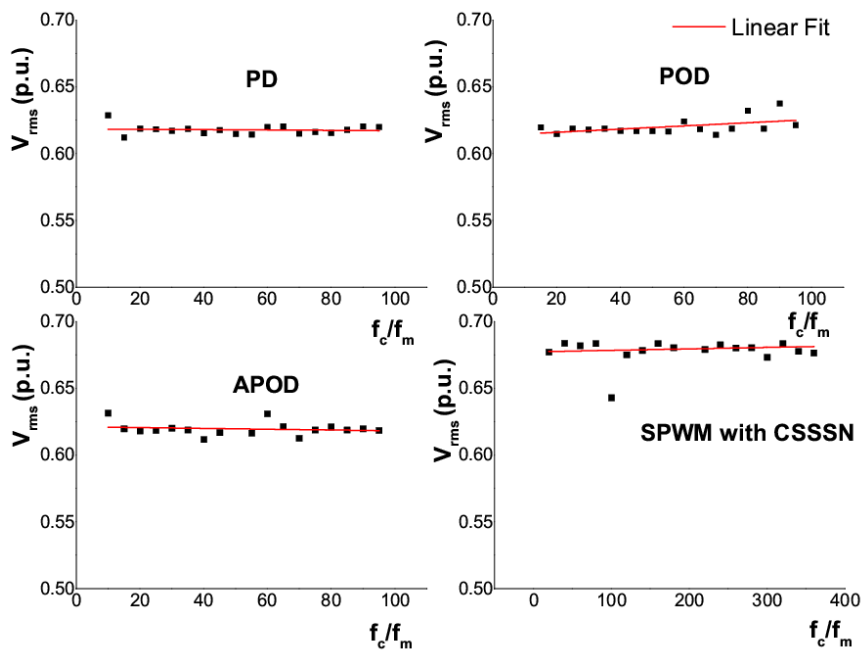


**Figure 4.3** Variation of rms value of output voltage with variation of (a)  $f_c/f_m$ , (b)  $m_a$ , for MWES with 5-level inverter

The plots of the rms value of the output voltage waveform during different amplitude modulation indexes and frequency modulation indexes are shown in Figure 4.3. It can be observed from the plots, in Figure 4.3, obtained using the above mentioned modulation schemes that the rms value of the output waveform is significantly improved in the MWES configuration employing the CSSS network. When the frequency modulation ratio is varied, the improvement in rms value is around a significant 5% over wide switching frequency ranges. Similar kind of improvement can be observed when amplitude modulation index is varied. The rms value of the output voltage is considerably better even during under-modulation region which may be considered as a significant outcome of using the CSSS network in controlling the series connected inverter. These results validate the mathematical analysis presented in section 3.6 and also justifies the selection of  $(V_m/2)$  as the CSSS network's threshold value for a five level inverter.

When a 7-level inverter was used in the MWES, similar improvements were observed. These results are shown in the plots of Figure 4.4.



(a)

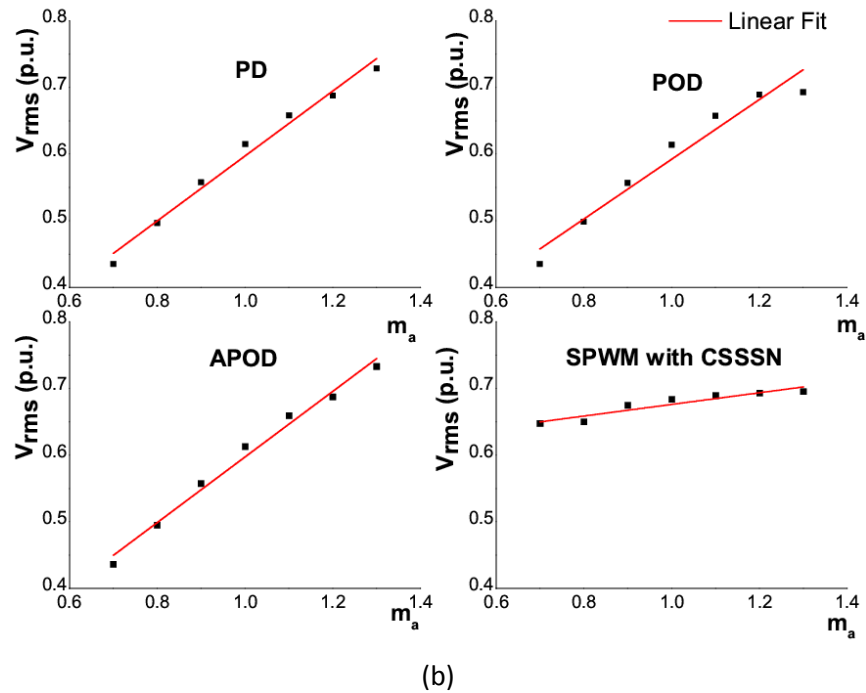
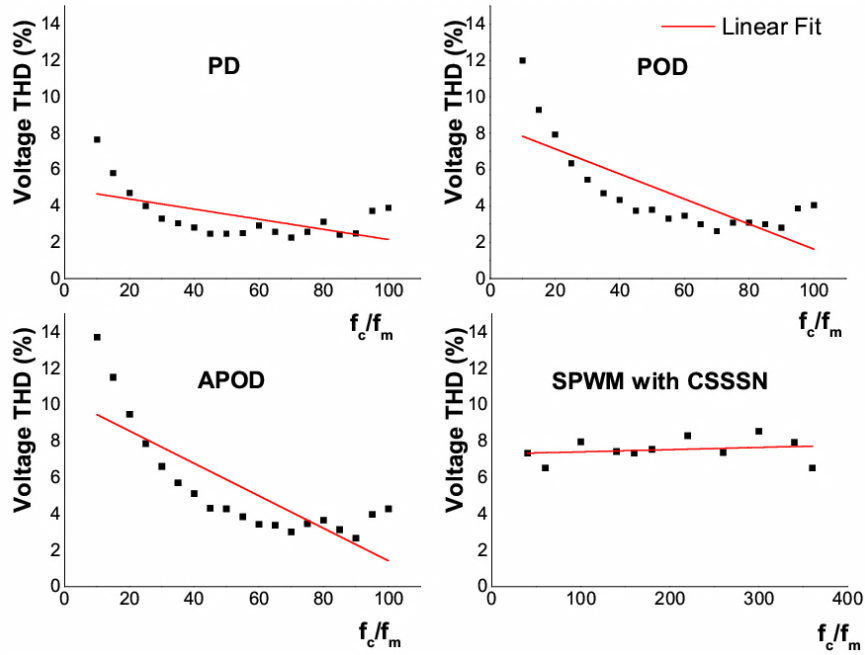


**Figure 4.4** Variation of rms value of output voltage with variation of (a)  $f_c/f_m$ , (b)  $m_a$ , for MWES with 7-level inverter

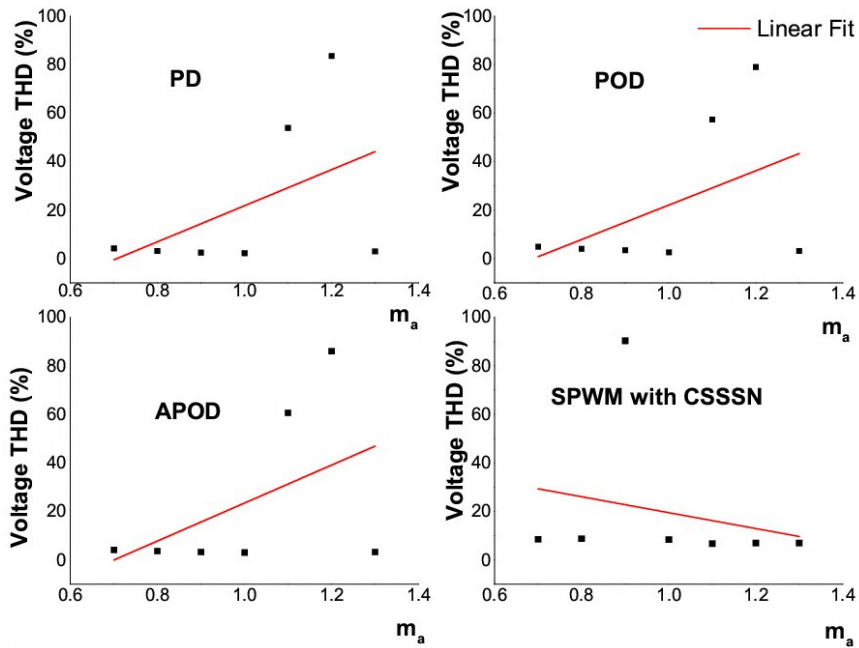
The plots of the voltage THD values with respect to variation in amplitude modulation index and frequency modulation index, for five level and seven level inverters, are shown in Figure 4.5 and Figure 4.6. When the series connected inverter is controlled using modulation schemes like PD, POD and APOD, and when the frequency modulation ratio is varied, it can be observed from Figure 4.5(a) that the THD in the output voltage is high during low switching frequencies. Also, it can be noted that the THD value reduces when the switching frequency is increased. Whereas, when CSSS network is employed, the THD values are almost constant during both low switching frequencies and high switching frequencies. The plots shown in Figure 4.5(b) indicate that the THD performance of the series connected inverter with CSSS network is almost constant, in both under-modulation and over-modulation region. Without the CSSS network, the inverter produces higher THD in the over-modulation region.

These plots of Figure 4.5 gives the inference that the series connected inverter with CSSS network can provide a stable performance, in terms of THD, for wide range of switching frequencies and modulation indexes. Similar kind of inference can be

derived from the plots of Figure 4.6, which shows the results of MWES with 7-level inverter.

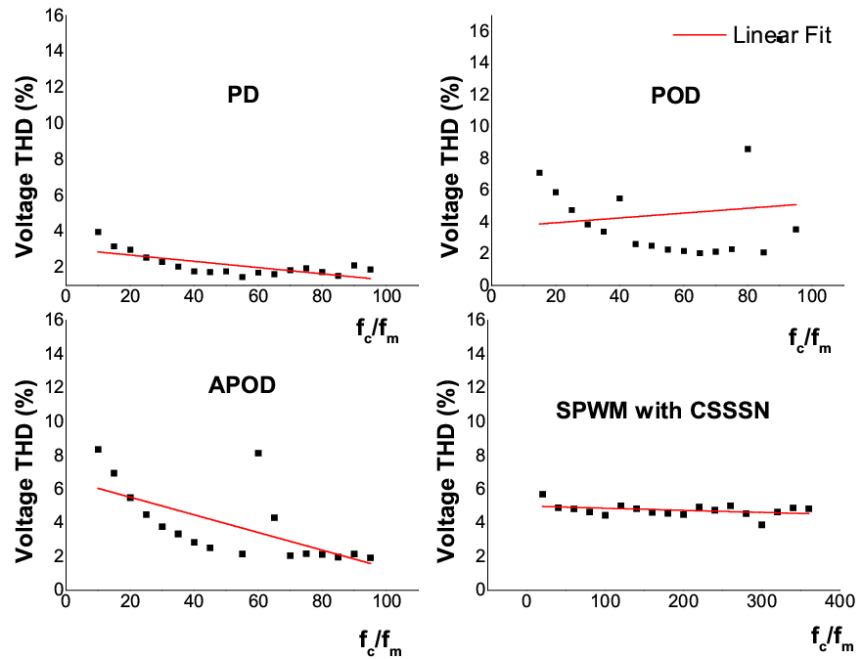


(a)

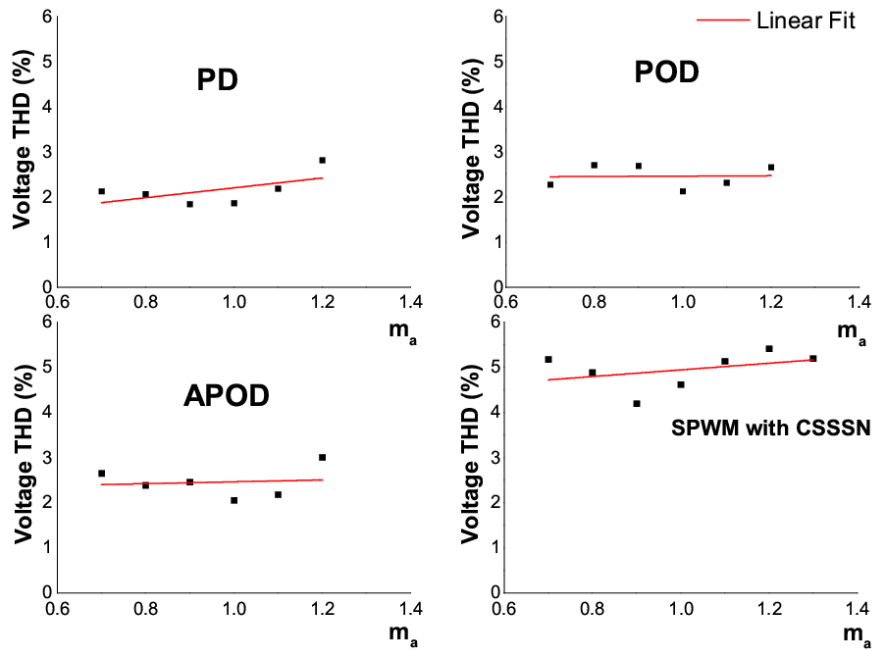


(b)

**Figure 4.5** Variation of voltage THD with variation of (a)  $f_c/f_m$ , (b)  $m_a$ , for MWES with 5-level inverter



(a)



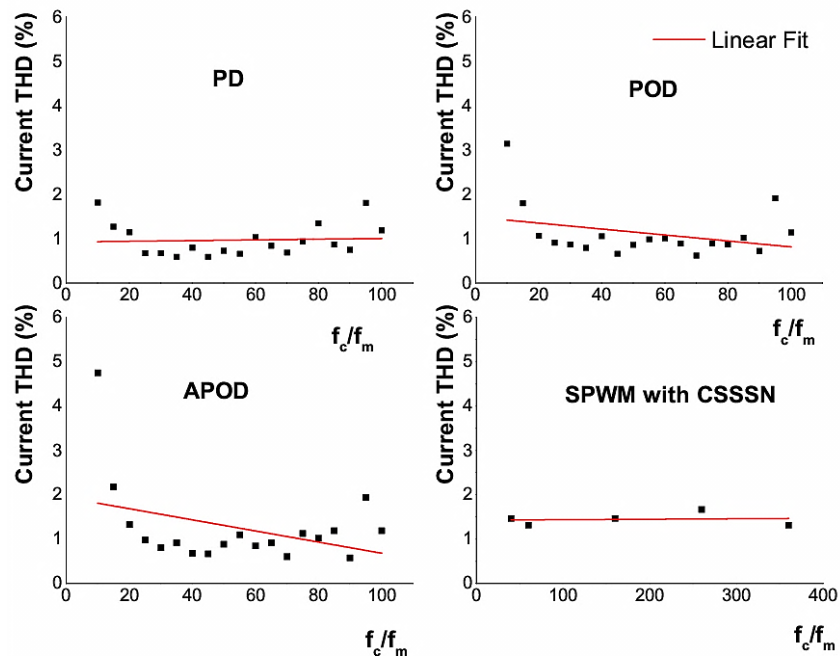
(b)

**Figure 4.6** Variation of voltage THD with variation of (a)  $f_c/f_m$  (b)  $m_a$ , for MWES with 7-level inverter

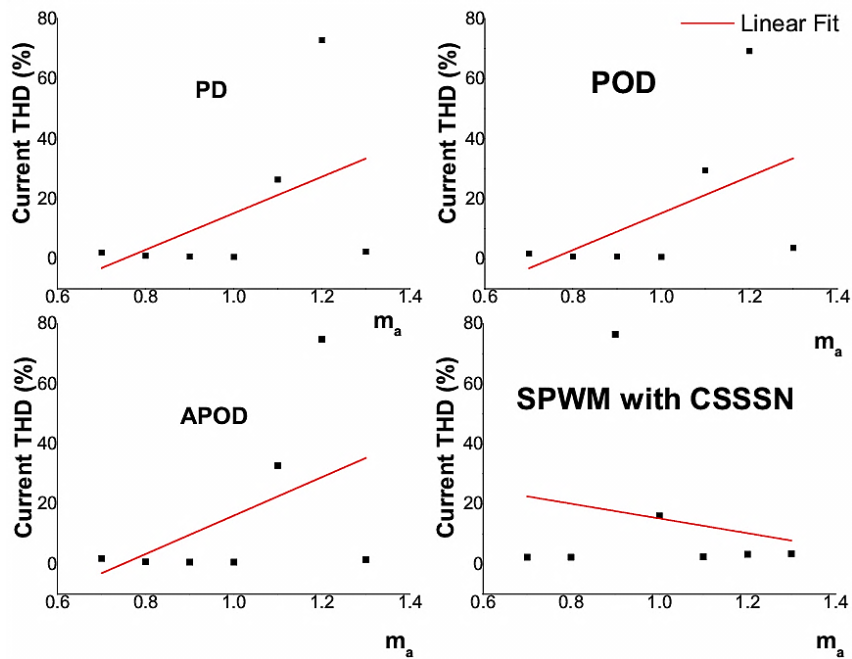
The plots of current THD with respect to amplitude modulation index and frequency modulation index for 5-level inverter and 7-level inverter configurations are shown in Figure 4.7 and Figure 4.8, respectively. Similar to the voltage THD



plots, it can be observed that the inverter with CSSS network gives a performance (in terms of current THD) which is almost stable over the entire operating region.



(a)

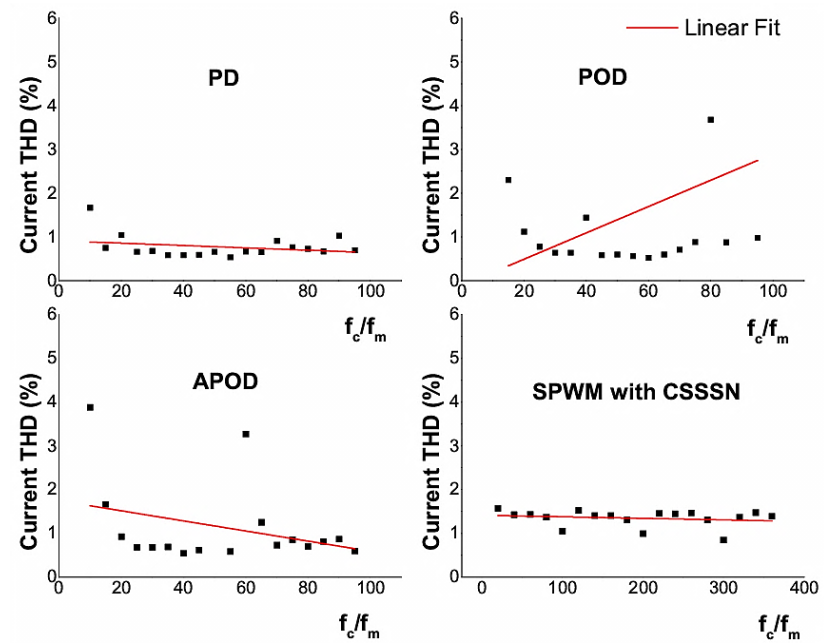


(b)

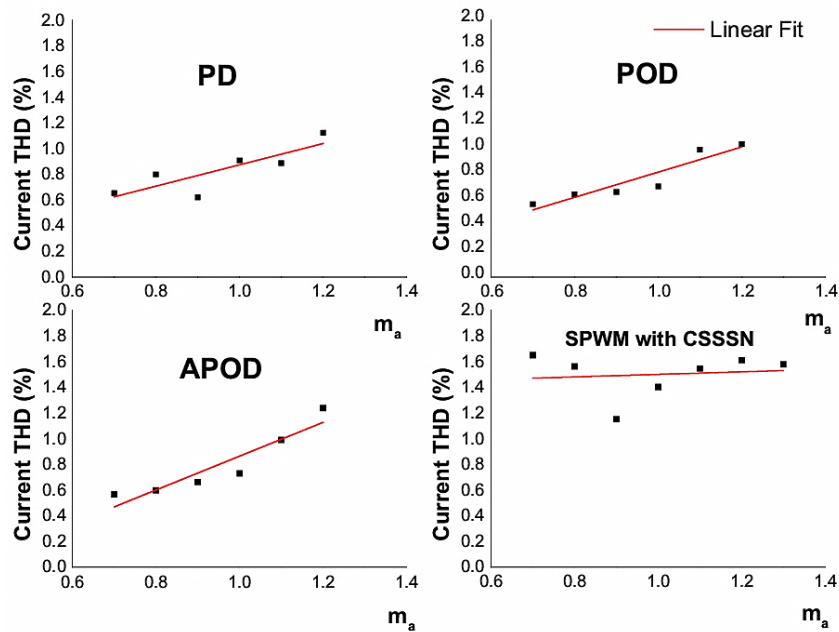
**Figure 4.7** Variation of current THD with variation of (a)  $f_c/f_m$  (b)  $m_a$ , for MWES with 7-level inverter

Also, the current THD values obtained from a CSSS network is comparable to the

values obtained using other modulation schemes. On comparing the linearly fitted line in Figure 4.7(a), it can be noted that the output current distortion is less and the current THD values are almost constant under different inverter switching frequencies.



(a)



(b)

**Figure 4.8** Variation of current THD with variation of (a)  $f_c/f_m$  (b)  $m_a$ , for MWES with 7-level inverter

A similar kind of stable performance is obtained when the amplitude modulation index is varied. It is evident from the plot of figure 4.7(b) that the inverter with CSSS network provides stable performance in both over-modulated and under-modulated regions unlike other modulation schemes where the performance is varying when the amplitude modulation index varies. The plots of Figure 4.8 and its analysis reiterate the conclusion derived above that the MWES inverter with CSSS network provides a stable performance over wide operating conditions.

When the micro wind energy systems forms a part of a distributed generation system, it usually employs distribution transformers. When these distribution transformers are feeding non-linear loads they are usually de-rated to avoid overheating due to the increased eddy currents caused by the harmonic currents of the non-linear loads. k-factor usually gives the information about how much a distribution transformer needs to be de-rated at the time of installation. K-factor is a weighting of the harmonic load currents according to their effects on transformer heating, as derived from ANSI/IEEE C57.110 (Khan and Ahmed 2007).

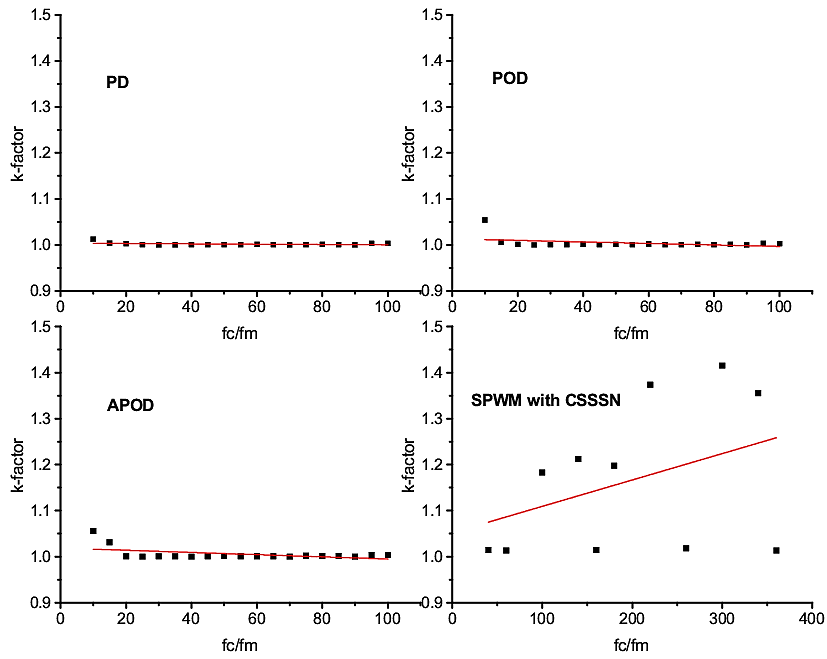
So, apart from the rms and THD values, the impact of the modulation schemes on the k-factor of the transformer is also analyzed. The expression used to compute k-factor is given by equation (4.1).

$$\text{k-factor} = \frac{i_1^2(1^2) + i_2^2(2^2) + i_3^2(3^2) + i_4^2(4^2) + \dots + i_n^2(n^2)}{i_1^2 + i_2^2 + i_3^2 + i_4^2 + \dots + i_n^2} \quad (4.1)$$

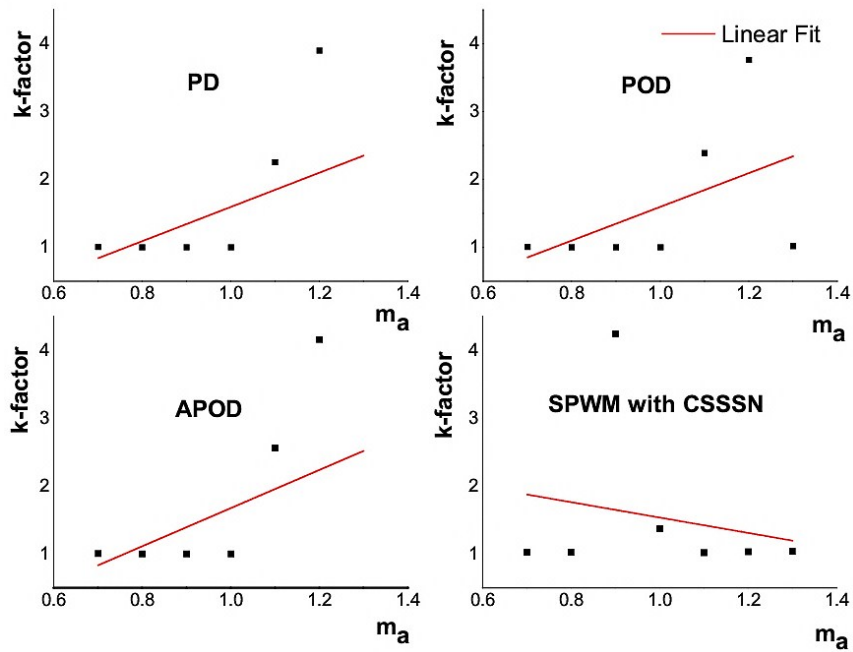
where  $i_1, i_2, i_3, \dots, i_n$  are the load current at the respective harmonics expressed in per unit. In this study, harmonic components up to 11 have been considered for computation of k-factor. Hence, equation (4.1) is rewritten as in equation (4.2).

$$\text{k-factor} = \sum_{n=1}^{11} \frac{i_n^2(i^n)}{(i^n)} \quad (4.2)$$

The variation of k-factor for a 5-level and 7-level inverter configurations when amplitude modulation index and frequency modulation index is varied has been presented in Figure 4.9 and Figure 4.10.



(a)



(b)

**Figure 4.9** Variation of k-factor with variation of (a)  $f_c/f_m$  (b)  $m_a$  for MWES with 5-level inverter

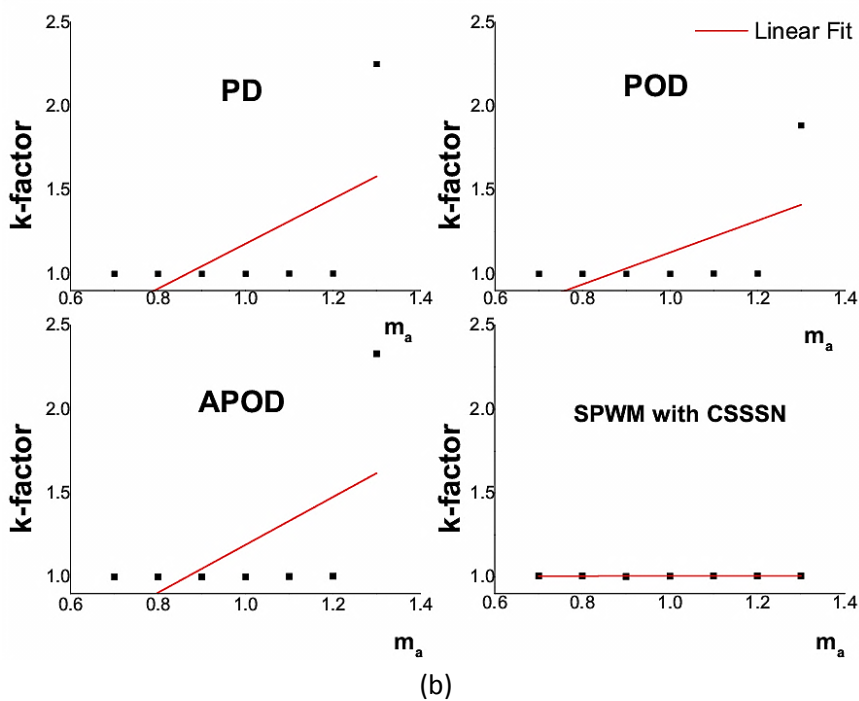
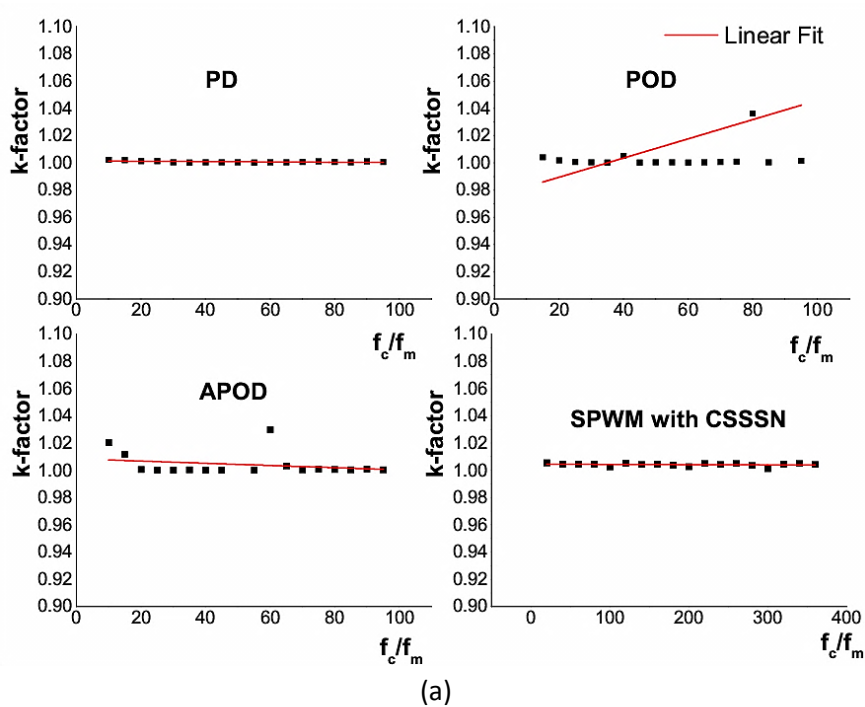


**Figure 4.10** Variation of k-factor with variation of (a)  $f_c/f_m$  (b)  $m_a$  for MWES with 7-level inverter

The load in the simulation study is a reactive load and its impedance value is held constant for all operating conditions. As a result of that, the k-factor is just above the value of ‘1’ in all the cases. In practical cases, when more non-linear loads like switching converter based loads are connected to the transformer, the k-factor may

further increase. Since the objective of the author is to prove that the proposed switching network can give comparable satisfactory performance to other modulation schemes, other types of non-linear loads are not used for simulation. It can be observed from Figure 4.9 and Figure 4.10 that the k-factor is almost constant for most of the operating conditions and comparable to other modulation schemes, when using the CSSS network in the MWES.

The results have been tabulated for the purpose of getting a clear picture of the performance of the MWES under various test conditions. Table 4.1 shows the range of values for voltage THD, current THD and k-factor when the frequency modulation index ( $f_c/f_m$ ) is varied. It can once again be noted that the performance remains almost stable for a wide range of input conditions when the proposed CSSS network is used to control the inverter.

**Table 4.1** Effect of variation of  $f_c/f_m$  on performance parameters under different modulation schemes

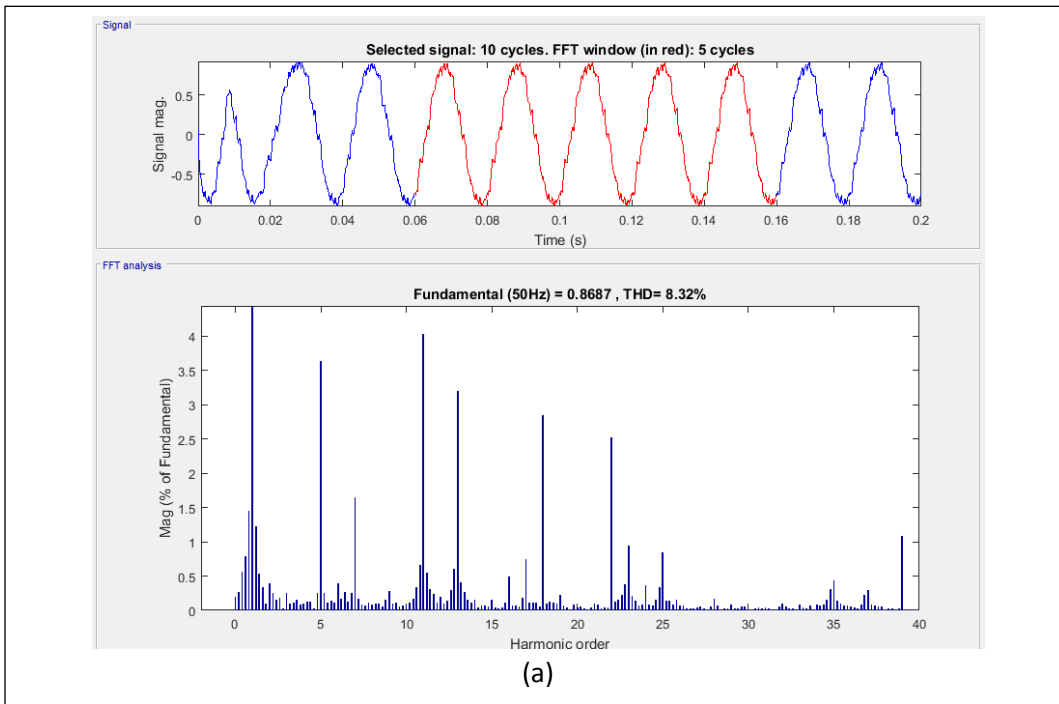
Performance parameters	Modulation Scheme	PD	POD	APOD	Proposed scheme with CSSSN
	Test Cases				
Voltage THD (%)	5-level	3-5	2.5 - 7.5	2 - 9	7.5 - 8
	7-level	3 - 1.5	4 - 5	2 - 6	4.5 - 5
Current THD (%)	5-level	0.5 - 1.5	0.5 - 1.5	0.5 - 2	~1.5
	7-level	0.5 - 1	0.5 - 2	0.5 - 1.5	1 - 1.5
k-factor	5-level	~ 1	~ 1	~ 1	1.1 1.3
	7-level	~ 1	0.95-1.05	~ 1	~ 1

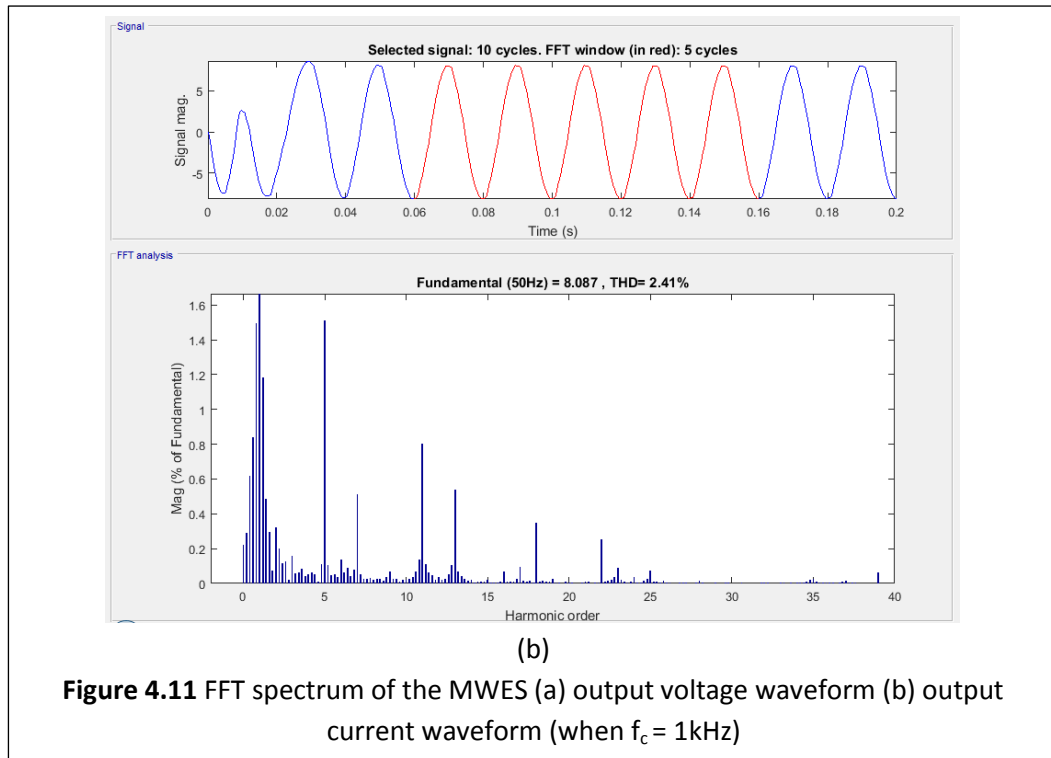
Table 4.2 shows the range of values for voltage THD, current THD and k-factor when the amplitude modulation index ( $m_a$ ) is varied. Two important conclusions can be derived from the results tabulated in Table 4.2. First, the performance of the inverter using the proposed CSSS network is comparable to the existing modulation techniques, when the modulation index is less than 1 (i.e. under-modulation region). Second, the performance is better and remains uniform under various test conditions, when the modulation index is more than 1 (i.e over-modulation region).

**Table 4.2** Effect of variation of  $m_a$  on performance parameters under different modulation schemes

Performance parameters	Modulation Scheme		PD	POD	APOD	Proposed scheme with CSSSN
	Test cases					
Voltage THD (in %)	5-level	Under-modulation	~ 5	~ 5	~ 5	~ 10
		Over-modulation	20 - 40	20 - 40	20 - 40	~10
	7-level	Under-modulation	2	2.5	2.5	~5
		Over-modulation	2-3	2-3	2-3	~5
Current THD (in %)	5-level	Under-modulation	~4	~4	~4	~7
		Over-modulation	4 - 30	4 - 30	4 - 30	~5
	7-level	Under-modulation	0 - 1	0.5 - 0.75	0.5 - 0.75	~1.6
		Over-modulation	1 - 1.5	0.75 - 1	0.75 - 1.5	~1.6
k-factor	5-level	Under-modulation	~ 1	~ 1	~ 1	~ 1
		Over-modulation	1 - 2.5	1 - 2.5	1 - 2.5	~ 1
	7-level	Under-modulation	~ 1	~ 1	~ 1	~ 1
		Over-modulation	1 - 1.5	1 - 1.5	1 - 1.5	~ 1

The FFT spectrum of the MWES output voltage and current waveform for one of the test cases (switching frequency of 1kHz) is shown in Figure 4.11.





## 4.2 MWES Inverters with Delta Modulator and CSSS Network

Many of the two level inverter modulation techniques like hysteresis control, sub-harmonic PWM, delta modulation have their own advantages and it would be advantageous if a multilevel inverter can be controlled using these techniques. The principles of the CSSS network enable the usage of any two level inverter modulation techniques (which are originally intended to control only a two level inverter) to literally control any levels of series connected inverters. In this section, the application of delta modulation technique to control five level series connected inverters in the MWES has been demonstrated.

The principle of delta modulation evolved from pulse code modulation used in communication networks. Attraction of the delta modulation (DM) technique is that it guarantees that the on and off time of the inverter switches will never fall below a given minimum value. Delta modulation technique is an established alternative to the traditional sinusoidal PWM switching used in commercial voltage source inverters driving AC motors (Anjum and Maswood 2008). It is considered as the simplest method for modulating an analog signal to



digital form. The entire process of generating switch control signals is based upon the process of converting an analog modulating (reference) signal into a digital signal by using quantizers. In delta modulation, the reference function  $x(t)$  is coded and decoded back to form a derived function  $x'(t)$ . Then both the functions are compared to generate 1-bit logic signal. These logic signals are then used to control the power switches of the inverters. The magnitude difference of  $x(t)$  and  $x'(t)$  forms a difference function  $y(t) = x(t) - x'(t)$ . The function  $x'(t)$  is made to oscillate within a specified band above and below the reference function  $x(t)$ , which in turn varies the difference function  $y(t)$  value. During the modulation process, the analog signal is sampled at a rate several times higher than the frequency of the modulating signal to adhere to the nyquist criterion. While doing so, a careful choice of sampling rate is made to avoid the problems due to granularity and oversampling. Figure 4.122 depicts the block diagram of a delta modulator and the waveforms generated and associated waveforms.

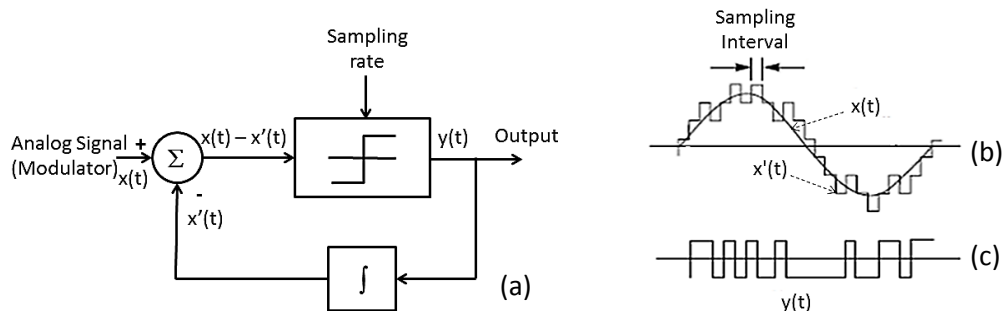


**Figure 4.12** (a) Delta modulator (b) Reference and Sampled waveforms (c) Pulse coded switching signals

The number of commutation intervals is controlled by controlling the following parameters:

- (i) Magnitude of the reference function
- (ii) Quantizing interval (sample frequency)
- (iii) Bandwidth threshold levels

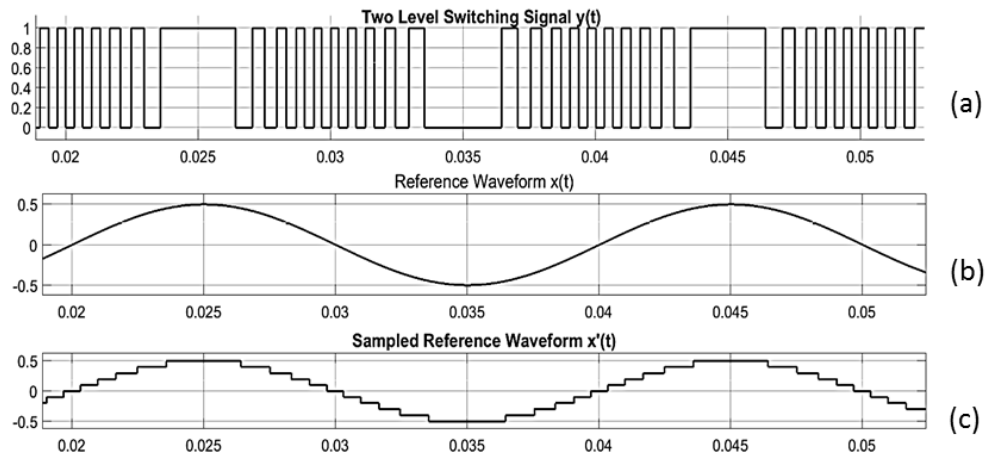


**Figure 4.13** (a) Two level switching signals generated by the delta modulator, (b) Reference signal, (c) Sampled reference signal.

The time period of the pulses in the output signal  $y(t)$  is proportional to the slope of the reference waveform. The inherent closed loop makes sure that the reference signal is tracked continuously. Figure 4.13 shows the reference sine wave (i.e. analog modulating signal), the sampled reference waveform and the pulse code modulated, two-level, switching signals.

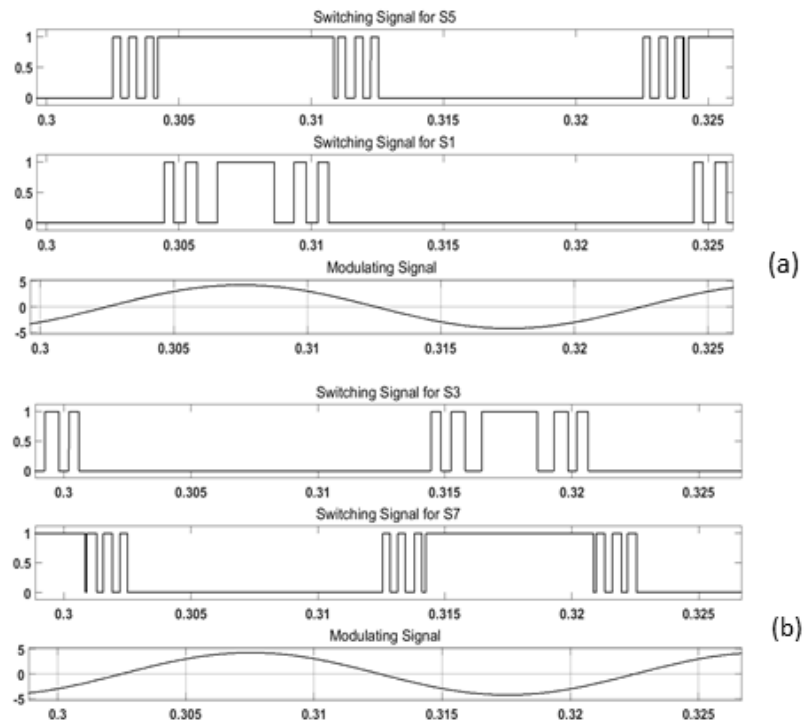


**Figure 4.14** Switching signals generated by the CSSSN during (a) positive cycle of the reference wave, (b) negative cycle of the reference wave.

The pulse code modulated signals generated by the delta modulator is fed to a CSSSN. In turn, the CSSSN network generates switching signals for all the power switches in the lower bridges and upper bridges of the 5-level inverters in the MWES. Figure 4.14 shows the switching signals generated by the CSSSN during positive and negative half of the reference waveform.

Figure 4.15 depicts the complete set of switching signals for all the eight switches (S1 through S8) of the five level inverter shown in Figure 3.15.

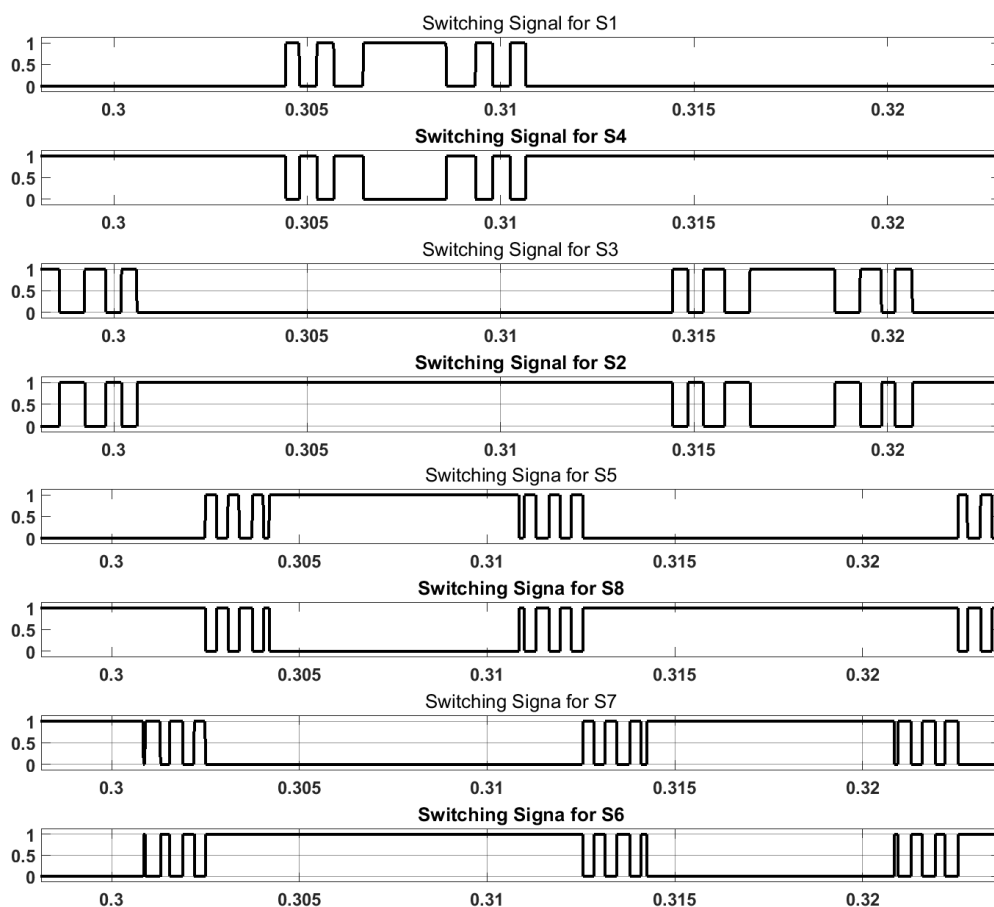


**Figure 4.15** Delta modulated switching signals generated by the CSSSN for all the eight switches of the 5-level inverter

The performance of the MWES with delta modulated 5-level series connected inverters is tested for various operating conditions. The Quantization Index (QI) of the delta modulator is varied from 0.1 to 0.4 to cover various sampling intervals. Care has been taken during the selection of QI that issues due to granularity and

over sampling are avoided. The switching frequency of the inverter is approximately estimated using the expression given in equation 4.3.

$$\text{Switching frequency } (f_s) = 4 * \frac{V_{ref}(p)}{QI} * 50 \quad (4.3)$$

where  $V_{ref}(p)$  is the peak value of the reference waveform. Figure 4.16 shows the output voltage(phase-line) waveform of the 5-level series connected inverter before the filter. Figure 4.17 depicts the filtered output voltage and current waveforms of the MWES during one of the test conditions.

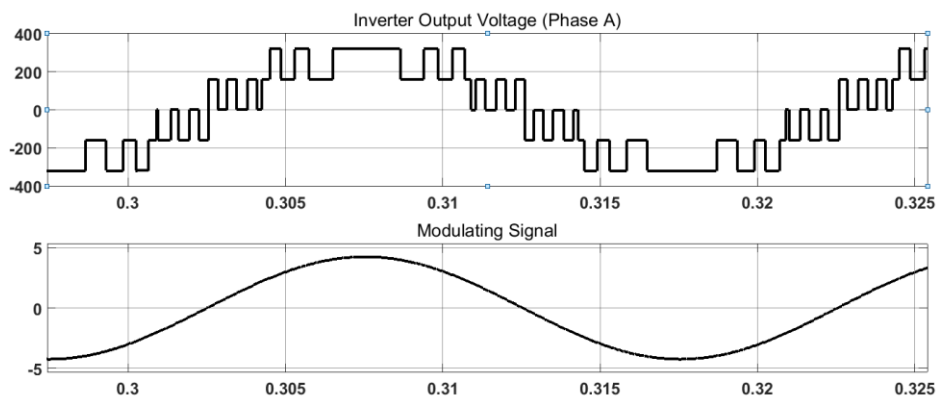


**Figure 4.16** Phase voltage of one of the 5-level inverters in the MWES

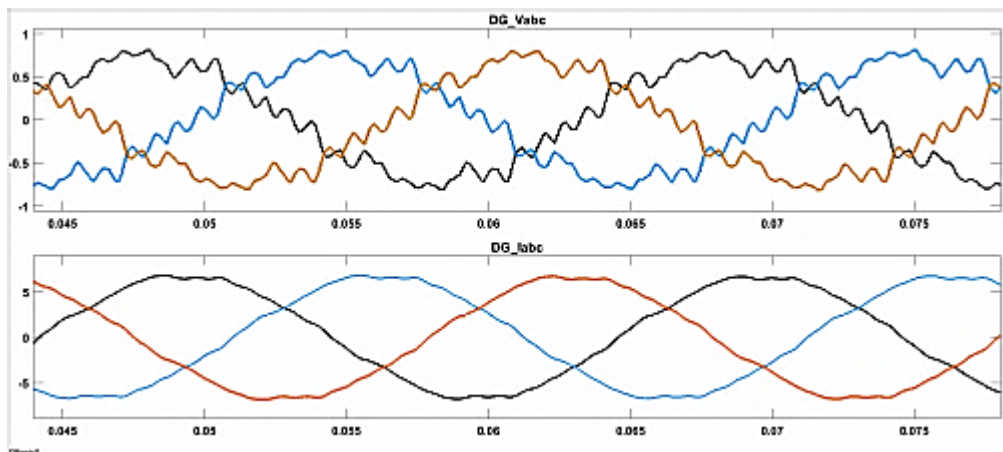


**Figure 4.17** 3-phase output voltage and current waveforms of the MWES employing delta modulation technique and CSSS network

The variations of output rms values, total harmonic distortion and k-factor are plotted for different quantization indexes which are shown in Figure 4.18 to 4.20.

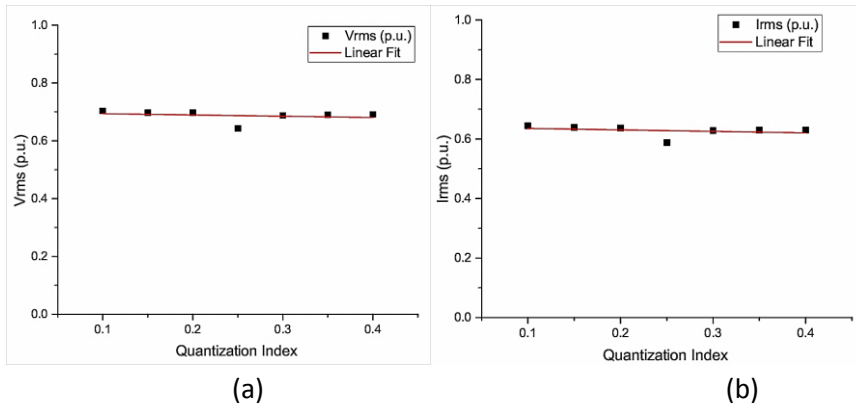


**Figure 4.18** Variation of rms value of voltage and current w.r.t variation in QI

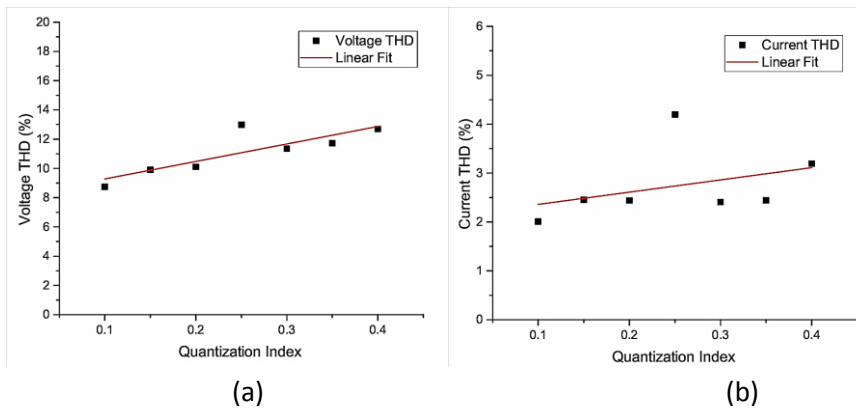


**Figure 4.19** Variation of voltage and current THD w.r.t variation in QI

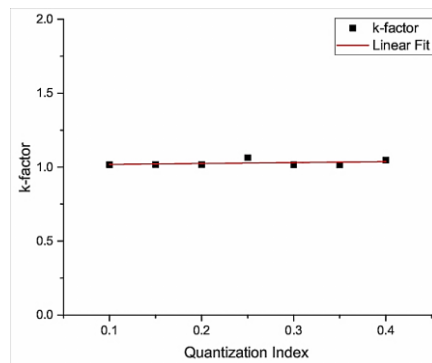


**Figure 4.20** Variation of k-factor w.r.t variation in QI

It can be observed from the above results that the performance of the MWES with delta modulation technique and CSSSN is very much comparable to the performance mentioned of MWES with SPWM and CSSSN.

### 4.3 MWES Inverters with Un-equal Sources

Under practical conditions, series connected inverters with independent sources rarely operate with equal input voltages. In a micro wind energy system where the dc voltages are derived from the conversion of wind turbine ac voltage, the output voltages of each turbine may differ depending on the variation of wind speed. Even if the wind speed is assumed constant around all the turbines operating in the area, the voltage produced by the turbine generators may not be equal. This unequal source condition affects the rms value of the output voltage of the series connected inverter. Not only the rms value changes in these conditions, but also the output waveforms get more distorted. So in these cases, the modulation technique has to perform the additional task of improving the rms value without distorting the output too much. A simple solution to handle this problem is provided by extending the principles of the proposed CSSS network.

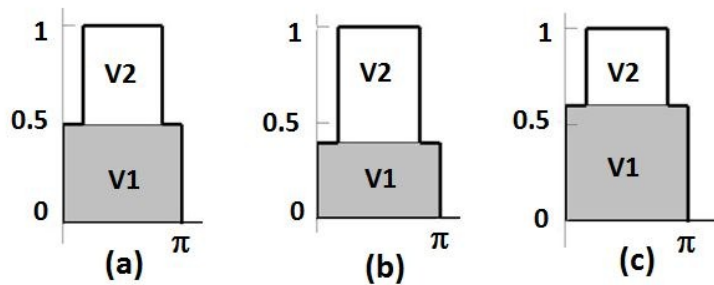


**Figure 4.21** Five level output under (a) equal source condition (b) un-equal source condition ( $V_1 < V_2$ ) (c) un-equal source condition ( $V_1 > V_2$ )

The operating principle of the extended CSSS network is derived based upon the analysis of the area covered by the output waveforms under different input magnitude conditions. Figure 4.21 shows the inverter output waveforms under equal source condition and un-equal source conditions. Let the area covered by the waveforms in Figure 4.21 (a), (b) and (c) be  $A_1$ ,  $A_2$  and  $A_3$ , respectively. Referring to the five level series connected inverter in Figure 4.22, it can be said that the shaded area of the waveforms in Figure 4.21 is formed due to lower bridge inverter source voltage  $V_1$ . The un-shaded area is formed due to the upper bridge inverter

source voltage  $V_2$ . The area of these waveforms can be generally expressed as in equation 4.4.

$$A = \{area\ formed\ by\ V_1\} + \{area\ formed\ by\ V_2\} \quad (4.4)$$

$$= \{V_1\pi\} + \left\{V_2 \left(\frac{5\pi}{6} - \frac{\pi}{6}\right)\right\}$$

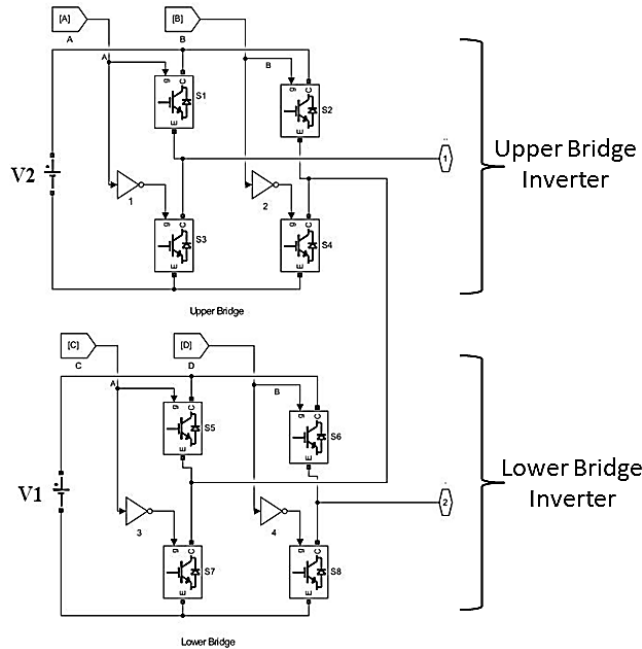


**Figure 4.22** A five level series connected inverter

The area of the waveform in Figure 4.21(a) (when the sources are having equal magnitude) is expressed as in equation 4.5,

$$A_1 = V_1 \left\{ \pi + \left( \frac{5\pi}{6} - \frac{\pi}{6} \right) \right\}, \text{ when } V_1 = V_2 \quad (4.5)$$

When the sources have un-equal magnitude as shown in Figure 4.21 (b) and (c), the two source voltages are related using the expression  $V_2 = xV_1$ . The area of these waveforms, under various un-equal source conditions, are expressed as in equation 4.6 and 4.7,

$$A_2 = V_1 \left\{ \pi + x \left( \frac{5\pi}{6} - \frac{\pi}{6} \right) \right\}, \text{ when } V_1 > V_2 \text{ and } x < 1 \quad (4.6)$$

and

$$A_3 = V_1 \left\{ \pi + x \left( \frac{5\pi}{6} - \frac{\pi}{6} \right) \right\}, \text{ when } V_1 < V_2 \text{ and } x > 1 \quad (4.7)$$

For example,

When  $V_1 = 0.5 p.u$ ,  $V_2 = 0.5 p.u$  (i.e.  $V_1 = V_2$  and  $x = 1$ ), the area of A1 is calculated using equation 4.4 as,

$$A_1 = 2.61$$

When  $V_1 = 0.6 p.u$ ,  $V_2 = 0.4 p.u$  (i.e.  $V_1 > V_2$  and  $x < 1$ ), the area of A2 is calculated using equation 4.4 as,

$$A_2 = 2.72$$

When  $V_1 = 0.4 p.u$ ,  $V_2 = 0.6 p.u$  (i.e.  $V_1 < V_2$  and  $x > 1$ ), the area of A3 is calculated using equation 4.4 as,

$$A_3 = 2.51$$

It can be inferred from the above derivation that the rms value can be improved significantly if the positions of the lower and upper bridges are interchanged during un-equal voltage conditions when  $V_1$  is less than  $V_2$ . By interchanging the bridges and thereby interchanging the source positions, the source with larger magnitude contributes more to the output voltage waveform, similar to the figure shown in Figure 4.21 (c). This interchange of sources results in significant increase in the rms value of the output waveforms.

Since physically interchanging positions of the bridges during the operation of the MWES is not possible, the switching signals used to control each inverter bridges may be interchanged when  $V_1 < V_2$ . The operation of the extended CSSS network is decided based on this inference and conclusion. The extended CSSSN monitors the magnitude of each inverter's input source voltage and the position of the individual inverter bridges is changed logically, if required, to improve the rms value of the output.



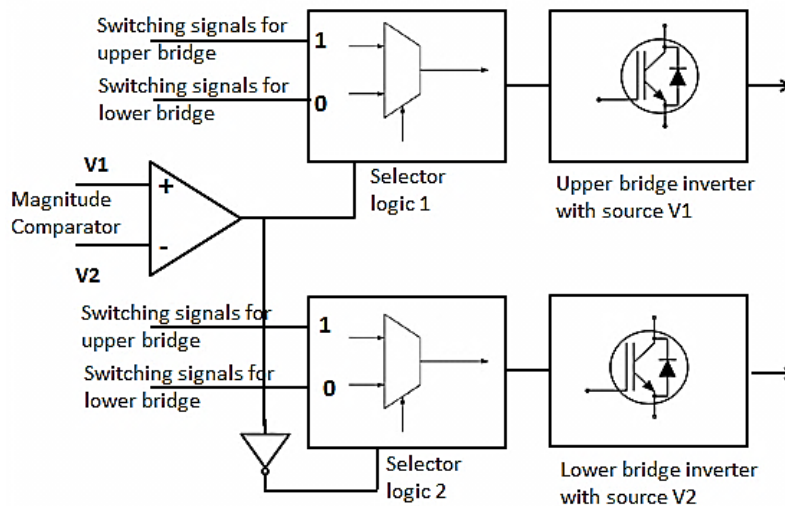


**Figure 4.23** Logic diagram for Extended-CSSS network in the MWES to handle unequal sources conditions

The logic of extended CSSS network is shown in Figure 4.23, which is intended for use in MWES to improve the output rms during unequal source conditions. As mentioned earlier, the lower bridge inverter's input voltage is referred as  $V_1$  and upper bridge voltage as  $V_2$ . A comparator compares the magnitude of  $V_1$  and  $V_2$ , and controls the functioning of the selector logic. Whenever  $V_1 < V_2$  (i.e. upper bridge inverter has a source magnitude greater than lower bridge inverter source magnitude), switching signals originally meant for controlling upper bridge inverter is given to lower bridge inverter and vice versa.

The inverter output voltage waveforms for different source voltage conditions ( $V_1 < V_2$  and  $V_1 > V_2$ ) with and without extended CSSSN network are shown in Figure 4.24. It can be noted from Figure 4.24 (c) and (d) that series connected inverter output waveforms looks the same as the extended-CSSS networks logically alters the inverter positions when  $V_1 = 140\text{V}$  and  $V_2 = 160\text{V}$ . The inverter h-bridge with 160V source is operated (as lower h-bridge) to produce the lower portion of the waveform and the inverter with 140V source is operated (as upper h-bridge) to produce the upper portion of the waveform, thus increasing the rms value obtainable from the output waveforms.

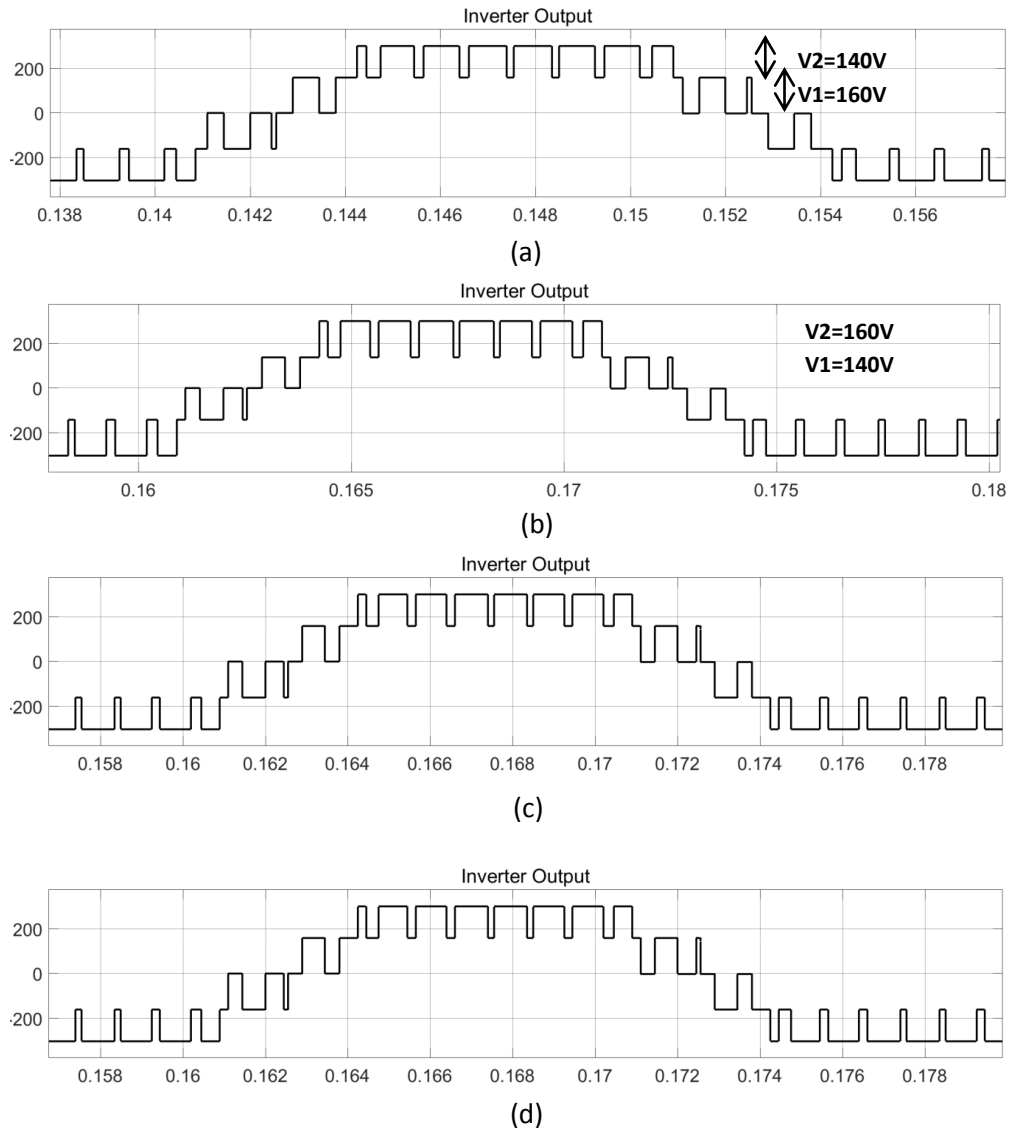
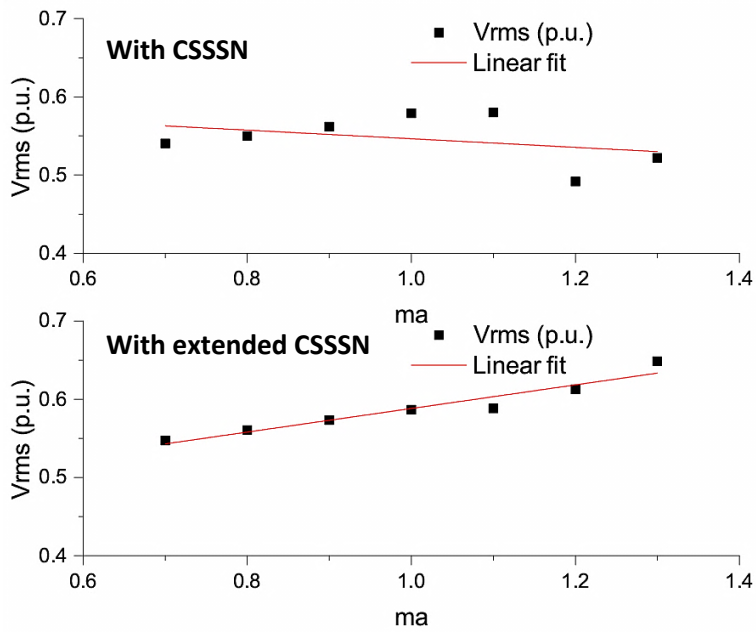
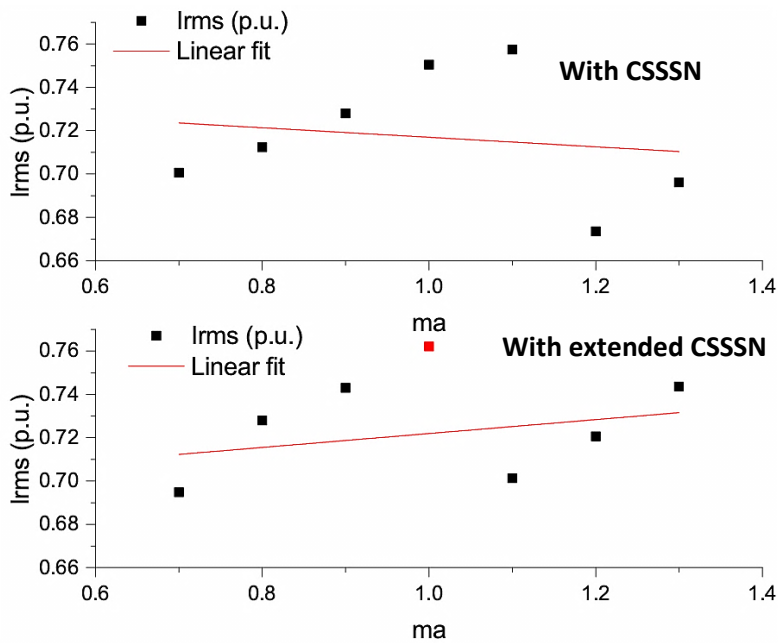


**Figure 4.24** Series connected inverter outputs (a) without extended-CSSN when  $V_1=160$  and  $V_2=140$ , (b) without extended-CSSN when  $V_1=140$  and  $V_2=160$ , (c) with extended-CSSN when  $V_1=160$  and  $V_2=140$ , (d) with extended-CSSN when  $V_1=140$  and  $V_2=160$

The overall results obtained as a result of simulating the MWES with extended CSSS network and 5-level series connected inverters, under equal and unequal sources conditions, are presented in Figure 4.25 and 4.26. For study purpose, the unequal voltage source conditions of  $V_1=0.87V_2$  (i.e.  $V_1=140v$ ,  $V_2=160v$ ) and  $V_1=1.147V_2$  ( $V_1=160v$ ,  $V_2=140v$ ). SPWM technique is used to generate the two level switching signals which are then distributed to various inverter bridges using the CSSS network.



(a)



(b)

**Figure 4.25** MWES performance under unequal source condition ( $V_1 < 0.8V_2$ )

(a) Variation of  $V_{rms}$  with CSSSN and with/without extended CSSSN

(a) Variation of  $I_{rms}$  with CSSSN and with/without extended CSSSN

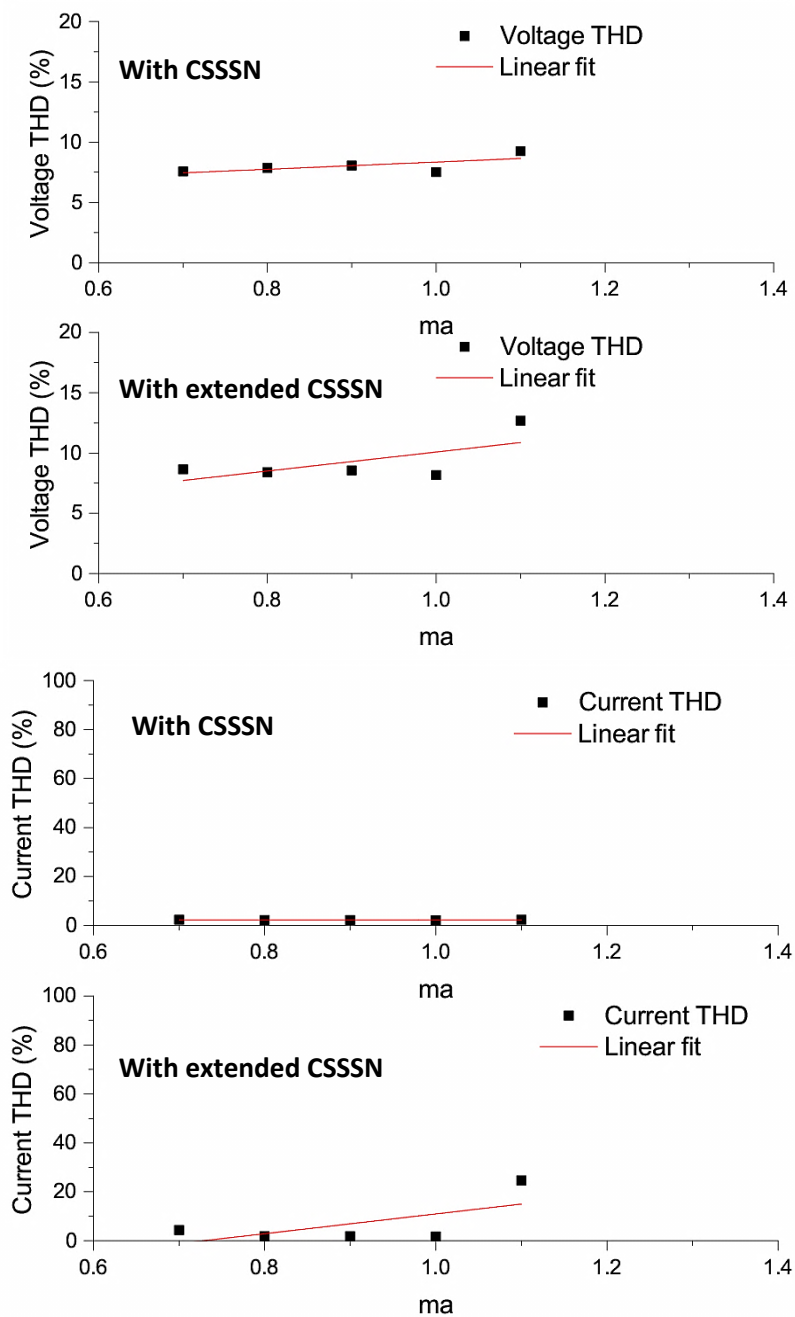


**Figure 4.24**

**Figure 4.26** MWES performance under unequal source condition ( $V_1 < 0.8V_2$ )

(a) Variation of  $V_{thd}$  with CSSN and with/without extended CSSN

(a) Variation of  $I_{thd}$  with CSSN and with/without extended CSSN

The analysis of the results indicates that the obtained results are in-line with the analytical conclusion derived earlier. The rms values of the MWES output current and voltage are improved when the extended CSSS network's functionality is used.

#### 4.4 Generation of Switching Signals using Digital Signal Controller (DSC)

In order to demonstrate how easily the switching signals can be generated for controlling a series controlled inverter using the CSSS network, the proposed network logic was implemented on Texas Instrument’s TMS320F28335 digital signal controller. The F28335 controller has many peripheral functions including six enhanced pulse width modulation (ePWM) units. The ePWM units were programmed to generate appropriate switching signals for all the eight switches of the 5-level series connected inverter similar to the one shown in Figure 3.15(c). The control program in the form of graphical language to control the DSC was written using Altair’s sT Embed tool. In its simplest form, the program includes a set of comparators and selector logic as shown in Figure 4.27. The ePWM units 1

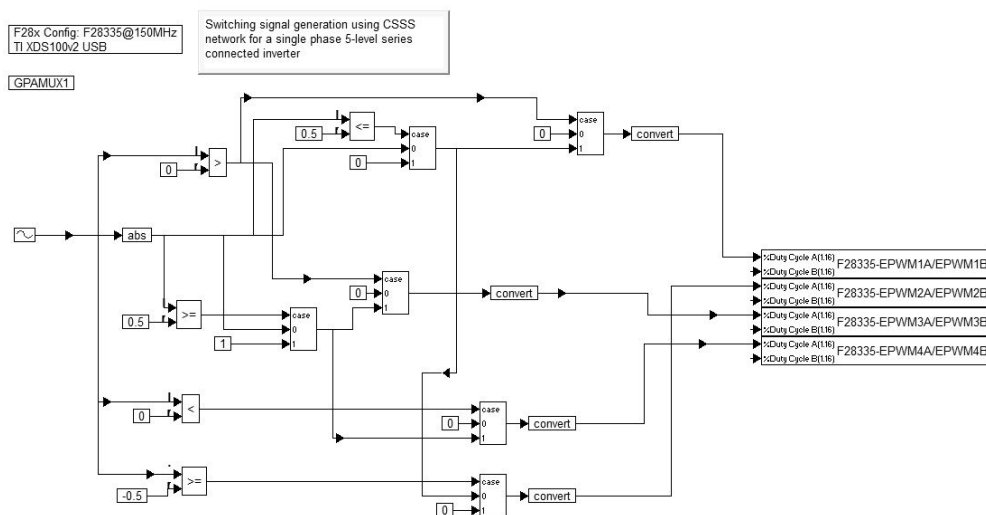
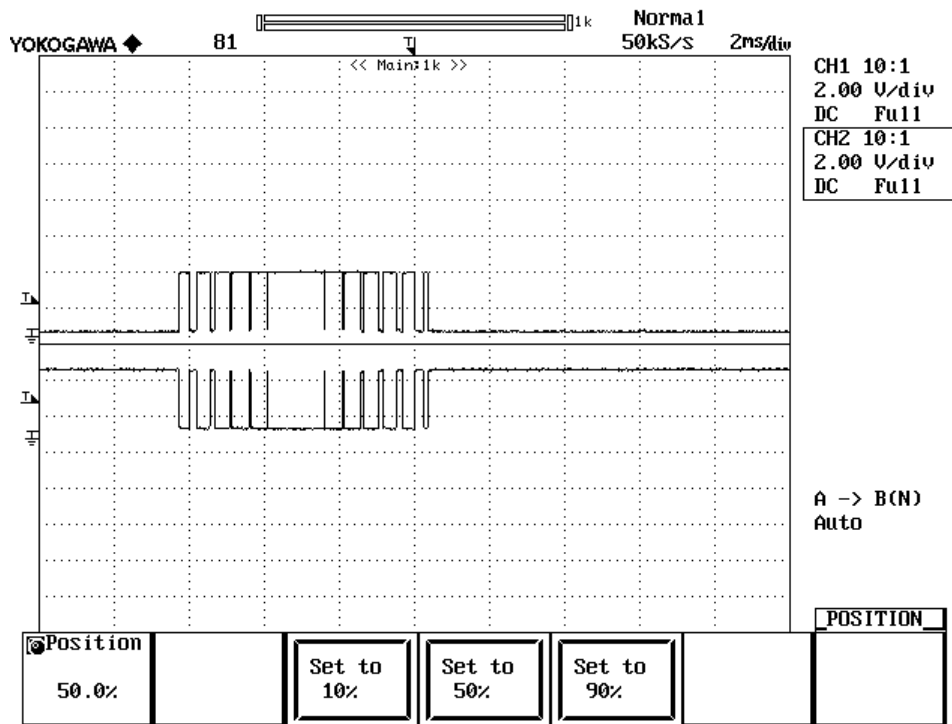
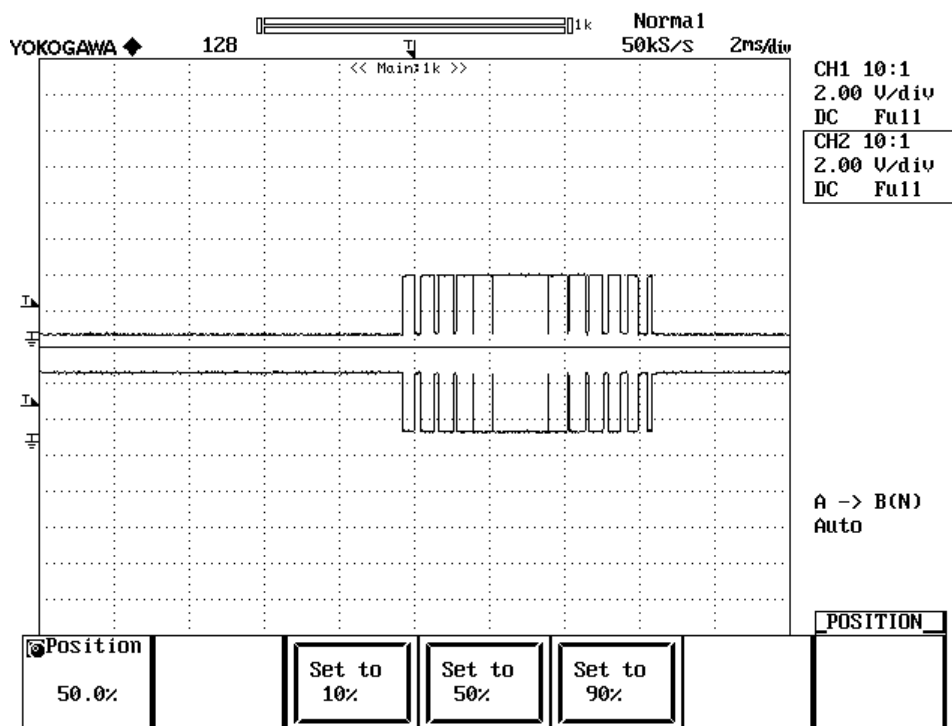


**Figure 4.27** : DSC Program to generate switching signals for a 5-level inverter

and 2 were programmed to generate switching signals for all the upper bridge switches (S1, S2, S3 and S4), whereas ePWM units 3 and 4 were programmed to generate switching signals for all the lower bridge switches (S5, S6, S7 and S8). The switching signals generated by the ePWM units of F28335 DSC (with carrier frequency of 2kHz) are shown in Figure 4.28 and Figure 4.29. Each of the ePWM units were programmed to generate complementary switching signals (with dead band) to control the upper and lower leg switches in each bridge.

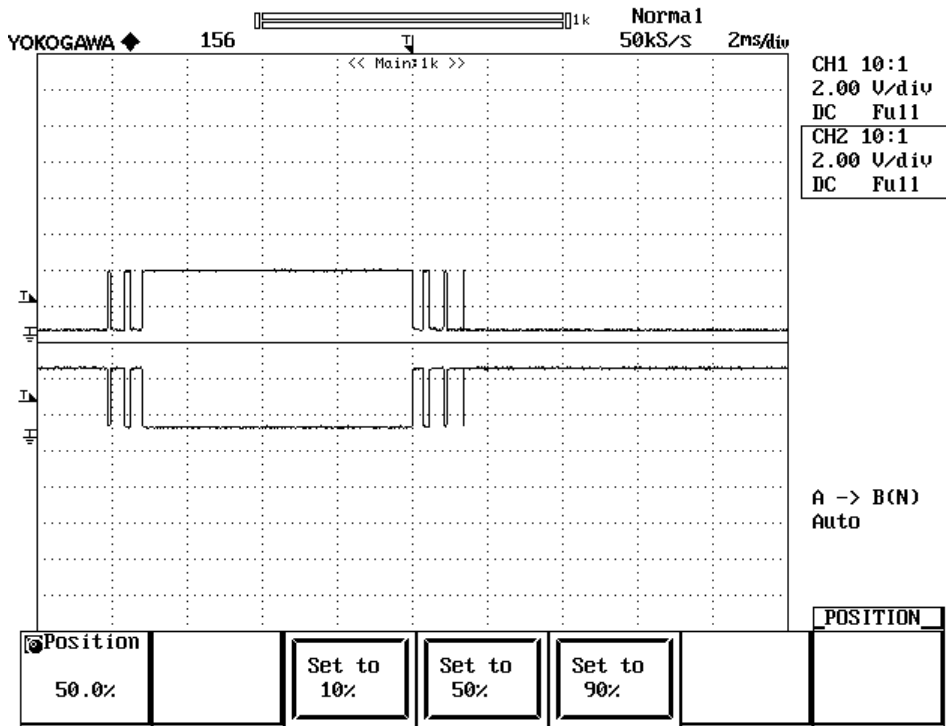


(a)

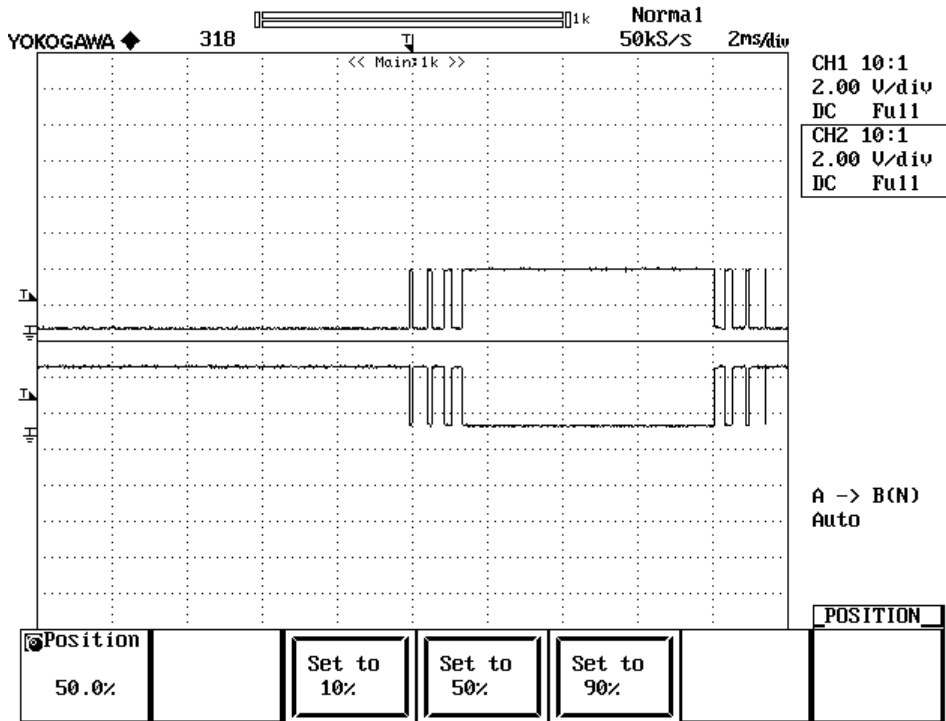


(b)

**Figure 4.28** : Switching signals generated by F28335 DSC for upper bridge switches (a) for switches S1, S4. (b) for switches S2, S3.



(a)



(b)


**Figure 4.29:** Switching signals generated by F28335 DSC for lower bridge switches (a) for switches S5, S8. (b) for switches S6, S7.

The compiled program consumes less than 2 kB in F28335 DSC's memory including the initialized data. The program can be easily modified to generate any number of switching signals which is restricted only by the hardware resources available in the selected DSC.

#### **4.5 Summary**

This chapter dealt with the analysis of performance of a micro wind energy system under various test conditions. The test cases include variations in amplitude modulation index and frequency modulation index for both conventional modulation strategies and the proposed comparators based switching signal selection network. As a result of analyzing the performance, it is concluded that the performance of MWES with the proposed CSSS network is comparable to that of the conventional techniques, yet simpler. In many of the cases it was observed that the performance with CSSS network is better than the conventional techniques. Also, this chapter explains about the functionality of extended CSSS network to deal with series connected inverter with unequal dc sources. The employment of extended CSSS network enabled the marginal increase of rms value of the inverter output voltage. The demonstration of how the CSSSN functionality can be implemented on a digital signal controller is also presented in this chapter.





# Chapter 5

## Conclusion

## 5. CONCLUSION

Due to increased human dependence on electricity, the gap between electricity supply and demand is steadily increasing. It is suggested through this research work that a fraction of this demand can be met by employing micro wind energy systems for electricity generation. An attempt has been made to analyze the performance of micro wind turbine based electricity generation systems and study the complexity in controlling the system using existing control techniques. Also, a simple solution has been proposed and suggested to overcome the complexity involved in controlling the inverters. This simple solution may encourage widespread use of micro wind turbines in standalone applications, without compromising on the performance.

The simulation experiments performed in this research work include micro wind energy systems with conventional configurations involving different types of converters and different types of control methodologies. MWES configurations involving two-level inverters, reactive elements and bulk step-up transformers were ruled out after thorough study, due to cost aspects and the kind of control complexity involved in obtaining satisfactory system performance. Studies and simulation experiments performed during the research lead to the conclusion that a series connected inverter is much more suitable for stand-alone applications and also in distributed generation applications. The overall cost factor, including maintenance and operation, could also be comparatively less for MWES configurations involving series connected inverters. The modular structure of series connected inverters offer an easy way for replacements and also offers the advantage of scalability to any levels.

During the simulation experiments, in order to control the series connected inverters, many of the existing modulation strategies were used. Even though each of these strategies was found to be having their own advantages, when it comes to meeting the requirements of a micro wind energy system, they had their limitations. The limitations can be mainly attributed to the complexity involved in

the switching signal generation process for obtaining a stable and satisfactory performance over wide operating conditions.

For a micro wind energy system where wind is the primary input energy source, the modulation strategy employed should control the inverters in such a way that the system produces as much power as possible during varying wind conditions. A modulation strategy which uses feedback information of some kind is a better option. As the process of finding apt modulation strategy is an important design step for any power converter based application, care was taken to explore all the possible strategies during simulation experiments. Performance parameters like rms value of the output current, rms value of output voltage, total harmonic distortion of output voltage, total harmonic distortion of output current and k-factor of the distribution transformer were used to analyze the performance of the MWES.

When selective harmonic elimination technique is used, reduction of even few of the lower order harmonics required lengthy solutions. Methods like graphical analysis technique is comparatively simpler but the process of finding the optimum solution have to be repeated whenever there is a change in the operational parameters. The need for computing the solutions every time complicated the control strategy further. On the other hand, when multicarrier modulation strategies were employed to control the inverters of MWES, it was noticed that the performance was not uniform under all the operating ranges. The amplitude modulation index and frequency modulation index were varied over a wide range during the simulation study. The performance was satisfactory only during certain operating conditions. Another issue noted with the multicarrier strategies was that the number of carrier waves required to generate switching signals for various inverter bridges increased as the number of output levels increase. This may be a discouraging factor during practical implementation when more number of level shifted or phase shifted carriers need to be generated. It was also observed during the analysis that the multicarrier strategies were not satisfactory in handling unequal source conditions.

After studying and analyzing the results obtained by simulating the MWES with much of the existing multilevel inverter modulation strategies, a novel switching network for controlling the inverters has been proposed in this research work. Based upon the working principle of the switching network, it's named as comparator based switching signal selection network (CSSSN). The network offers a simple solution to generate switching signals for any levels of series connected inverter. Also, the network enables the use of any existing two level inverter modulation schemes to control any multilevel inverter of literally any levels. The performance analysis of the micro wind energy system employing the novel CSSS network shows that the performance is very much comparable to the performance using existing techniques. In fact, during certain operating conditions the performance of the MWES is observed to be better than the existing techniques. A generalized algorithm has also been suggested to implement the functionality of CSSS network using any programmable computing device.

An extended CSSS network has also been proposed to deal with unequal source conditions in series connected inverter. The performance analysis of MWES with extended CSSSN indicates that by including this extended feature, the output rms value (and thereby the amount of power delivered to the load) can be improved significantly, without deteriorating the output THD much.

It can be rightfully concluded that when micro wind energy systems are used in standalone applications, the simple system configuration with CSSS network proposed in this research work may very well be employed to obtain stable and satisfactory performance over wide operating conditions. The generalized algorithm proposed to implement the CSSSN functionality can be readily transformed into an embedded-C code to program a DSP, FPGA or a microcontroller, thus simplifying the control algorithm implementation process.

### **5.1 Future Scope of the Research Work**

The potential of micro wind turbines are yet to be fully utilized in electricity generation applications. The study of the micro wind energy systems with CSSS network can be done for distributed generation plants in grid connected mode.

Further research can be done to analyze the aspects of power quality, stability and reliability of MWES in grid connected mode.

The research work provides additional scope for expanding the application of the proposed CSSS network to other areas like electric vehicle drives, industrial drives, static var compensation, active filters etc. In fact, all areas where the three major multilevel inverter topology can be potentially employed, offer a scope for application of the CSSS network.



# APPENDIX

## APPENDIX I

### Specification of SPVAWT1-650W VAWT

General	Model	SPVAWT1-650W
	Rotational axis	Vertical Axis Wind Turbine
	Number of blades	6 Nos
	Materials used	Aluminum blades. Galvanized Mild Steel rotors and static tube.
	Rotor diameter	510 mm
	Shaft height	2100 mm
	Generator	Axial Flux Permanent Magnet direct coupled synchronous generator.
	Weight	46 Kgs
Performance	Peak Electrical power	650W
	Rated Voltage	24/48V DC
	Rated Wind Speed	15m/s
	Start up wind speed	1.5m/s
	Charging start speed	2.8m/s
	Cut out wind speed	25m/s
Rotor	Wind direction sensing	Omni directional
	Yaw control	Not required
Stator	Inductance	33mH per phase
	Resistance	38 ohm per phase
	No. of poles	8

## APPENDIX I

### C Program for generating switching signals using CSSSN

```
/** solidThinking Embed 2017.2 Build 28 Automatic C Code Generator Version  
15.0 Build 28 ***/
```

```
#include "math.h"  
#include "cgen.h"  
#include "c2000.h"  
int MHZ=150;  
#define _SYS_MHZ_ 150  
  
static SIM_STATE tSim={0,0,0  
,0,0,0,0,0,0,0,0,0,1,1,0,0,0,0,0,0};  
SIM_STATE *sim=&tSim;  
static INTERRUPT void cgMain()  
{  
static CGDOUBLE _cnt22=1000;  
CGDOUBLE t22;  
int t5;  
CGDOUBLE t12;  
CGDOUBLE t23;  
CGDOUBLE t28;  
CGDOUBLE t32;  
CGDOUBLE t10;  
CGDOUBLE t11;  
CGDOUBLE t13;  
ADCTRL2 |= 0x4040; // Reset ADC Seq  
ADCTRL2 |= 0x2020; // Trigger ADC  
PIEACK = 0x1; // Reset PIE IFLG  
t22 = sin(++_cnt22 > 1000?_cnt22=0:_cnt22)*0.00627690839878081);  
t5 = ( t22> 0);  
t12 = fabs( t22);  
t23 = ( t12<=0.5)?0.: t12;  
t28 = t5? t23:0.;  
t32 = ( t22>=-0.5)?0.: t23;  
t10 = ( t12>=0.5)?1.: t12;  
t11 = t5? t10:0.;  
t13 = ( t22< 0)? t10:0.;  
GPAMUX1 = (GPAMUX1&0xFFFFF01) | 0x5554;  
{ long _duty32 = (long)(int)( t28 * 32768)*37501;  
CMPA1 = (int)(_duty32>>15);  
}  
;  
{ long _duty32 = (long)(int)( t32 * 32768)*37501;  
CMPA2 = (int)(_duty32>>15);
```



```

}
;
{ long _duty32 = (long)(int)( t11 * 32768)*37501;
  CMPA3 = (int)(_duty32>>15);
}
;
{ long _duty32 = (long)(int)( t13 * 32768)*37501;
  CMPA4 = (int)(_duty32>>15);
}
;

endOfSampleCount = TIMER0TIM;

}

void main()
{
  EALLOW;
  PLLSTS = 0x10; // reset clk check
  WDCR=0x00ef; // Disable Watchdog
  asm(" clrc DBGM");
  if (!(PLLSTS&8)) // Skip PLL set if OSC failure
  { PLLSTS = 0x40; //Disable OSC check
    PLLSTS = 0x100; //Enable OSC check (&F283xx /2 mode)
    PLLCR = 0xa; // set PLL to 5xOSC = 150 MHZ;
  }
  PCLKCR1 = 0xF;
  PCLKCR3 = 0x1100;
  EDIS;
  TBPRD1 = 0x927c;
  AQCTLA1 = 0x90;
  AQCTLB1 = 0x0;
  DBCTL1 = 0xb;
  DBRED1 = 0x32;
  DBFED1 = 0x32;
  EALLOW;
  TZCTL1 = 0x0;
  TZSEL1 = 0x0;
  EDIS;
  TBPRD2 = 0x927c;
  AQCTLA2 = 0x90;
  AQCTLB2 = 0x0;
  DBCTL2 = 0xb;
  DBRED2 = 0x32;
  DBFED2 = 0x32;
  EALLOW;
  TZCTL2 = 0x0;

```

```

TZSEL2 = 0x0;
EDIS;
TBPRD3 = 0x927c;
AQCTLA3 = 0x90;
AQCTLB3 = 0x0;
DBCTL3 = 0xb;
DBRED3 = 0x32;
DBFED3 = 0x32;
EALLOW;
TZCTL3 = 0x0;
TZSEL3 = 0x0;
EDIS;
TBPRD4 = 0x927c;
AQCTLA4 = 0x90;
AQCTLB4 = 0x0;
DBCTL4 = 0xb;
DBRED4 = 0x32;
DBFED4 = 0x32;
EALLOW;
TZCTL4 = 0x0;
TZSEL4 = 0x0;
EDIS;
simInit( 0 );
EALLOW;
GPAMUX1 = 0x5555;
EDIS;
startSimDsp();
installInterruptVec(1,7,&cgMain);
TIMER0PRD = 0xbb8; // 32-bit Timer Period Low
TIMER0PRDH = 0x0; // 32-bit Timer Period High
TIMER0TCR |= 0x4020; //Interrupt enable, Timer Reset
EALLOW;
PIECTRL = 1; // Enable PIE Interrupts
EDIS;
IER |= 0x1; //CPU Interrupt enable
resetInterrupts();
enable_interrupts(); // Global Start Interrupts
TBCTL1 = 0x2; // Start timer
TBCTL2 = 0x2; // Start timer
TBCTL3 = 0x2; // Start timer
TBCTL4 = 0x2; // Start timer
EALLOW;
PCLKCR0 |= 0x4; // Start all PWM timers
EDIS;
dspWaitStandAlone();
}

```



# REFERENCES

## REFERENCES

- Ahshan, R., M. T. Iqbal and G. K. I. Mann (2008). "Controller for a small induction-generator based wind-turbine." *Applied Energy Journal*, 85(4): 218-227.
- Al-Othman, A. K. and T. H. Abdelhamid (2008). "Elimination of harmonics in multilevel inverters with non-equal DC sources using PSO". *Energy Conversion and Management*, Volume 50, Issue 3, March 2009, Pages 756-764
- Anaya-Lara, O., N. Jenkins, J. Ekanayake, P. Cartwright and F. M. Hughes (2009). "Wind Energy Generation: Modeling and Control." *John Wiley & Sons, Ltd.*
- Anjum, S. and A. I. Maswood (2008). "Delta modulation with PI controller a comparative study." *2008 IEEE Power and Energy Society General Meeting - Conversion and Delivery of Electrical Energy in the 21st Century*, Pittsburgh, USA.
- Baroudi, J. A., V. Dinavahi and A. M. Knight (2005). "A review of power converter topologies for wind generators." *2005 IEEE International Conference on Electric Machines and Drives*. San Antonio, TX, USA.
- Burton, T., D. Sharpe, N. Jenkins and E. Bossanyi (2002). "Wind Energy Handbook." *John Wiley & Sons, Ltd.*
- Carrasco, J. M., L. G. Franquelo, J. T. Bialasiewicz, E. Galvan, R. C. PortilloGuisado, M. A. M. Prats, J. I. Leon and N. Moreno-Alfonso (2006). "Power-Electronic Systems for the Grid Integration of Renewable Energy Sources: A Survey." *IEEE Transactions on Industrial Electronics*, 53(4): 1002-1016.
- Chiasson, J. N., L. M. Tolbert, K. J. McKenzie and D. Zhong (2005). "Elimination of harmonics in a multilevel converter using the theory of symmetric polynomials and resultants." *IEEE Transactions on Control Systems Technology* 13(2): 216-223.

- Colak, I., E. Kabalci and R. Bayindir (2011). "Review of multilevel voltage source inverter topologies and control schemes." *Energy Conversion and Management*, 52(2): 1114-1128.
- Contributors, Wikipedia. (11 February 2018). "Vertical axis wind turbine." Retrieved 2<sup>nd</sup> February, 2018 from [https://en.wikipedia.org/w/index.php?title=Vertical\\_axis\\_wind\\_turbine&oldid=825098287](https://en.wikipedia.org/w/index.php?title=Vertical_axis_wind_turbine&oldid=825098287)
- Desai, V. K. (2017). "Huge scope of small wind turbines in India." Retrieved 28<sup>th</sup> January, 2018, from <https://tinytechindia.com/blog/huge-scope-of-small-wind-turbines-in-india/>
- Grainger, J. J. and W. D. Stevenson (1994). "Power system analysis." *McGraw-Hill*.
- Hansen, L. H., P. H. Madsen, F. Blaabjerg, H. C. Christensen, U. Lindhard and K. Eskildsen (2001). "Generators and power electronics technology for wind turbines." *The 27th Annual Conference of the IEEE Industrial Electronics Society IECON '01*, 2001, Denver, CO, USA.
- Holmes, D. G. and T. A. Lipo (2003). "Pulse Width Modulation for Power Converters: Principles and Practice." *John Wiley & Sons*.
- Jih-Sheng, L. and P. Fang Zheng (1996). "Multilevel converters-a new breed of power converters." *IEEE Transactions on Industry Applications* 32(3): 509-517.
- Khan, S. and G. Ahmed (2007). "Industrial Power Systems." *CRC Press*.
- Kharu, R. (2018) "Market Development of Small Wind Turbines and Wind Solar Hybrid Systems In India." Retrieved 2<sup>nd</sup> February, 2018, from <http://www.wisein.org/wise-conference-exhibition/Brain-Storming-Session-on-SWT/WISE.pdf>

- Kortabarria, I., E. Ibarra, I. M. d. Alegría, J. Andreu and A. Ascarza (2010). "Power converters used in grid connected small wind turbines: Analysis of alternatives." *5th IET International Conference on Power Electronics, Machines and Drives (PEMD 2010)*. Brighton, UK.
- Kshirsagar, U. (July, 2016)." Small Wind Turbines & Hybrid Systems : Opportunities & Suggestions India Small Wind Association." Published by Spitzen Energy, Pune.
- Lezana, P. and G. Ortiz (2009). "Extended Operation of Cascade Multicell Converters Under Fault Condition." *IEEE Transactions on Industrial Electronics* 56(7): 2697-2703.
- Li, D., S. Wang and P. Yuan (2010). "A Review of Micro Wind Turbines in the Built Environment." *2010 Asia-Pacific Power and Energy Engineering Conference*. Chengdu, China.
- Liang, W. and W. Liu (2010). "Key technologies analysis of small scale non-grid-connected wind turbines: A review." *2010 World Non-Grid-Connected Wind Power and Energy Conference*. Nanjing, China.
- Lu, X., M. B. McElroy and J. Kiviluoma (2009). "Global potential for wind-generated electricity." *Proceedings of the National Academy of Sciences* 106(27): 10933.
- Malinowski, M., K. Gopakumar, J. Rodriguez and M. A. Perez (2010). "A Survey on Cascaded Multilevel Inverters." *IEEE Transactions on Industrial Electronics* 57(7): 2197-2206.
- Mathworks. (2017). "Simulink documentation." Retrieved 24th February, 2017, from <https://in.mathworks.com/help/physmod/sps/powersys/ref/permanentmagnetsynchronousmachine.html>
- Melicio, R., V. M. F. Mendes and J. P. S. Catalao (2008). "Two-level and multilevel converters for wind energy systems: A comparative study." *2008*

*13th International Power Electronics and Motion Control Conference.*  
Poznan, Poland.

Mittal M L, Sharma C and S. R (2012). "Estimates of emissions from coal fired thermal power plants in India." *Proceeding of international emission inventory conference.*

Nicolas, C. V., F. Blazquez, D. Ramirez, M. Lafoz and J. Iglesias (2002). "Guidelines for the design and control of electrical generator systems for new grid connected wind turbine generators." *IEEE 2002 28th Annual Conference of the Industrial Electronics Society. IECON 02.* Sevilla, Spain.

NITI Aayog (June, 2017). "Draft Energy Policy." Published by *NITI Aayog*, Government of India.

Pathmanathan, M., C. Tang, W. L. Soong and N. Ertugrul (2008). "Comparison of power converters for small-scale wind turbine operation." *2008 Australasian Universities Power Engineering Conference.* Sydney, NSW, Australia.

Power, Sunair. (2015) "SUNAIR 650W VAWT Specifications." Retrieved 6<sup>th</sup> August, 2015 from <http://www.sunairpower.co.in/?spvawt1-650w,6>.

Rishi Dwivedi, L. F., Steve Sawyer and Shruti Shukla (2016). "Indian Wind Energy- A brief outlook." Global Wind Energy Council, 2016.

Sathyajith, M. and G. Susan Philip (2011). "Advances in Wind Energy Conversion Technology" Springer-Verlag Berlin Heidelberg.

Svitil, K. (July, 2011). "Wind-turbine placement produces tenfold power increase, researchers say." Retrieved 2<sup>nd</sup> February, 2018, from <https://phys.org/news/2011-07-wind-turbine-placement-tenfold-power.html>

Technologies, X. (2017). "K-Factor Defined." Retrieved 5<sup>th</sup> August, 2017, from [www.xitrontech.com/assets/002/5787.pdf](http://www.xitrontech.com/assets/002/5787.pdf)

Tolbert, L. M., J. N. Chiasson, D. Zhong and K. J. McKenzie (2005). "Elimination of harmonics in a multilevel converter with nonequal DC sources." *IEEE Transactions on Industry Applications* 41(1): 75-82.

Wang, H., C. Nayar, J. Su and M. Ding (2011). "Control and Interfacing of a Grid-Connected Small-Scale Wind Turbine Generator." *IEEE Transactions on Energy Conversion* 26(2): 428-434.



## **DETAILS OF PUBLICATIONS**

1. Kodeeswara Kumaran G and P. Parthiban, "Performance Analysis of Micro Wind Turbine Based Energy Systems with Series Connected Inverters and a Novel Switching Network", Journal of Green Engineering, volume 7, Issue 3, July 2017, page:385-400. doi: 10.13052/jge1904-4720.733. SCImago Journal Rank: 0.132.
2. Kodeeswara Kumaran G and P. Parthiban, "Application of delta modulation strategy to series connected inverters," 2016 IEEE International Conference on Circuits, Controls, Communications and Computing (I4C), Bangalore, 2016, pp. 1-4. doi:10.1109/CIMCA.2016.8053303
3. Chandan Mandal, Kodeeswara Kumaran G and P.Parthiban, "Selective harmonic elimination using graphical method in a 5-level CHB MLI fed from equal and non-equal dc sources", National Conference on Power Electronics, Belagavi. pp. 19-21. January, 2016.

## **BRIEF BIODATA**

<b>Name</b>	Kodeeswara kumaran G
<b>Qualification</b>	M.Tech (Power Electronics & Drives)
<b>Contact Information</b>	Department of Electrical & Electronics Engineering, M. S. Ramaiah Institute of Technology, Bangalore-560054. India.
<b>e-mail id</b>	kkumaran@msrit.edu